

UC Davis

UC Davis Electronic Theses and Dissertations

Title

Bugs Behaving Badly: Insect Pest Behavior and Pathogen-Induced Cannibalism

Permalink

<https://escholarship.org/uc/item/4rf8p505>

Author

Culshaw-Maurer, Michael

Publication Date

2021

Peer reviewed|Thesis/dissertation

Bugs Behaving Badly:
Insect Pest Behavior and Pathogen-Induced Cannibalism

By

MICHAEL CULSHAW-MAURER
DISSERTATION

Submitted in partial satisfaction of the requirements for the degree of

DOCTOR OF PHILOSOPHY

in

Ecology

in the

OFFICE OF GRADUATE STUDIES

of the

UNIVERSITY OF CALIFORNIA

DAVIS

Approved:

Jay Rosenheim, Co-Chair

Sebastian Schreiber, Co-Chair

Andrew Sih

Committee in Charge

2021

Acknowledgments

In the course of an endeavor as long as a PhD, there are simply too many people to thank, but I will do my best to cover my bases. I would like to acknowledge Jay Rosenheim, Sebastian Schreiber, and Andy Sih as not only the members of my dissertation committee, but sources of support, motivation, and kindness over the last 6 years. I would like to thank my wife, Lea Pollack, for being a partner in the truest sense of the word. I could not have done it without her support and companionship, and for playing roles from editor, to coauthor, to pump-up playlist maker and beyond. I'd like to thank our dog, Gouda, for helping us both stay marginally more sane during the last year of COVID lockdown. I would like to thank my family for their constant support and love. I would also like to thank everyone in the GGE and broader "ecology plus" community at UC Davis. It has been an honor to be a part of such a vibrant, brilliant, and caring community of scientists. I am particularly grateful to all the amazing members of the Rosenheim and Schreiber labs who I have gotten to know as friends and colleagues over the years. I would like to thank all my wonderful collaborators through the years, both formal and informal, for making science a more stimulating and rewarding endeavor. Finally, I would like to dedicate this work to the memory of Nick Booster, a friend and scientist missed by all who knew him.



Abstract

The study of insect behavior in agroecosystems offers opportunities to understand fundamental concepts in behavioral ecology and to improve the management of pests for the sake of agricultural production. The following dissertation is a series of papers focused on insect pest behavior and trait-mediated effects. Chapter 1 is a synthetic review paper that develops a framework for utilizing the large body of literature on enemy-risk effects to improve arthropod pest management. While the field of biological control of pests is built on natural enemy ecology, insights gleaned from the study of enemy-risk effects have not been fully incorporated into biological control practice. This paper provides an overview of key concepts from both fields, reviews the literature where they intersect, and provides both conceptual discussions and case studies of particularly relevant applications. Chapter 2 is a paper modeling the collective movement behavior of a devastating pest, the Australian plague locust, using combined agent-based and partial differential equation models. While many models of locust movement rely on interactions between individuals, we demonstrate that foraging behavior generates the characteristic traveling wave pattern of Australian plague locust hopper bands. Finally, Chapter 3 is a manuscript investigating an agent-based model of the population and disease dynamics of a system where infection induces cannibalistic behavior. This study was inspired in part by the case of *Geocoris pallens*, a common beneficial insect in agricultural systems, whose California populations have suffered from increased cannibalism in the face of a novel pathogen. While only empirically documented in a few systems, disease often induces energetic stress, a key trigger of cannibalistic behavior, which is widespread among animal taxa. I present the results of a series of *in silico* experiments investigating the interacting effects of pathogenic virulence and

pathogen-induced cannibalism, showing that the combination can lead to drastic suppression of host populations and even host extinction.

REVIEW AND SYNTHESES

Bugs scaring bugs: enemy-risk effects in biological control systems

Michael Culshaw-Maurer,^{1,2*} 
 Andrew Sih³  and
 Jay A. Rosenheim¹

¹Department of Entomology and Nematology, University of California, Davis, CA 95616, USA

²Department of Evolution and Ecology, University of California, Davis, CA 95616, USA

³Department of Environmental Science and Policy, University of California, Davis, CA 95616, USA

*Correspondence: E-mail: mjculshawmaurer@ucdavis.edu

Abstract

Enemy-risk effects, often referred to as non-consumptive effects (NCEs), are an important feature of predator–prey ecology, but their significance has had little impact on the conceptual underpinning or practice of biological control. We provide an overview of enemy-risk effects in predator–prey interactions, discuss ways in which risk effects may impact biocontrol programs and suggest avenues for further integration of natural enemy ecology and integrated pest management. Enemy-risk effects can have important influences on different stages of biological control programs, including natural enemy selection, efficacy testing and quantification of non-target impacts. Enemy-risk effects can also shape the interactions of biological control with other pest management practices. Biocontrol systems also provide community ecologists with some of the richest examples of behaviourally mediated trophic cascades and demonstrations of how enemy-risk effects play out among species with no shared evolutionary history, important topics for invasion biology and conservation. We conclude that the longstanding use of ecological theory by biocontrol practitioners should be expanded to incorporate enemy-risk effects, and that community ecologists will find many opportunities to study enemy-risk effects in biocontrol settings.

Keywords

Agricultural ecology, behavioural ecology, biological control, enemy-risk effects, natural enemies, non-consumptive effects, pest management, predation risk, predator–prey ecology, trophic cascades.

Ecology Letters (2020)

INTRODUCTION

Biological control (or biocontrol) is the use of an organism to reduce or prevent the unwanted impact of another organism, typically through an exploitative interaction (Eilenberg *et al.*, 2001). While competitive relationships are sometimes utilised (Tyndale-Biscoe and Vogt, 1996), most biological control agents, including predators, parasitoids, pathogens and herbivores, are consumers of pest organisms (Heimpel and Mills, 2017). Perhaps the best-known form of biological control is ‘classical’ or importation biological control, where a natural enemy is imported from a region other than the target area, often from the native home range of the pest. Today, this involves a rigorous process of enemy selection, efficacy testing and non-target testing (Bigler *et al.*, 2006), since history is filled with examples of exotic enemies wreaking havoc on naïve, native communities (Simberloff and Stiling, 1996). Inundative and inoculative releases of natural enemies, collectively referred to as ‘augmentative control’, involve the release of large numbers of enemies, either to bolster existing populations or to provide a short pulse of control without long-term establishment. In contrast, conservation biological control is the attempt to increase the effectiveness of already-present enemies. Methods include the provision of alternative resources for biocontrol agents (e.g. extrafloral or floral nectar, pollen), changes in landscape complexity and the preservation of natural areas beneficial to enemies (Bianchi *et al.*,

2006; Tscharrntke *et al.*, 2007, 2016). Altogether, these various methods of biological control provide significant ecosystem services in both natural and agricultural ecosystems (Losey and Vaughan, 2006; Zhang and Swinton, 2012; Naranjo *et al.*, 2015).

Biological control and predator–prey/parasitoid–host (‘natural enemy’) ecology have a long relationship (Hassell and Varley, 1969; McMurtry *et al.*, 1970; Murdoch *et al.*, 1985). Early theory in natural enemy ecology was heavily influenced by examples of classical biological control, and broader natural enemy ecology has served to inform biocontrol practice. However, biological control has lagged behind natural enemy ecology by not recognising the impact and importance of enemy-risk effects, often referred to as non-consumptive effects (NCEs), fear effects, risk effects, non-lethal effects or trait-mediated effects. Biocontrol typically focuses on direct lethal effects of enemies on pests, whether through consumption or parasitism (which we refer to as consumptive effects or CEs) or through infection. However, natural enemy ecology has long recognised the importance of enemy-risk effects (Abrams *et al.*, 1996; Werner and Anholt, 1996; Schmitz, 1998; Werner and Peacor, 2003). Enemies induce behavioural, physiological, morphological or life-history changes in their prey that can lead to significant changes in individual fitness, population dynamics and community dynamics. Meta-analyses and reviews have noted that even when natural enemies kill relatively few prey or hosts, they can have major

impacts via enemy-risk effects (Preisser *et al.*, 2005; Peckarsky *et al.*, 2008; Preisser and Bolnick, 2008; Schmitz *et al.*, 2008; Sih *et al.*, 2010; Buchanan *et al.*, 2017). While numerous studies have demonstrated major enemy-risk effects in many biological control systems, this knowledge has not been implemented in standard thinking about biocontrol. Several ways that enemy-risk effects connect to biocontrol include understanding: (1) the dynamics of trophic cascades where natural enemies have positive impacts on plants not only by killing pests (CEs), but also by altering pest traits; (2) the role of risk effects in governing interactions in biocontrol systems with multiple enemies, intra-guild predation (IGP) and bottom-up effects; (3) the impacts of enemy-induced pest dispersal on the spatiotemporal ecology of biocontrol; and (4) how effects of natural enemies differ on co-evolved versus naïve prey, as is common for target versus non-target prey respectively. Insights about enemy-risk effects can thus help to better guide agent selection, non-target testing, integrated pest management (IPM) programs and other biocontrol practices. Conversely, biocontrol systems are ideal for the general study of enemy-risk effects, offering opportunities to study risk at multiple scales, across multiple trophic levels, with varying levels of co-evolution, and in systems amenable to experimental manipulation.

We provide a systematic overview of insights gained from integrating enemy-risk effects into the ecology of biocontrol, focusing on management of arthropod pests. We begin with a conceptual overview of current literature on enemy-risk effects, including work outside of biocontrol systems, then review studies of enemy-risk effects in biocontrol and finish by demonstrating and discussing in some detail how a conceptual knowledge of risk effects can inform and improve pest management and biocontrol programs (see Box 1 for a well-studied example).

ENEMY-RISK EFFECTS: A BRIEF CONCEPTUAL OVERVIEW

Many organisms exhibit responses to natural enemies (predators and parasitoids; we frequently use ‘predator/prey’ as a catchall that includes parasitoid/host relationships), including within-generation changes in behaviour (e.g. reduced activity, increased refuge use, increased group size; Lima, 1998), physiology (Hawlena and Schmitz, 2010; Clinchy *et al.*, 2013), morphology (Bourdeau and Johansson, 2012; Hulthén *et al.*, 2014) and life history (Miner *et al.*, 2005; LaManna and Martin, 2016; Relyea *et al.*, 2018). These responses typically have costs in terms of reduced feeding and growth rates and, ultimately, reduced fitness (Kerfoot and Sih, 1987; Stamps, 2007; Orrock *et al.*, 2013) and population growth rates (Creel and Christianson, 2008). Because these responses often involve niche shifts (e.g. in prey diets or habitat use), they also affect prey interactions with other species (Werner and Peacor, 2003). For example, anti-predator responses can alter competition among prey (Werner and Anholt, 1996), increase exposure to other predators (Sih *et al.*, 1998; Fouzai *et al.*, 2019) or to diseases (Duffy *et al.*, 2011; Shang *et al.*, 2019) and alter impacts on their own resources (Schmitz *et al.*, 2004). Notably, if prey exhibit strong, effective anti-enemy responses, predators might actually kill few prey (i.e. have weak consumptive effects, CEs) but instead have

large impacts on prey fitness and prey interactions with the rest of their community (Preisser *et al.*, 2005). These three levels of effect (individual response, impacts on fitness/populations and community effects) are best defined as **enemy-induced trait responses**, **non-consumptive effects** and **trait-mediated indirect effects** (Peacor *et al.*, 2020). Box 2 discusses this terminology in greater detail.

LITERATURE REVIEW OF BIOLOGICAL CONTROL ENEMY-RISK EFFECT STUDIES

We carried out a systematic review of empirical studies on enemy-risk effects in biocontrol systems using combinations of the search terms “biological control”, “biocontrol”, and “pest” with the terms “non-consumptive”, “nonconsumptive”, “non-lethal”, “nonlethal”, “sub-lethal”, “sublethal”, “risk effect*”, “anti-predator”, or “anti-predator.” Studies were included if they were on arthropod pests, investigated some stage of the enemy-risk effect pathway depicted in Fig. 1, and demonstrated some relevance to pest control. Our review of the literature yields several takeaway messages: (1) enemy-risk effects are prevalent in arthropod pest systems, (2) enemy-induced trait shifts can interact with other aspects of agroecosystems, such as plant defences, trap crops and plant pathogen transmission, (3) risk effects produced by predators have been studied more extensively than those produced by parasitoids, (4) the importance of enemy-risk effects on non-target species has received little attention and (5) few studies have examined the consequences of enemy-risk effects for plant damage in the field.

We organised papers in Table 1 according to the ‘level’ of study, ranging from documentation of enemy-induced trait responses to explicit measure of NCEs on pest control and trait-mediated indirect effects on crops (see Supporting Information for expanded table format). This categorisation is not meant to rank the quality or usefulness of studies, but rather to demonstrate where research has been focused and where room for growth remains. Fifty-four per cent of studies (32 of 59) aimed to assess the strength of pest responses, which is a critical step in the inclusion of enemy-risk effects in the design and implementation of biocontrol programs. Many of these studies incorporated other aspects relevant to pest management, such as variation in spatial scale (Lee *et al.*, 2014), ability to transmit plant pathogens (Tholt *et al.*, 2018), interactions with trap cropping (Lee *et al.*, 2011) and plant defence (Thaler *et al.*, 2014). Of the 27 remaining studies, about half documented demographic consequences for pests, and half documented the levels of pest damage. Four studies measured changes in plant damage in the field (Griffin and Thaler, 2006; Thaler and Griffin, 2008; Steffan and Snyder, 2010; Hermann and Thaler, 2018). Only two studies measured the risk effects of enemies on non-target species (Walzer and Schausberger, 2009; Fill *et al.*, 2012); these effects are likely overlooked in many evaluations of host range, as we discuss in the following section.

It can be difficult to scale up enemy-risk effect studies from measuring pest responses to the measures of biocontrol efficacy, including effects on pest population dynamics or crop yield, as these typically require longer timescales and broader

Box 1 Enemy-risk effects and the biological control of the red imported fire ant

The red imported fire ant, *Solenopsis invicta*, was inadvertently introduced from South America into the port city of Mobile, Alabama in the 1930s. Expanding its range across much of the southern United States, it achieved exceptionally high densities (5–10 times greater than in their native range), displacing native ants, damaging agricultural production and creating a sting hazard for anyone active outdoors (Porter and Gilbert, 2004; Oi *et al.*, 2015). After a massive and controversial insecticide-based eradication effort failed, attention turned to classical biological control. Studies in the native range of the ants revealed over 20 species of parasitoid flies in the genus *Pseudacteon* (family Phoridae), most of which appeared to be host specific and thus to be potentially acceptable in terms of low risk of non-target impacts. *Pseudacteon* spp. parasitoids lay eggs in adult worker ants, the resulting parasitoid larvae completing their development in the heads of their host ants, which fall off as the larvae develop (hence their common name: decapitating flies).

Early investigations of *Pseudacteon* spp. in the native ranges of the fire ants concluded, however, that they were poor candidates for effective biological control, because they achieved very low rates of parasitism (Jouvenaz *et al.* 1981). Extensive year-long sampling across multiple sites confirmed that parasitism was indeed rare, with only 0.24% of workers parasitised on average (Calcaterra *et al.*, 2008). Retrospective analyses of the extensive literature on the introductions of parasitoids as classical biological control agents by Hawkins *et al.* (1993) and Hawkins and Cornell (1994) suggested that a threshold for success exists: parasitoids that fail to achieve maximum parasitism rates of >32% in their native ranges, or >33–36% in their introduced ranges, have been unable to produce economically acceptable levels of pest suppression. Because the entire *Pseudacteon* spp. complex exerted a maximum of only 2.81% parasitism in the native range (Calcaterra *et al.*, 2008), the suggestion that these flies would be of ‘dubious value’ for biological control (Jouvenaz *et al.* 1981) was not hard to understand.

However, as argued by Feener and Brown (1992) and Porter and Gilbert (2004), a reliance on parasitism rates alone might lead us to grossly underestimate the potential value of *Pseudacteon* spp. parasitoids as control agents. Earlier studies had shown that phorid parasitoids attacking a different ant, while also generating little parasitism, elicited dramatic anti-predator defences. Ants responded to the presence of flies by fleeing back to the nest or by sheltering from fly attacks in the leaf litter, causing the ants to lose their status as competitive dominants in their interactions with other ants (Feener, 1981). Subsequent studies of *S. invicta* revealed a similar pattern: in response to a fly’s arrival, workers retreated underground, took cover below sticks or pebbles, or adopted stereotypic defensive postures with their sting-bearing gasters raised (Orr *et al.*, 1995; Porter *et al.*, 1995). This eliminated their ability to recruit foragers to food sources, with other ants immediately exploiting the now-available resources. Just a single parasitoid could arrest the foraging activity of hundreds of fire ant workers (Porter *et al.*, 1995). Thus, *S. invicta* display dramatic and costly anti-predator defences, and the non-consumptive effects of phorid flies on fire ants may allow native ants to compete effectively with these invaders.

Thus, recognition of the potential importance of enemy-risk effects of *Pseudacteon* spp. motivated the decision to import these species as classical biological control agents. Six species have been introduced to the United States to date, with different species attacking different subsets of worker ants, based on ant size, time of activity or foraging location (at the nest or at foraging trails; reviewed by Oi *et al.*, 2015). Importantly, host-range testing included assessments not only of parasitism of non-targets, but also the attraction to worker ants and expression of the hovering attacks that elicit defensive responses (Porter and Gilbert, 2004). Whether the enemy-risk effects will prove to be sufficient to control *S. invicta* in its invasive range remains, however, an open question, as *Pseudacteon* spp. continue to build their populations and expand their ranges while monitoring continues (Chen and Fadamiro, 2018; Oi *et al.*, 2019).

spatial scales (Hermann and Landis, 2017). However, when moving from pest–agent interactions to the harvest and sale of a crop, there are many steps where the enemy-risk effects may attenuate (Hamburg and Hassell, 1984; Godfray and Waage, 1991; Collier and Van Steenwyk, 2004; Kaplan *et al.*, 2014). Additionally, there may be many interacting effects on pests and crop yield, ranging from environmental factors to pesticide applications. Due to these complications, enemy-risk effect studies that do not measure outcomes beyond pest responses may not fully capture the relevance of enemy-risk effects in pest management.

Some of the most fruitful areas for further research include (1) separating NCEs and CEs to improve predictions of pest population dynamics (see Box 4), (2) considering enemy-risk effects that include qualitative shifts, such as spatiotemporal location, and how they interact with agricultural practices in ways that differentiate them from CEs, (3) including enemy-

risk effects in assessment of agent efficacy and non-target impacts, (4) expanding taxonomic breadth to include more parasitoids and (5) expanding scales of study to better understand the impacts on crop production. We believe ongoing empirical work would be well served by incorporating theory from the broader study of enemy-risk effects, which would facilitate predictions about when and where risk effects may play an important role in the efficacy of pest management programs.

ENEMY-RISK EFFECTS AND THE EVALUATION OF BIOLOGICAL CONTROL AGENTS

A primary task of biocontrol researchers is evaluating the impact of biological control agents on target and non-target organisms. Evaluations occur during each stage of a biocontrol project, whether the program is classical, augmentative or

Box 2 Categorising enemy-risk effects

The term NCE is frequently used to describe processes at three levels: the enemy-induced trait response (e.g. increased refuge use), the consequences for the individual prey/host (e.g. reduced growth rate) or the consequences at the prey/host population level (e.g. increased emigration). Referring to all three levels as NCEs reduces the important distinctions between them, we advocate for a more explicit framework (Fig. 1), and clearer terminology (also see Peacor *et al.*, 2020). We will use the terms **enemy-risk effect** to refer to the overall process, **enemy-induced trait response** to refer to the mechanism of response, **NCE** to refer to fitness/population consequences and **trait-mediated indirect effect** to refer to effects cascading to trophic levels below the prey/host. A complementary way of conceptualising enemy-risk effects is to take a more phenomenological approach, focusing on the aspects of a pest population: its *per capita* impact, abundance and distribution (box shading in Fig. 1).

Behavioural shifts are a commonly studied trait responses in arthropods, and are generally the most rapid and reversible. Examples include changes in time spent feeding (Thaler and Griffin, 2008; Jandricic *et al.*, 2016; Ingerslew and Finke, 2017), food source (Schmitz *et al.*, 1997), microhabitat and refuge use (Lucas *et al.*, 2000; Lawson-Balagbo *et al.*, 2007; Penfold *et al.*, 2017), oviposition rate (Deas and Hunter, 2013; Hermann and Thaler, 2018), oviposition site selection (Angelon and Petranka, 2002; Vonesh and Blaustein, 2010; Silberbush and Blaustein, 2011), short-distance escape (Tamaki *et al.*, 1970; Nelson, 2007; Fill *et al.*, 2012) and dispersal (Höller *et al.*, 1994; Henry *et al.*, 2010; Welch and Harwood, 2014; Otsuki and Yano, 2014b).

Physiological shifts can be direct responses to risk, but they are often the consequences of behavioural shifts. For example, a reduction in individual growth rate (physiological) is often a result of reduced foraging effort (behavioural). This can make physiological shifts difficult to categorise within the framework shown in Fig. 1. Examples include changes in growth rate (Kaplan *et al.*, 2014), development time (Bellamy and Alto, 2018) and assimilation efficiency (Thaler *et al.*, 2014).

Morphological shifts are generally slower to appear and more difficult to reverse than behavioural or even physiological shifts. They have been less described in terrestrial arthropods, but thoroughly studied in systems such as *Daphnia pulex*, where predator cues trigger production of carapace protrusions that decrease vulnerability to predation (Havel and Dodson, 1984; Tollrian, 1995; Rabus and Laforsch, 2011). **Life-history shifts** frequently occur over a long timescale and are irreversible for an individual prey/host. They include changes in timing of reproduction or metamorphosis (Ims, 1990; Benard, 2004; Relyea, 2007), quality and quantity of offspring produced (Map pes *et al.*, 1997) and production of winged morphs (Sloggett and Weisser, 2002; Kunert and Weisser, 2003).

Trait responses carry costs for individuals, and we can categorise **NCEs** based on these costs. These costs are ultimately tied to individual fitness, including reduced fecundity (Map pes *et al.*, 1997) and reduced survival (Walzer and Schausberger, 2009).

Both responses and consequences at the individual level can cascade to affect the entire prey/host population. Finally, community-level impacts include both **trait-mediated indirect effects**, wherein an NCE reduces the prey population such that they have a smaller effect on a lower trophic level, and **interaction modifications**, wherein a trait response causes an existing interaction with another species to change. As seen in Fig. 1, these community effects can occur via different pathways that may not be captured equally in all studies.

Experiments to evaluate the relative strength of CEs and NCEs typically contrast the total effect of actual predators (CE + NCEs) with the effect of constrained predators (e.g. predators caged or artificially manipulated to prevent use of mouthparts) or predator cues (NCEs only) on prey. A meta-analysis of these experiments found that the importance of NCEs was highly variable, but on average roughly the same magnitude as CEs (Preisser *et al.*, 2005). For biocontrol, trait-mediated indirect effects cascading to the plant may be even more relevant. Enemies frequently have very strong positive effects on plants due to trait shifts by herbivores, even when CEs are relatively small (Schmitz *et al.*, 2004; Creel and Christianson, 2008).

Behavioural ecology theory and experiments suggest that prey typically exhibit stronger trait responses when perceived risk is higher and when the marginal costs of response are lower (Lima, 1998). When perceived risk reflects actual risk, predators that are more dangerous in the absence of prey defences can induce such strong anti-predator responses that they kill fewer prey (but cause stronger NCEs) than less dangerous predators. Thus, predation rate is often not a good measure of predation risk, and therefore not always a good indicator of total effect on prey (CEs + NCEs). Perceived risk, however, is not always proportional to actual risk. Perceived risk depends on not just the type of predator and its attack success, but also on the type and strength of predator cues or prey alarm cues (Kats and Dill, 1998; Stankowich and Blumstein, 2005; Ferrari *et al.*, 2010), on the habitat *per se* (Verdolin, 2006; Thaker *et al.*, 2011) and on prey sensory/cognitive capacities (Kats and Dill, 1998; Ferrari *et al.*, 2010; Bedoya-Perez *et al.*, 2019). Predators that are not very dangerous, but difficult to locate and assess (e.g. ambush predators) can induce strong anti-predator responses and thus strong NCEs (Sih, 1992; Preisser *et al.*, 2007). Prey may even respond to an organism that is incapable of killing them if the cues are sufficiently close to those of a dangerous enemy (Fill *et al.*, 2012). Box 3 discusses how prey perceive risk in more detail and implications for enemy-risk effects and biocontrol.

conservation biocontrol. First, the initial step in most biocontrol programs is to describe, as quantitatively as possible, the natural enemy community associated with a target pest; for invasive species, this may involve describing food webs in both the native and invaded ranges. Second, as part of

classical biological control programs, and in some cases augmentative biological control, candidate agents need to be screened for host/prey specificity to assess the risks of non-target impacts and to identify the most promising agent(s) for mass-rearing and release. Finally, after classical biocontrol

Box 3 Prey perception of risk

A large literature in behavioural and sensory ecology has examined prey perception of danger based on cues that provide information on the levels of enemy risk (Weissburg *et al.*, 2014; Ehlman *et al.*, 2019). Arthropods perceive risk using chemical (both airborne and via direct contact; Dicke and Grostal, 2001; Sitvarin and Rypstra, 2012; Hermann and Thaler, 2014), visual (Gonçalves-Souza *et al.*, 2008), vibratory (Castellanos and Barbosa, 2006), auditory (Skals, 2005) and tactile cues (Castellanos *et al.*, 2011; Okada and Akamine, 2012). Organisms often use multiple cue modalities, which can vary depending on prey perceptual ability and the types of enemies.

A primary source of risk cues is the enemy itself, whether directly as sounds, vibrations, chemical cues or visual presence, or indirectly as chemical footprints, faeces, molts and silk. Organisms can also respond to indicators of risk before they actually detect enemies; for example by responding to 'alarm cues' associated with other prey being attacked, injured or killed (Schoeppner and Relyea, 2005; Vandermoten *et al.*, 2012). Alarm cues can induce a range of responses and can even be shared across species (Agarwala *et al.*, 2003; Goodale and Nieh, 2012). Another cue may be habitat or microhabitat type. If certain habitat types are associated with enemy risk, then risk avoidance may drive habitat selection, regardless of direct cues from enemies or even conspecifics (Lucas *et al.*, 2000).

Cues can vary widely in spatiotemporal extent, affecting different numbers of prey over varying timescales. For example, because chemical cues can spread widely and remain detectable for long periods, they can cause risk effects to persist long after enemies have left an area (Wilson and Leather, 2012; Ninkovic *et al.*, 2013). Theory suggests that because the cost of under-responding to risk (i.e. getting killed) is often much greater than the cost of over-responding (e.g. hiding unnecessarily and losing feeding opportunities), when cues provide imprecise information about the presence (versus absence) of predators, this uncertainty can induce strong enemy-risk effects even when predators are only occasionally present (Sih, 1992). This may be true for many prey facing the risk of attack by ambush predators. In contrast, seeing or coming into physical contact with an enemy is usually a more definitive risk indicator.

The links between cue generation, detection and anti-enemy response are complex, involving multiple steps and interactions. Environmental context can strongly affect both the strength and detection of a cue (e.g. wind may disperse a chemical cue) and the perception of risk upon detection (e.g. perceived risk may be lower if a refuge is nearby). Response to risk can be highly state dependent; a starving organism may be more likely to accept higher risk to avoid starvation, and a larger, faster individual may assess risk differently than a smaller, more vulnerable organism. In some cases, it can take a combination of multiple cues to trigger a response (Gish *et al.*, 2011). Recent theoretical work has suggested that cues indicating risk should be integrated with other cues indicating safety to shape responses (Trimmer *et al.*, 2017; Ehlman *et al.*, 2019), and supporting evidence has emerged from recent studies with desert isopods (Zaguri and Hawlena, 2019).

A key insight from signal detection theory is that all cues are imperfect indicators. Cues can vary in strength; a chemical cue can be diluted or concentrated, a visual cue can be obscured by other objects and an auditory cue can be disrupted by ambient sounds. On top of variance in cue strength, the specificity of cue modalities can vary. The visual cue of a looming shape could come from a dangerous enemy or a harmless passing organism, the chemical and tactile cue of a parasitoid could come from a species that parasitises the pest or another, closely related parasitoid that does not (Fill *et al.*, 2012), and cues that elicit stress and reduce population growth can come from activity of commensal organisms (Jensen and Toft, 2020). The reliability of cues may change with the introduction of novel organisms (Ehlman *et al.*, 2019) or through habituation to the cue. The consistent application of synthetic alarm pheromone may cause decreased sensitivity of aphids to the cue, but this insensitivity may in turn increase CEs by coccinellid predators (de Vos *et al.*, 2010). Finally, synthetic predator kairomones can increase mosquito mortality synergistically with *Bacillus thuringiensis* applications, even when completely decoupled from real predators (Op de Beeck *et al.*, 2016; Delnat *et al.*, 2020). Biocontrol practices might benefit from deeper understanding of pest perception of cues associated with enemy risk.

Marginal costs of enemy-induced trait responses are higher (and prey exhibit weaker trait responses) if prey are energy stressed (hungry), resources or mates are abundant but more accessible only if prey show little anti-predator response, or if prey have high reproductive value (more to lose; Houston *et al.*, 1999; Clark, 1994). For herbivores, the strength of the enemy-risk effect depends on, among other things, plant abundance and quality, herbivore condition and life-history stage (McArthur *et al.*, 2012; Stephan *et al.*, 2017).

The role of enemy-risk effects in community dynamics becomes more complex when we consider multiple enemies and IGP, common occurrences in biocontrol systems. With multiple agents of mortality, enemy-risk effects can often blend into CEs where a trait response to an enemy (e.g. a shift in microhabitat use) increases mortality from another enemy (Sih *et al.*, 1998), environmental stressors (Schmitz *et al.*, 1997) or even pesticides (Janssens and Stoks, 2013). With IGP, predators are also potentially prey, and thus also exhibit enemy-induced trait responses and NCEs. The mix of CEs and NCEs involving multiple species then influences community outcomes including biocontrol efficacy. We discuss this in more detail in a later section.

Many of these predictions about enemy-risk effects assume that prey exhibit adaptive responses to enemies that they have coevolved with. Prey lacking evolutionary (or developmental) history with enemies (or specific enemies) often exhibit much weaker anti-enemy responses and thus suffer heavy mortality (strong CEs) when novel enemies appear (e.g. island prey or prey in fishless ponds; Cox and Lima, 2006; Carthey and Blumstein, 2018). This depends on the cue or functional similarity of new enemies to the prey's familiar enemies (Sih *et al.*, 2010; Carthey and Banks, 2014; Saul and Jeschke, 2015). Given that biocontrol often involves introducing enemies that have a co-evolutionary history with the target pest, but not with non-target organisms, the effect of evolutionary history on CEs versus NCEs is clearly a salient issue that we discuss in more detail below.

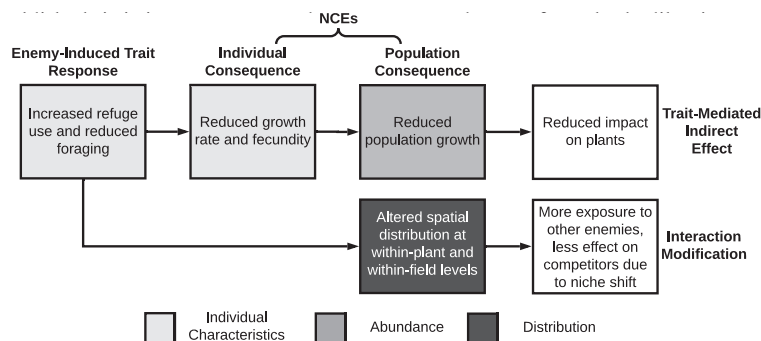


Figure 1 Demonstration of a particular enemy-risk effect fitting in to the broader framework we describe in Box 2. An enemy-risk effect is described by both the stage, beginning with individual response and ending with community effects, as well as by the effects on the abundance, distribution and characteristics of a pest population.

TABLE 1 Table of biocontrol enemy-risk effect studies, organised according to the level of study

'Highest' level of study	Other aspects	Citation
Behavioural/ Physiological/ Morphological Response (32)	None (8)	Angelon and Petranka, (2002), Silberbush <i>et al.</i> (2010), Silberbush and Blaustein, (2011), Warburg <i>et al.</i> (2011), Thaler <i>et al.</i> (2012), Fischhoff <i>et al.</i> (2018), Dupuy and Ramirez, (2019), La-Spina <i>et al.</i> (2019)
	Variation among agents (8)	Pallini <i>et al.</i> (1999), Wuellner <i>et al.</i> (2002), Ramirez <i>et al.</i> (2010), Hoki <i>et al.</i> (2014), Otsuki and Yano, (2014b), Dias <i>et al.</i> (2016), Jacobsen <i>et al.</i> (2016), Staats <i>et al.</i> (2016)
	Variation among pests (1)	Wilson and Leather, (2012)
	Variation among agents and pests (3)	Nelson and Rosenheim, (2006), Ingerslew and Finke, (2017), Francesena <i>et al.</i> (2019)
	Interaction with competition (1)	Stav <i>et al.</i> (2010)
	Variation of cues (2)	Ninkovic <i>et al.</i> (2013), Hermann and Thaler, (2014)
	Variation among agents, pests, cues (1)	Roberts, (2014)
	Interaction with resources (2)	Wasserberg <i>et al.</i> (2013), Silberbush <i>et al.</i> (2014)
	Interaction with plant defence (1)	Thaler <i>et al.</i> (2014)
	Variation of spatial scales (1)	Lee <i>et al.</i> (2014)
	Interaction with trap cropping, variation among agents (1)	Lee <i>et al.</i> (2011)
	Variation in plant variety (1)	Cuny <i>et al.</i> (2019)
	Ability to transmit plant pathogen (1)	Tholt <i>et al.</i> (2018)
	Indirect effects on other pest (1)	Prasad <i>et al.</i> (2018)
Individual Fitness Consequences (3)	None (1)	Matsumoto <i>et al.</i> (2003)
	Variation in agents and cues (1)	Gyuris <i>et al.</i> (2017)
Demographic Consequences (11)	Effects of enemy on survival while infected with pathogen (1)	Ugine and Thaler, (2020)
	None (2)	Nelson, (2007), Xiong <i>et al.</i> (2015)
	Interaction with temperature (1)	Bannerman <i>et al.</i> (2011)
	Variation among agents (1)	Folgarait and Gilber, (1999)
	Variation among agents and pests (1)	Weisser <i>et al.</i> (1999)
	Variation of NCE pathways (1)	Fievet <i>et al.</i> (2008)
	Interaction with plant defence (2)	Kaplan and Thaler, (2012), Kersch-Becker and Thaler, (2015)
	Non-target effects (1)	Fill <i>et al.</i> (2012)
	Multiple-enemy effects (1)	Bilu and Coll, (2007)
	Effects driven by commensal species (1)	Jensen and Toft, (2020)
	None (4)	Snyder and Wise, (2000), Maanak <i>et al.</i> (2013), Jandricic <i>et al.</i> (2016), Rendon <i>et al.</i> (2016)
Plant Damage (13)	Variation among agents (2)	Hlivko and Rypstra, (2003), Hogg <i>et al.</i> (2014)
	Variation among pests and agents (1)	Rypstra and Buddle, (2012)
	Interaction with plant defence (1)	Kaplan and Thaler, (2010)
	Non-target effects, variation among agents (1)	Walzer and Schausberger, (2009)
	In field (4)	Griffin and Thaler, (2006), Thaler and Griffin, (2008), Steffan and Snyder, (2010), Hermann and Thaler, (2018)

it may be important to consider enemy-risk effects. In some cases, even the simple in-quarantine host-range testing protocols using small and simplified microcosms and short exposures to natural enemies can reveal some evidence of enemy-risk effects. For example, host-range tests of candidate parasitoid species may reveal elevated mortality of individual hosts that do not produce parasitoid offspring (e.g. Abram *et al.*, 2016; Bulgarella *et al.*, 2017); in these cases, hosts may die following parasitoid probes without oviposition, or parasitoid oviposition may lead to early mortality of both the host and the parasitoid eggs prior to any consumption of the host. In some cases, such parasitoid-generated host mortality has been found in host species on which parasitoids never successfully produce offspring (Hoddle and Pandey, 2014; Valente *et al.*, 2017), emphasising that parasitism rates alone may not suffice to capture non-target effects (Abram *et al.*, 2019). Depending on response variables measured in target or non-target hosts or prey, including altered movement or microhabitat selection, development rates, feeding behaviour or reproduction, other risk effects could potentially also be detected in a quarantine setting, but current host-range testing generally sidesteps the possible importance of these effects. Like indirect effects, however, many possible enemy-risk effects, including those expressed via longer range movements, are not readily evaluated within a quarantine facility.

More encouragingly, many widely used protocols for assessing the efficacy of biological control measure either target (or non-target) population density as the primary response variables (Table 2), thereby capturing the combined influences of CEs and NCEs. This is particularly true in studies of

conservation biocontrol, which also frequently incorporate larger spatiotemporal scales and whole communities of enemies. Although it may sometimes be of academic interest to separate the roles of CEs and NCEs (but see Box 4), these protocols accomplish the central objective of capturing the full range of pathways through which natural enemies may contribute to herbivore population suppression.

ECO-EVOLUTIONARY EXPERIENCE AND RESPONSES TO BIOLOGICAL CONTROL AGENTS

Recent research on prey responses to exotic enemies emphasises the importance of prey's eco-evolutionary experience (EEE) with enemies (Blumstein, 2006; Cox and Lima, 2006; Sih *et al.*, 2010; Saul and Jeschke, 2015; Trimmer *et al.*, 2017; Carthey and Blumstein, 2018; Ehlman *et al.*, 2019). By 'eco-evolutionary experience' we mean either an evolutionary history, or an earlier ecological (developmental) history that allowed prey to either evolve or learn to cope with a predator. Naïve prey that lack previous experience with a novel predator often respond insufficiently, suffering heavy predation (high CEs). Examples include the devastating impacts of novel predators (humans, other mammals, brown tree snakes) on naïve island prey, or of novel predatory fish on naïve prey in previously fishless lakes (Cox and Lima, 2006). For classical biological control, the expectation is that if the target pest has had an extensive evolutionary history with the imported enemy, it will likely exhibit adaptive responses (and thus NCEs) that reduce CEs. In contrast, non-target prey that have not had previous EEE with the biocontrol agent might exhibit much

Box 4 Consequences of NCEs vs. CEs for prey and predator population dynamics

A central difference between CEs and NCEs is their consequences for natural enemy reproduction (Abram *et al.*, 2019). CEs, on the one hand, generally lead to an increase in natural enemy birth rates: an immature parasitoid develops to the reproductive adult stage by attacking and killing a host, and a predator survives and reproduces by consuming prey. NCEs, on the other hand, do not result in any increase in the natural enemy's population, and if they reduce the victim population through increased mortality or decreased fecundity, they actually shrink the resource pool available to the natural enemy. A natural enemy that induced NCEs only would eventually go extinct, as it would never be able to reproduce. It is worth noting that a generalist enemy may impose strictly NCEs on some of its prey taxa, as long as it is able to consume other species of prey or engage in omnivory. If NCEs are not explicitly accounted for, a gap between high pest mortality and low enemy reproduction may be erroneously attributed to other causes, such as poor assimilation efficiency or natural enemy mortality.

CEs and NCEs may also vary in how their overall magnitudes at the population level are influenced by predator density. A large decrease in the number of predators may lead to a large decrease in consumption of prey, but the small number of predators may still be enough to induce significant NCEs (Carpenter *et al.*, 1987). The strength of NCEs can also be linked to CEs, creating potential feedbacks between the two effect pathways (Weissburg and Beauvais, 2015). Understanding the perception of risk and thresholds prey use to make decisions can help determine how NCE strength may vary with enemy population compared to CE strength (see Box 3 for a more thorough discussion of prey perception and risk management).

The inclusion of enemy-risk effects in models has varying effects on the resulting dynamics, ranging from increased to decreased stability, the appearance of population cycles and even the reversal of predicted trophic cascades (Abrams and Matsuda, 1997; Abrams, 2008; Peckarsky *et al.*, 2008; Larsen, 2012). The classic example of predator-prey dynamics involving lynx and snowshoe hares has discrepancies between observed data and CE-only predictions, but the inclusion of enemy-risk effects can help improve the match between prediction and observation (Hik, 1995; Boonstra *et al.*, 1998). The relative contributions of NCEs and CEs to population dynamics can vary with environmental factors and the spatiotemporal scales of study, so these interactions must be accounted for if possible. Considering enemy-risk effects in population dynamics is not simply the addition of ecological complexity for its own sake, but a way to improve predictions of population modelling.

TABLE 2 Methods used, either singly or in combination, to evaluate the impact of biological control agents on target and non-target organisms

Method	Useful for predators, parasitoids or both	Measures consumptive effects?	Measures non-consumptive effects?
Artificial sentinel prey models (e.g. clay caterpillars) evaluated for removal or marks of attack	Mostly Predators	✓	✗
Live tethered or outplanted sentinel prey/hosts (usually immobile stages, like eggs or pupae; but also confined larval stages)	Both	✓	✗
<i>Post hoc</i> assessment of natural enemy impact via detection of bite-marks or other physical damage to prey	Predators	✓	✗
<i>Post hoc</i> assessment of natural enemy impact via detection of distinctive host remains, host-feeding tubes or damage, remains of developing parasitoids (egg chorions, larval or pupal exuvia, meconia, cocoons), or distinctive parasitoid or host emergence holes	Parasitoids	✓	✗
Dissection of hosts to record parasitoid eggs, larvae or pupae; or rearing of hosts	Parasitoids	✓	✗
Monoclonal antibody-ELISA or DNA-based assays of hosts to detect internally developing parasitoids	Parasitoids	✓	✗
Gut content analyses – detection of prey remains using simple dissections and visual inspection	Predators	✓	✗
Monoclonal antibody-ELISA, immunomarking or DNA-based assays of consumer gut contents	Predators and host-feeding parasitoids	✓	✗
Focal observations of prey/hosts, using human observers or video cameras	Both	✓	Partially*
Field life table construction by repeated sampling of a cohort of developing hosts/prey to quantify survival and rate of development from eggs to adults; often used with immobile hosts/prey	Both	✓	Partially†
Short-term (i.e. too short for prey reproduction) mesocosm assays using hand removal or caging treatments to contrast the effects of natural enemy presence/absence; response variable = prey survival	both	✓	Partially†
Long-term (i.e. long enough to permit substantial prey reproduction) mesocosm assays using hand removal or caging treatments to contrast the effects of natural enemy presence/absence; response variable = prey population size or growth rate	both	✓	✓
Experimental removal of natural enemy populations using selective insecticides; response variable = prey/host population size or growth rate	both	✓	✓
Experimental addition of natural enemy populations by controlling ants that otherwise exclude the nature enemy; response variable = prey/host population size or growth rate	both	✓	✓
Observational field methods comparing natural enemy present vs. absent (e.g. in classical biocontrol settings: pre- vs. post-release, or release site vs. non-release site); response variable = prey/host population size or growth rate‡	both	✓	✓

*Focal observations might reveal some NCEs related to the expression of anti-predator behaviours, although would be unlikely to quantify the costs of such behaviours.

†This method could capture the costs of some NCEs if those costs were expressed through a reduction in developmental survival rates.

‡Purely correlative studies examining associations between densities of predators and prey or hosts and parasitoids are also sometimes reported. But, without additional evidence of a causal link (and support for the direction of causality) such studies are often open to multiple interpretations. Thus, we omit them from the current discussion.

weaker, if any, anti-predator response. If the predator can attack these non-target prey, then the biocontrol agent might prefer and exert strong CE on non-target prey and less consumptive impact on the targeted pest.

Some naïve prey, however, exhibit appropriate responses to novel predators. One key factor is the prey's past history not with the specific novel predator, but with predation pressure in general. Prey that have experienced little predation pressure of any sort tend to be bolder and thus exhibit weaker response to novel predators, as compared to those that have evolved with moderate to heavy predation pressure (Ferrari *et al.*, 2015). Therefore, non-target prey should be particularly vulnerable to novel biocontrol agents if those prey species have evolved with little predation (demonstrated by novel invasive social insects in Hawaii; Wilson *et al.*, 2009; Krushelnycky *et al.*, 2017). Recent

work adds that if prey have experienced persistent high predation risk, then they should also be bold, not cautious. If predators are persistently present, prey cannot hide indefinitely, and should only respond strongly to cues that indicate particularly high impending risk (Trimmer *et al.*, 2017; Ehlman *et al.*, 2019). Additionally, though we focus on arthropod pests, work on invasive plants suggests that invasive species facing no top-down pressure may evolve to devote fewer resources to anti-enemy responses and more to competitive ability (Blossey and Notzold, 1995). This process may be rapidly reversed upon the reintroduction of natural enemies through biological control programs, with invasive species rapidly developing anti-enemy responses that could drastically change the initial CE–NCE ratio (Stastny and Sargent, 2017).

Another key factor in predicting prey response to an introduced biocontrol agent is its similarity to familiar, native predators. Even if non-target prey have never experienced the particular novel predator, the ‘cue similarity’ hypothesis posits that if the introduced predator resembles familiar predators, ‘naïve’ prey are likely to respond (Sih *et al.*, 2010; Saul and Jeschke, 2015). Understanding the sensory/cognitive ecology of how target versus non-target prey perceive risk from biocontrol agents is then key (see Box 3). Even if prey correctly perceive the risk and respond, they can still suffer heavy predation if they show an inappropriate response (e.g. freeze when they should flee) or if their response is ineffective (e.g. they flee but the predator is too fast; Sih *et al.*, 2010; Carthey and Blumstein, 2018). Sih *et al.* (2010) suggested that the effectiveness of naïve prey responses to novel predators should depend on the functional ‘attack mode’ similarity of novel and familiar predators, and on whether prey rely on generalised responses (that work well against a broad range of predators) or specialised ones (that work very well, but only with specific predators). If the novel predator exhibits cue similarity but attack mode dissimilarity to familiar predators, it might induce both strong but ineffective responses that result in high CEs and high NCEs. This scenario could be ideal for suppressing target prey, but disastrous if it applies to non-target prey.

A community-level prediction is that prey should be more likely to respond well to a novel predator if the prey have EEE with a greater diversity of predator archetypes (Blumstein, 2006; Cox and Lima, 2006; Ehlman *et al.*, 2019). If prey have EEE with only one main type of predator, they might exhibit predator-specific defences. In contrast, if either target or non-target prey have EEE with a broad range of predators, they should be more likely to exhibit a diversity of specialised and generalised defences that could be effective against novel biocontrol agents.

Finally, it is possible that contemporary evolution could occur during a long-term biocontrol relationship. While there are examples of evolved resistance to parasitism through enhanced immune responses (Berberet *et al.*, 2003), we know of no cases where arthropod pests evolve anti-enemy responses to biocontrol agents. Hufbauer and Roderick (2005) thoroughly reviewed microevolution in biocontrol, which may provide insights along with those gleaned from evolution of prey responses to invasive predators. Studying this directly in biocontrol systems would require measuring enemy-risk effects over long timescales, which could become a routine part of long-term efficacy studies.

SPATIOTEMPORAL ASPECTS OF ENEMY-RISK EFFECTS

Enemy-risk effects and direct consumptive effects frequently occur on different spatiotemporal scales, with many risk effects occurring over larger areas and longer times than CEs. This means that many studies focusing on CEs lack the scale necessary to capture enemy-risk effects, a topic that has been reviewed elsewhere (Hermann and Landis, 2017) and covered with respect to biological control in Table 2. Beyond expanding the scales of biocontrol enemy-risk effect research in the future, current theory and evidence from the broader

literature may help biocontrol practitioners conceptualise and predict how enemy risk affects pest abundance and interactions with other pest management measures in time and space.

Just as pests act within a ‘landscape of fear’ shaped by enemy cues that are heterogeneous through time and space (Laundré *et al.*, 2001), agricultural landscapes exhibit spatiotemporal variability across multiple scales. Agroecosystems are spatially heterogeneous at the within-plant, between-plant, within-field and between-field scales, especially when farmers use practices such as intercropping or planting hedgerows. They also change throughout time, as many crops undergo a relatively predictable growth pattern, changing in vulnerability to various pests and in their spatial structure. Farmers apply pesticides, irrigate and harvest crops according to schedules, creating temporal patterns of disturbance. By superimposing the temporally variable landscape of risk and the temporally variable agricultural landscape, we may be able to integrate enemy-risk effects into predictions on interactions between biocontrol agents and other IPM strategies. We outline specific ways in which enemy-risk effects in space and time may interact with agricultural practices in the following sections.

Enemy-Risk Effects in Space

At smaller spatial scales, enemy risk may alter microhabitat use as pests seek refuges or move to lower quality parts of the plant (Lee *et al.*, 2011; Paterson *et al.*, 2013; Calvet *et al.*, 2018). Pest fitness may be affected by decreased foraging time due to refuge use or consistent foraging on lower quality resources. Some pests, particularly aphids, will drop off a plant in response to enemy risk (Humphreys and Ruxton, 2019). This behaviour incurs significant costs, as dropping reduces feeding time (Nelson and Rosenheim, 2006; Nelson, 2007). It may also expose pests to a new set of mortality sources, such as ground-dwelling enemies or increased exposure to extreme temperatures. Conversely, increased refuge use due to enemy risk may decrease pesticide exposure (Jallow and Hoy, 2005; Martini *et al.*, 2012). Additionally, shifts in microhabitat use by pests may reduce the reliability of field sampling methods based on the inspections of certain parts of the plant (Southwood and Henderson, 2000).

At larger spatial scales, enemies may influence pest dispersal and habitat selection at within-field and between-field scales. Foraging models, such as the Ideal Free Distribution (IFD), are often used to predict pest movement and abundance within a patchy habitat, but the inclusion of mobile enemies and prey perception of enemies can drastically alter those predictions (Sih *et al.*, 1998; Brown and Kotler, 2004; Fraker and Luttbeg, 2012). Natural enemies can change the threshold at which pests disperse, either increasing dispersal by making patches riskier, or decreasing dispersal by making the movement between patches riskier (Sih and Wooster, 1994; Hamill *et al.*, 2015). Modelling work has shown that this can lead to seemingly counterintuitive results at the metapopulation level; if prey immigration is not affected by enemy presence, but emigration is reduced by it, then prey density can be higher in patches with enemies. Whether or not natural enemy distributions match the distributions of their prey can depend

on mobility of the pests and enemies, the resource needs of each and other density-dependent effects for each population (Winder *et al.*, 2001; Nachman, 2006; Pearce and Zalucki, 2006). In general, understanding how natural enemies affect spatial patterns of pest abundance, such as higher density near field borders, may allow for more precise pest sampling and pesticide spraying, increasing the efficacy and cost effectiveness of these methods. Boxes 5, 6 and 7 all describe particular cases in which enemy-induced dispersal aids or hinders specific pest management goals, including disease transmission, pesticide resistance and trap cropping.

Enemy-Risk Effects in Time

Temporal scaling of enemy-risk effects is complex, since pests can respond to enemies on multiple scales, and consequences of those responses can appear at multiple scales as well. Short-term behavioural changes by pests can lead to two main categories of outcomes: there may be a long-term fitness consequence of short-term changes, or there may be compensation for the short-term effect in the long-term. Other pest responses occur only over a longer timescale, such as changes in life-history events. The goals of a biocontrol program affect the importance of different enemy-risk effects across time.

Short-term behavioural responses may lead to long-term fitness consequences. The accumulation of small fitness losses, such as reduced feeding, mating opportunities or increased energy expenditure, can lead to long-term reductions in population growth. Short-term reductions in feeding rate during a vulnerable life stage may also delay development, which may lead to increased pest mortality due to high CEs (Uesugi, 2015). Furthermore, if the focus of a study is solely on short-term effects, these long-term changes may not be measured. Similarly, if long-term population growth is studied without looking at short-term mechanisms, NCEs might be missed entirely, and the change in growth rate may be attributed solely to CEs (see Hermann and Landis, 2017 for a more in depth discussion of appropriate timescales).

Pests may also compensate for short-term enemy-induced trait responses in the long-term, leading to no NCEs and little impact on the pest population as a whole. If enemy risk is variable, pests that suffer losses in feeding or mating during high-risk periods may be able to compensate during periods of low risk (Houston *et al.*, 1993). Compensatory mortality can also occur in biological control systems, as when density-dependent mortality is replaced by enemy-induced mortality, leading to no overall difference in mortality (Cloutier and Bauduin, 1995; Suh *et al.*, 2000). While this has been demonstrated in CEs, the same could occur for NCEs, where strong effects during one life stage lead to no difference in later population size.

Short-term behavioural shifts alone may have a significant impact on biocontrol outcomes if they can be aligned with periods of crop vulnerability. Pests are often only damaging during a particular crop or pest growth stage (Hokkanen, 1991; Wiedenmann and Smith, 1997). The use of temporal asynchrony between crop and pest stages, achieved through precise timing of crop production, can exploit the narrowness of the crop vulnerability window to reduce pest impact

(Letourneau and Bruggen, 2006). Similarly, if pest pressure can be reduced during that time through enemy-induced behavioural responses, crop damage may be decreased regardless of impacts on pest population growth.

Some trait responses to natural enemies only occur in the long-term, and as such, their consequences only appear in the long-term as well. Pests can shift their life history in response to enemy risk, including increasing developmental rate (Thaler *et al.*, 2012; Elliott *et al.*, 2016; Rendon *et al.*, 2016). Speeding up the development of a vulnerable life stage may reduce overall exposure to natural enemies, but incur costs later on. If shorter development means less time in a crop-damaging life stage (e.g. less time spent as a crop-feeding caterpillar), this may be beneficial to the crop, though it may also increase the rate of pest population growth. Different pests, even within the same order, may allocate risk avoidance behaviour to different life stages, either exhibiting oviposition site selection or juvenile enemy-avoidance behaviour (Stav *et al.*, 2000, 2010; Kiflawi *et al.*, 2003; Brown and Kotler, 2004; Blaustein *et al.*, 2005).

It is important to consider the goals of the biocontrol program when addressing temporal components of enemy-risk effects. In a classical biocontrol program, where the goal is the long-term establishment of the natural enemy, some level of CEs is necessary to sustain the enemy population, even if NCEs are initially very high. However, with an augmentative release, high enemy densities are expected to remain for only a short time. In this case, strong short-term behavioural changes, such as temporarily reduced feeding, or short-term behaviours that lead to long-term fitness consequences may be enough to significantly impact the pest, though the enemy does not establish. For example, if an augmentative release of enemies leads to a large reduction in pest feeding during a week of high crop vulnerability, then long-term impacts on pest population may be of little concern since the damaging behaviour itself was prevented.

ENEMY-RISK EFFECTS WITH MULTIPLE BIOCONTROL AGENTS

Effects of multiple enemies on pests

An extensive literature has established that combinations of multiple predator species can have any of three outcomes on prey suppression: (1) additive, independent effects; (2) greater than additive, or synergistic effects; or (3) less than additive, or disruptive effects (Jonsson *et al.*, 2017). Much of this literature has emphasised consumptive effects as the drivers of these outcomes; thus, synergistic effects may be generated by various forms of complementarity, including complementary use of space (e.g. consuming prey in different microhabitats) or time (e.g. consuming prey during different times of day or seasons), or differences in the host/prey stages or species attacked (Finke and Snyder, 2008; Straub and Snyder, 2008; Northfield *et al.*, 2010), whereas disruptive effects may be generated by IGP or various forms of competitive interference (Vance-Chalcraft *et al.*, 2007).

Enemy-risk effects may, however, also play important roles in shaping non-additive effects of multiple predators (Sih *et al.*, 1998). In particular, when prey defensive responses to

Box 5 Enemy-risk effects and biological control of vectors of plant disease

One of the most damaging ways that insect herbivores affect their host plants is by acting as vectors of plant pathogens. Biological control agents can clearly slow the spread of vectored pathogens by suppressing vector population densities; as both consumptive and non-consumptive effects can depress population growth rates of insect vector populations, both can contribute to this ecosystem service (Landis and Van der Werf, 1997; Moore *et al.*, 2009; Finke, 2012; Long and Finke, 2015; Clark *et al.*, 2019).

However, it is now widely recognised that enemy-risk effects may also have a somewhat counterintuitive and unhelpful influence on the epidemiology of insect-vectored pathogens: in some cases, anti-enemy behaviours may involve increased movement of insect vectors on both local and regional scales, accelerating disease transmission. Thus, the net effect of biological control on disease prevalence can be negative, neutral or positive, depending on the relative magnitudes of consumptive effects and enemy-risk effects and the details of the interactions (Finke, 2012; Crowder *et al.*, 2019). The empirical record has shown that outcomes can depend on the identity of the biocontrol agents, the herbivore and the pathogen (Nelson and Rosenheim, 2006; Belliure *et al.*, 2011; Dumont *et al.*, 2015; Clark *et al.*, 2019); in particular, predator–prey interactions that result in strong prey dispersal in response to predation risk or actual predator attacks often result in short-term increases in disease transmission any time pathogen acquisition and transmission by the vector is not interrupted by the decision to leave a feeding site.

The empirical literature shows that a widespread response of insect vectors of plant disease to predator presence and, especially actual predator attacks is to move away from the attack site via local movements (Weber *et al.*, 2006; Belliure *et al.*, 2011; Hodge *et al.*, 2011; Dáder *et al.*, 2012; Long and Finke, 2015). Aphids, which vector more than half of all plant viruses, release alarm pheromones when attacked by predators, causing clone-mates to run away or, in some cases, to drop from the host plant (Vander moten *et al.*, 2012). Especially in cases where disease transmission requires rapid movement between two host plants (common for viruses that are transmitted via transient contamination of aphid mouthparts), this can accelerate disease transmission.

Predators can also shape longer distance movements via two potentially offsetting processes. First, many herbivores show density-dependent induction of winged morphs or other forms of density-dependent dispersal (Denno and Peterson, 1995; Pepi *et al.*, 2016); in this case, suppression of vector population densities via consumptive or non-consumptive effects has the potential to slow disease spread (Michaud and Belliure, 2001). Second, however, many herbivores also induce winged forms in response to detection of predator cues, including, for aphids, alarm pheromones (Weisser *et al.*, 1999; Mondor *et al.*, 2005; Vander moten *et al.*, 2012), potentially leading to substantial increases in potential for disease transmission over larger spatial scales. Although experimental studies have demonstrated the potential for both of these effects, how this plays out in nature is unknown.

The preponderance of evidence from experimental studies supports the hypothesis that natural enemies accelerate disease transmission in crop plant populations (Long and Finke, 2015). However, because most published studies are quite short duration, they can reveal the immediate effects of increased vector movement, but may underestimate the importance of vector population suppression, which often requires multiple generations of predator–herbivore interactions. Also, because most studies have been performed in laboratory or greenhouse settings, the importance of predators as elicitors of vector movement may be exaggerated relative to its true effect in the field, where many other factors can trigger the same trivial movements (e.g. effects of wind, mechanical disturbances and contacts with other herbivores; Bailey *et al.*, 1995; Nelson and Rosenheim, 2006). Nevertheless, it is clear that biological control can be a double-edged sword when directed against disease vectors.

one predator increase vulnerability to a second predator ('risk enhancement'), the outcome is often predator facilitation and synergistic impacts on prey mortality. This is the case when pea aphids are attacked by combinations of the ladybird beetle *Coccinella septempunctata* and the carabid beetle *Harpalus pennsylvanicus*. Pea aphids drop off plants when threatened by the foliage-foraging *C. septempunctata*, and despite adaptations for re-grasping the plant as they fall (Meresman *et al.*, 2017), some still reach the ground, where they are attacked by the strictly ground-foraging *H. pennsylvanicus* (Losey and Denno, 1998). Similarly, strong risk enhancement is seen when *Tetranychus kanzawai* spider mites are driven out of their web refuges by specialised predatory mites *Neoseiulus womersleyi*, only to fall prey to ants that forage only outside of their webbing (Otsuki and Yano, 2014a).

Enemy-risk effects can also contribute to predator interference. If defensive responses to one predator also confer

protection against a second predator ('risk reduction'), then total predation may be less than expected when both predators are present (Vance-Chalcraft and Soluk, 2005). Alternatively, even when defensive responses appear to conflict, the presence of multiple predators may sometimes improve prey survival. For example, Meadows *et al.* (2017) showed that *Culex* mosquito larvae respond to a complex of mesopredators by diving towards the bottom of water bodies; however, in the presence of top predators, dragonfly larvae, which forage lower in the water column, diving responses by *Culex* are suppressed. Because the diving behaviour is costly, suppression of this response doubled the survival of larval mosquitoes to pupation. Thus, enemy-risk effects often play key roles in shaping the emergent non-additive impacts of multiple predators.

Box 6 Enemy-risk effects, between-plant movement and insecticide resistance management

Predator-induced between-plant movement by herbivores can disrupt schemes that are intended to delay the evolution of resistance to insecticides. A significant recent change in agricultural pest management has been the introduction of crop plants genetically engineered to produce their own insecticidal proteins, derived from the bacterium *Bacillus thuringiensis* ('Bt'; Tab ashnik *et al.*, 2013). Although Bt crops can reduce the need for widespread applications of insecticides, planting a crop that constitutively produces an insecticidal toxin is a recipe for rapid evolution of resistance. To reduce this risk, evolutionary biologists working with regulators and seed companies designed and implemented the 'high dose, refuge' strategy of resistance management. Assuming a monogenic basis for resistance with susceptible allele *S* and resistance-conferring allele *R*, a 'high dose' means that both susceptible homozygotes (genotype *SS*) and heterozygotes (*RS*) are killed on Bt plants. Only the rare resistant homozygotes (*RR*) can survive. The 'refuge' refers to a planted block of non-Bt plants, which are expected to produce relatively large numbers of *SS* individuals. The rare *RR* homozygotes surviving on Bt plants are then expected to mate with one of the abundant *SS* individuals developing in the refuge, and the offspring (genotype *RS*) are subsequently killed on the Bt crops, removing *R* alleles from the population. In this way, the models suggest, resistance can be dramatically delayed (Tab ashnik *et al.*, 2013).

A key problem, however, has been farmer compliance with planting the block of non-Bt refuge plants (Carroll *et al.*, 2012; Garcia *et al.*, 2016). In response to this, seed companies have introduced the notion of a 'refuge in a bag': planting seed is sold as a mixture of Bt and non-Bt seed, which generates a field with spatially interspersed Bt and non-Bt plants. This approach is now being adopted on a global scale (Tab ashnik *et al.*, 2013; Carrière *et al.*, 2016). But if pests move frequently between plants in response to unsuccessful predator attacks, two problems are introduced (Mallet and Porter, 1992; Carroll *et al.*, 2012; Carrière *et al.*, 2016). First, the efficacy of the refuge may be eroded. The refuge in a bag idea relies on the expectation that individual non-Bt plants, surrounded by Bt plants, can still support the development of *SS* individuals. If, however, *SS* individuals move between plants, individuals beginning their development on a non-Bt refuge plant may move to a Bt plant and be killed (Head *et al.*, 2014). Second, the efficacy of the high dose may be eroded. *RS* heterozygotes, which must be killed under the high-dose strategy, can survive, favouring a rapid increase in *R* allele frequency, in either of two ways. First, herbivores may begin their lives on a non-Bt plant, where the highly vulnerable early developmental instars can be passed safely, and then move to Bt plants as later instar larvae, which are often more tolerant of Bt toxins, allowing *RS* individuals to survive (e.g. Head *et al.*, 2014). Second, young *RS* individuals who start their feeding on a Bt plant may be exposed to toxins, but if they move to non-Bt plants before they ingest a lethal dose they may survive. Thus, enemy-risk effects of predators that cause increases in herbivore movement, even on the very small spatial scale required to move between adjacent plants, can have major effects on the evolutionary trajectory of pest populations.

Enemy-risk effects and predator–predator interactions

Insect herbivores face the dual challenge of well-defended host plants and natural enemies (Polis, 1999). It has become increasingly well established that predators must also forage for defended food resources (their prey) under the risk of predation. Enemy risk can stem from specialist higher order enemies (e.g. obligate hyperparasitoids); intraguild predators (competitors that also engage in uni- or bidirectional predation with the focal predator); or cannibalistic conspecifics (Polis, 1981; Polis *et al.*, 1989; Rosenheim *et al.*, 1995; Rosenheim, 1998; Schausberger, 2003; Wise, 2006). And, just as for herbivores, the impacts of higher order predators, intraguild predators and cannibals can be both consumptive and non-consumptive (reviewed by Snyder and Ives, 2008; Frago, 2016). Although enemy-risk effects expressed by predators reacting to other predators are generally viewed as adaptations to reduce their own risk of predation, in most cases it is difficult to separate benefits from reducing the costs of predation versus reducing the costs of competition, or even other costs of high density, such as transmission of diseases that have broad host ranges. Predation risk reduction can, however, be clearly identified as the driver when competition and disease can be ruled out, such as when a primary parasitoid

abandons host patches where it detects pheromones produced by an obligate hyperparasitoid (Höller *et al.*, 1994).

Natural enemies express a broad array of responses to their own predators. A common response is to move away from areas where predator risk is perceived; this may be measured experimentally as shorter patch residency times (Nakashima and Senoo, 2003; Meisner *et al.*, 2011; Frago and Godfray, 2014), reduced oviposition or prey consumption (Agarwala *et al.*, 2003; Magalhães *et al.*, 2004; Meisner *et al.*, 2011; Choh *et al.*, 2015) or outright avoidance of patches where predators or predator-associated cues are detected (Magalhães *et al.*, 2004; Choh *et al.*, 2015; Cotes *et al.*, 2015; Seiter and Schausberger, 2015). Occasionally, parasitoids have been found to increase, rather than decrease, their oviposition activity in host patches with elevated predation risk, likely due to high patch quality even considering predator presence (e.g. Velasco-Hernández *et al.*, 2013). Other common responses include modulation of overall foraging activity (either increased or decreased; Magalhães *et al.*, 2004; Bucher *et al.*, 2014; Walzer *et al.*, 2015; Hentley *et al.*, 2016) and increased use of refuges (Venzon *et al.*, 2000). Developmental effects include increased mortality, delayed (or sometimes accelerated) development, decreased (or sometimes increased) adult body size and shortened pre-oviposition periods for adults (Walzer *et al.*, 2015; Michaud *et al.*, 2016). Compensatory

Box 7 NCEs, trap crops and push-pull systems

Enemy-induced dispersal can create large-scale shifts in spatiotemporal pest distribution, a phenomenon that may be put to use to improve pest management programs. For example, enemies that induce stable, predictable spatiotemporal pest patterns may allow for more precisely targeted pesticide applications. Another potential route is to use enemy-induced dispersal in tandem with trap cropping or push-pull systems. Trap cropping is the use of highly attractive 'trap' plants to lure pests out of the main crop, whereas push-pull systems add a repellent 'push' intercrop to the 'pull' trap crop (Cook *et al.*, 2007). Enemies may be utilised as a second 'push', driving pests out of the main crop and into the trap crop. This effect was studied by Lee *et al.* (2011) who demonstrated an increased level of whitefly dispersal from poinsettia into the cucumber trap crop when natural enemies were present in poinsettia. Whiteflies preferred settling in cucumber over poinsettia, but once settled in poinsettia, they did not tend to move to cucumber. Of the three natural enemies tested, only one increased whitefly dispersal into cucumber, demonstrating the importance of the specific pest and enemy pairing in this scenario.

Predictable and stable movement of pests from the main crop into the trap crop may be more likely with certain combinations of enemy, pest and plant traits. Ideally, enemies would primarily occupy the main crop, making it more dangerous than the trap crop and inducing pest dispersal into the trap crop. This could occur when enemies are habitat specialists with a strong preference for the main crop, due to plant chemical cues (Reddy, 2002), oviposition site preferences (Coll, 1996; Lundgren and Fergen, 2006) or omnivorous needs (Coll, 1996; Kopta *et al.*, 2012). It could also occur if enemies are relatively immobile and can be released solely into the trap crop, which could be possible with inundative or inoculative biological control. Reduction of natural enemy dispersal has been a goal in other contexts, such as releasing wingless ladybirds to prevent them from leaving the focal field (Lommen *et al.*, 2008), and it is possible that similar efforts could work at a within-field scale as well.

Complications may arise if enemies do not primarily occupy the main crop, instead preferring the trap crop, the spaces between crops or matching pest abundance. If the enemy prefers the trap crop, it may have the opposite effect as intended, reducing pest preference for the trap crop and increasing abundance in the main crop. However, if enemies prefer the trap crop, but pests still disperse into it, the trap crop may still be effective, and enemies may then have strong effects on the pests that establish there. If enemies, perhaps ground-dwelling predators, prefer spaces between crops, then they may increase the risk of dispersal in any direction, reducing effectiveness of the trap crop. Finally, if enemies track pest distribution, they may induce dispersal both into and out of the trap crop. This could have a range of effects, depending on the timing of dispersal, cost of dispersal and amount of trap crop. For example, if enemies track pests, forcing them to move back and forth between trap and main crops, but dispersal is very costly, the repeated dispersal may have high fitness costs for the pest. In this case, the lack of unidirectional movement into the trap crop may be more than made up for.

Just as multiple enemies may have additive, synergistic or disruptive effects on pests, so too might natural enemies and trap cropping techniques. Pest management outcomes may be optimised with a careful consideration of pest, enemy and crop combinations, necessitating more research on this topic beyond the promising existing studies.

Arthropod movement between fields is of particular interest when considering field-scale implementation of biocontrol. Under a classical biocontrol program, where the goal is typically for an agent to disperse widely and match the pest range, enemy-induced dispersal may not be a cause for alarm, as the enemy would be predicted to follow its prey. However, if enemy dispersal does not match pest dispersal, certain augmentative biocontrol releases may simply result in the pest problem being pushed from one farm to another. For example, flightless morphs of ladybeetles have been shown to control aphid populations more effectively due to their longer residency time in the crop (Koch, 2003). However, some ladybeetles can induce strong increases in alate production (Kaplan and Thaler, 2012) and aphid dispersal, potentially exporting the pest problem.

Finally, oviposition site selection can be strongly influenced by enemy presence. Many arthropods can detect enemies when making oviposition choices and prefer low-risk sites (Kraus and Vonesh, 2010; Livingston *et al.*, 2017), which may lead to heterogeneous patterns within or between fields. If natural enemies are in fields prior to oviposition, they may even completely deter pest establishment, referred to as biotic resistance (Gruner, 2005; Wanger *et al.*, 2011). This would be more likely to occur with generalist predators, since their populations may be sustained by other species prior to the arrival of the target pest. Conservation biological control, being most focused on supporting native enemy populations, utilises biotic resistance most strongly, though any natural enemy with sufficient density prior to pest establishment may help prevent establishment.

growth has been recorded following the periods of elevated predation risk that slowed growth (Walzer *et al.*, 2015). In many cases, predators respond not to reduce their own risk of predation, but rather to reduce the likelihood that their more vulnerable offspring will be attacked. Transgenerational phenotypic plasticity in response to predation risk has been recorded (Seiter and Schausberger, 2015), and in cases where

predator-prey role reversals are possible, adult predators that witness a heterospecific predator attacking juvenile members of its own species may subsequently be more aggressive in reciprocal attacks on juveniles of the attacking species (Choh *et al.*, 2014). Predators may even invade central locations within colonies of their prey to secure the predation risk-reduction benefits of a selfish herd (Dumont *et al.*, 2015).

What influence these responses have on the overall success of biological control is uncertain. Much of the literature is framed around the idea that anti-enemy behaviour of intraguild prey ameliorate the impact of IGP, potentially facilitating the coexistence of multiple natural enemies, and presumably enhancing the suppression of pest populations. In the short-term, however, anti-predator responses that reduce potential IGP or cannibalism often results in reduced overall consumption of prey (Sih *et al.*, 1998; Vance-Chalcraft *et al.*, 2007). Localised loss of contributions to biological control ascribed to non-consumptive effects of intraguild predators or hyperparasitoids has indeed been reported (Höller *et al.*, 1994; Raymond *et al.*, 2000; Meisner *et al.*, 2011; Frago and Godfray, 2014). But it is easier to record the potential erosion of biocontrol in a focal patch of prey than to document the possibly enhanced biocontrol elsewhere (for one study that investigated but did not find such an outcome, see Frago and Godfray, 2014). Predators that abandon patches of rich host/prey resources due to the presence of other natural enemies presumably weaken biocontrol in those patches, but may strengthen biocontrol elsewhere. Furthermore, consumptive and non-consumptive effects have not been separated in these studies, and doing so while still assessing the overall level of biocontrol success would not be easy: treatments (e.g. mouthpart manipulations) that could be applied to an intraguild predator to eliminate CEs imposed on an intermediate predator would also, unfortunately, eliminate CEs on the shared herbivore prey. Studies of hyperparasitoids could avoid this problem. In some cases the herbivores themselves have been shown to recognise localised enemy-free space generated by hyperparasitoids and to respond with elevated *per capita* reproductive output, perhaps as a consequence of reduced expression of costly anti-predator defences (Van Veen *et al.* 2001). To our knowledge, no one has attempted to measure or model the global effects of fear-mediated redistribution of natural enemies (but see Northfield *et al.* 2017 for a model that could provide a useful framework for such an investigation).

ENEMY-RISK EFFECTS AND BOTTOM-UP EFFECTS

Interactions between top-down and bottom-up pressures have received much attention in broader natural enemy ecology, but specific breakdown of CEs and NCEs has been less common (but see Kaplan and Thaler, 2010, 2012; Thaler *et al.*, 2014). A general framework for understanding the role of plant defences in altering the CE:NCE ratio focuses on the cost-benefit ratio of engaging in anti-enemy behaviour. An enemy-avoidance behaviour that reduces foraging time may have a higher relative cost if food quality is low, leading to a reduction in that behaviour and resulting NCEs. The degree to which plant defences shift the trade-off between foraging and enemy avoidance can depend on whether the pest is a generalist or specialist (Kaplan *et al.*, 2014). Though a reduction in only NCEs would shift the CE:NCE ratio towards consumptive effects, plant defences can also affect the rates of enemy consumption. Generalist enemies may reduce consumption of a particular prey if plant quality or defences reduce prey biomass, prey quality or the chemical cues used by enemies to locate prey (Kersch-Becker *et al.*, 2017).

Bottom-up effects do not always affect anti-enemy behaviours simply by changing the cost-benefit ratio of those behaviours. Additive effects may be possible if pests respond to plant defences and enemy risk in qualitatively different ways. For example, phytohormones have been shown to reduce aphid population growth, while natural enemies induce the production of winged morphs (Kaplan and Thaler, 2012). Here, the pathways operate independently, leading to additive effects of anti-enemy behaviour and plant defence. In other studies, short-distance dispersal and plant defences have been shown to interact strongly, with low plant quality and natural enemies synergistically increasing aphid dispersal (Kersch-Becker and Thaler, 2015). Additionally, the effects of reduced plant quality and NCEs may occur on longer timescales than CEs. Pests can exploit these longer timescales by engaging in compensatory mechanisms to reduce the overall negative effects. Caterpillars facing predation risk can reduce their feeding rate but temporarily increase conversion efficiency to maintain a normal growth rate (Thaler *et al.*, 2012). However, this cannot continue forever and may be dependent on the threat duration (Kaplan *et al.*, 2014).

Finally, many biocontrol agents are omnivorous, meaning plant defences may affect their fitness directly. If high-quality plants increase omnivorous enemy populations, consumption of prey may increase. However, high-quality plants may also reduce the omnivore's need to forage for prey, reducing *per capita* consumptive rates and NCEs. The interactions between plant defences and natural enemies are numerous, including risk effect pathways and others not discussed here, which have been more thoroughly reviewed elsewhere (Pappas *et al.*, 2017). Due to these complexities, studies aiming to assess enemy-risk effects in the field should consider what interactions with bottom-up effects may occur.

CONCLUSION

The study of enemy-risk effects has advanced greatly in the past two decades, developing into a more fully realised field, incorporating theoretical frameworks, many experimental methods and even predictive models. However, the field of biological control is still catching up to broader natural enemy ecology, and the incorporation of enemy-risk effects into the biocontrol framework is still in its infancy. There is a significant body of research documenting the importance of risk effects in biocontrol systems, but there is much room to grow beyond this. We have outlined several areas in which risk effect literature may provide insight into biocontrol practice, and hope that further studies will investigate specific interactions between enemy-risk effects and IPM programs more thoroughly.

Community ecologists likewise can find, in biological control systems, rich examples where the consequences of risk effects play out in well-characterised predator-prey systems, including both coevolved versus novel predator-prey associations. Agricultural systems provide ideal settings for examining both the shorter- and the longer term consequences of risk effects, on both smaller and larger spatial scales. Opportunities exist to examine how risk effects shape trophic cascades, the distributions of prey populations in space and even microevolutionary responses to plant defensive traits.

One of the most crucial aspects of the merging of the fields will be broadly considering biocontrol of arthropods as an inherently behavioural issue. A focus on preventing unwanted and damaging pest behaviour, whether through killing pests or changing their behaviour, broadens the scope of interactions that may be utilised in biological control. The historical focus on population density is no longer sufficient in light of research demonstrating the importance of enemy-risk effects and how they can cascade to the level of plants.

Studies of risk effects in biocontrol systems should also include more holistic studies of the numerous interactions, either synergistic or antagonistic, between pest behaviour and broader IPM practices. Studies in this area can simultaneously investigate core ecological concepts and provide more concrete suggestions for biocontrol practitioners.

Finally, we recognise that it may not be feasible to investigate all possible enemy-risk effects in a given agroecosystem when attempting to predict the effects of a biocontrol agent, which is why we propose the incorporation of theory and predictive models from risk effect research into biocontrol decision-making processes. By considering the evolutionary history of the pest, bottom-up effects of the crop and spatiotemporal dynamics of the agroecosystem, pest management programs may be able to predict the relative importance of various types of risk effects and how they may interact with management practices. Just as other detailed aspects of pest and agent biology are incorporated into management decisions, we advocate for the inclusion of enemy-risk effect knowledge as well.

ACKNOWLEDGEMENTS

We acknowledge Sara Hermann, Paul Abram and Lea Pollock for their thoughtful comments on drafts of the manuscript and members of the Rosenheim Lab for insightful discussions on various topics covered in the manuscript. MCM was supported by a USDA NIFA Predoctoral Fellowship (Award 2019-67011-29710) during stages of writing the manuscript. We dedicate this paper in the memory of Leon Blaustein, an important contributor to the field of enemy risk ecology and former UC Davis student, who passed away during the preparation of this manuscript.

AUTHORSHIP

All the authors discussed ideas and structure, wrote sections of the manuscript, reviewed literature and contributed substantially to revisions.

PEER REVIEW

The peer review history for this article is available at <https://publons.com/publon/10.1111/ele.13601>.

DATA AVAILABILITY STATEMENT

No original data were used in the manuscript, and all search terms and articles from the literature review are described and cited.

REFERENCES

- Abram, P.K., Brodeur, J., Burte, V. & Boivin, G. (2016). Parasitoid-induced host egg abortion: An underappreciated component of biological control services provided by egg parasitoids. *Biol. Control*, 98, 52–60.
- Abram, P.K., Brodeur, J., Urbaneja, A. & Tena, A. (2019). Nonreproductive effects of insect parasitoids on their hosts. *Annu. Rev. Entomol.*, 64, 259–276.
- Abrams, P.A. (2008). Measuring the population-level consequences of predator-induced prey movement. *Evol. Ecol. Res.*, 10, 333–350.
- Abrams, P.A. & Matsuda, H. (1997). Prey adaptation as a cause of predator-prey cycles. *Evolution*, 51, 10.
- Abrams, P.A., Menge, B.A., Mittelbach, G.G., Spiller, D.A. & Yodzis, P. (1996). The role of indirect effects in food webs. In: *Food Webs* (eds Polis, G.A. & Winemiller, K.O.). Springer, Boston, MA, pp. 371–395.
- Agarwala, B.K., Yasuda, H. & Kajita, Y. (2003). Effect of conspecific and heterospecific feces on foraging and oviposition of two predatory ladybirds: role of fecal cues in predator avoidance. *J. Chem. Ecol.*, 29, 357–376.
- Angelon, K.I.M.A. & Petranka, J.W. (2002). Chemicals of predatory mosquitofish (*Gambusia affinis*) influence selection of oviposition sites by *Culex* mosquitoes. *J. Chem. Ecol.* 28, 797–807.
- Bailey, S.M., Irwin, M.E., Kampmeier, G.E., Eastman, C.E. & Hewings, A.D. (1995). Physical and biological perturbations: their effect on the movement of apterous *Rhopalosiphum padi* (Homoptera: Aphididae) and localized spread of barley yellow dwarf virus. *Environ. Entomol.*, 24, 24–33.
- Bannerman, J.A., Gillespie, D.R. & Roitberg, B.D. (2011). The impacts of extreme and fluctuating temperatures on trait-mediated indirect aphid-parasitoid interactions. *Ecol. Entomol.*, 36, 490–498.
- Barratt, B.I.P., Howarth, F.G., Withers, T.M., Kean, J.M. & Ridley, G.S. (2010). Progress in risk assessment for classical biological control. *Biol. Control*, 52, 245–254.
- Bedoya-Perez, M.A., Smith, K.L., Kevin, R.C., Luo, J.L., Crowther, M.S. & McGregor, I.S. (2019). Parameters that affect fear responses in rodents and how to use them for management. *Front. Ecol. Evol.*, 7, 136.
- Bellamy, S.K. & Alto, B.W. (2018). Mosquito responses to trait- and density-mediated interactions of predation. *Oecologia*, 187, 233–243.
- Belliure, B., Amorós-Jiménez, R., Fereres, A. & Marcos-García, M.Á. (2011). Antipredator behaviour of *Myzus persicae* affects transmission efficiency of Broad bean wilt virus 1. *Virus Res.*, 159, 206–214.
- Benard, M.F. (2004). Predator-induced phenotypic plasticity in organisms with complex life histories. *Annu. Rev. Ecol. Syst.*, 35, 651–673.
- Berberet, R.C., Zarrabi, A.A., Payton, M.E. & Bisges, A.D. (2003). Reduction in Effective Parasitism of *Hypera postica* (Coleoptera: Curculionidae) by *Bathyplectes curculionis* (Hymenoptera: Ichneumonidae) Due to Encapsulation. *Environ. Entomol.*, 32, 1123–1130.
- Bianchi, F.J.J., Booij, C.J.H. & Tscharntke, T. (2006). Sustainable pest regulation in agricultural landscapes: a review on landscape composition, biodiversity and natural pest control. *Proc. Biol. Sci.*, 273, 1715–1727.
- Babendreier, D., Bigler, F. & Kuhlmann, U. (2006). Current status and constraints in the assessment of non-target effects. *Environmental impact of invertebrates for biological control of arthropods: methods and risk assessment* (eds Babendreier, D., Bigler, F. & Kuhlmann, U.). CABI Publishing, Cambridge, MA.
- Bilu, E. & Coll, M. (2007). The importance of intraguild interactions to the combined effect of a parasitoid and a predator on aphid population suppression. *Biocontrol*, 52, 753–763.
- Blaustein, L., Blaustein, J. & Chase, J. (2005). Chemical detection of the predator *Notonecta irrorata* by ovipositing *Culex* mosquitoes. *J. Vector Ecol.*, 30, 3.
- Blossey, B. & Notzold, R. (1995). Evolution of increased competitive ability in invasive nonindigenous plants: A hypothesis. *J. Ecol.*, 83, 887.
- Blumstein, D.T. (2006). The multipredator hypothesis and the evolutionary persistence of antipredator behavior. *Ethology*, 112, 209–217.

- Boonstra, R., Hik, D., Singleton, G.R. & Tinnikov, A. (1998). The impact of predator-induced stress on the snowshoe hare cycle. *Ecol. Monogr.*, 68, 371–394.
- Bourdeau, P.E. & Johansson, F. (2012). Predator-induced morphological defences as by-products of prey behaviour: A review and prospectus. *Oikos*, 121, 1175–1190.
- Brown, J.S. & Kotler, B.P. (2004). Hazardous duty pay and the foraging cost of predation. *Ecol. Lett.*, 7, 999–1014.
- Buchanan, A.L., Hermann, S.L., Lund, M., & Szendrei, Z. (2017). A meta-analysis of non-consumptive predator effects in arthropods: the influence of organismal and environmental characteristics. *Oikos*, 126, 1233–1240. <https://doi.org/10.1111/oik.04384>
- Bucher, R., Binz, H., Menzel, F. & Entling, M.H. (2014). Effects of spider chemotactile cues on arthropod behavior. *J. Insect Behav.*, 27, 567–580.
- Bulgarella, M., Quiroga, M.A., Boulton, R.A., Ramírez, I.E., Moon, R.D., Causton, C.E. *et al.* (2017). Life cycle and host specificity of the parasitoid *Conura annulifera* (Hymenoptera: Chalcididae), a potential biological control agent of *Philornis downsi* (Diptera: Muscidae) in the Galápagos Islands. *Ann. Entomol. Soc. Am.*, 110, 317–328.
- Calcaterra, L.A., Delgado, A. & Tsutsui, N.D. (2008). Activity patterns and parasitism rates of fire ant-decapitating flies (Diptera: Phoridae: *Pseudacteon* spp.) in their native Argentina. *Ann. Entomol. Soc. Am.*, 101, 539–550.
- Calvet, É.C., Lima, D.B., Melo, J.W.S. & Gondim, M.G.C. (2018). Chemosensory cues of predators and competitors influence search for refuge in fruit by the coconut mite *Aceria guerrerensis*. *Exp. Appl. Acarol.*, 74, 249–259.
- Carpenter, S.R., Kitchell, J.F., Hodgson, J.R., Cochran, P.A., Elser, J.J., Elser, M.M. *et al.* (1987). Regulation of lake primary productivity by food web structure. *Ecology*, 68, 1863–1876.
- Carrière, Y., Fabrick, J.A. & Tabashnik, B.E. (2016). Can pyramids and seed mixtures delay resistance to Bt crops? *Trends Biotechnol.*, 34, 291–302.
- Carroll, M.W., Head, G. & Caprio, M. (2012). When and where a seed mix refuge makes sense for managing insect resistance to Bt plants. *Crop Prot.*, 38, 74–79.
- Carthey, A.J. & Blumstein, D.T. (2018). Predicting predator recognition in a changing world. *Trends Ecol. Evol.*, 33, 106–115.
- Carthey, A.J.R. & Banks, P.B. (2014). Naïveté in novel ecological interactions: lessons from theory and experimental evidence. *Biol. Rev. Camb. Philos. Soc.*, 89, 932–949.
- Castellanos, I. & Barbosa, P. (2006). Evaluation of predation risk by a caterpillar using substrate-borne vibrations. *Anim. Behav.*, 72, 461–469.
- Castellanos, I., Barbosa, P., Zuria, I., Tammaru, T. & Christman, M.C. (2011). Contact with caterpillar hairs triggers predator-specific defensive responses. *Behav. Ecol.*, 22, 1020–1025.
- Chen, L. & Fadamiro, H.Y. (2018). Pseudacteon phorid flies: Host specificity and impacts on solenopsis fire ants. *Annu. Rev. Entomol.*, 63, 47–67.
- Choh, Y., Sabelis, M.W. & Janssen, A. (2015). Distribution and oviposition site selection by predatory mites in the presence of intraguild predators. *Exp. Appl. Acarol.*, 67, 477–491.
- Choh, Y., Takabayashi, J., Sabelis, M.W. & Janssen, A. (2014). Witnessing predation can affect strength of counterattack in phytoseiids with ontogenetic predator-prey role reversal. *Anim. Behav.*, 93, 9–13.
- Clark, C.W. (1994). Antipredator behavior and the asset-protection principle. *Behav. Ecol.*, 5, 159–170.
- Clark, R.E., Basu, S., Lee, B.W. & Crowder, D.W. (2019). Tri-trophic interactions mediate the spread of a vector-borne plant pathogen. *Ecology*, 100, 1–8.
- Clinchy, M., Sheriff, M.J. & Zanette, L.Y. (2013). Predator-induced stress and the ecology of fear. *Funct. Ecol.*, 27, 56–65.
- Cloutier, C. & Bauduin, F. (1995). Biological control of the colorado potato beetle *leptinotarsa decemlineata* (Coleoptera: Chrysomelidae) In Quebec By Augmentative Releases Of The Two-spotted Stinkbug *Perillus bioculatus* (Hemiptera: Pentatomidae). *Can. Entomol.*, 127, 195–212.
- Coll, M. (1996). Feeding and ovipositing on plants by an omnivorous insect predator. *Oecologia*, 105, 214–220.
- Collier, T. & Van Steenwyk, R. (2004). A critical evaluation of augmentative biological control. *Biol. Control*, 31, 245–256.
- Cook, S.M., Khan, Z.R., Pickett, J.A. (2007). The use of push-pull strategies in integrated pest management. *Annu. Rev. Entomol.*, 52, 375–400.
- Cotes, B., Rännbäck, L.-M., Björkman, M., Norli, H.R., Meyling, N.V., Rämert, B. *et al.* (2015). Habitat selection of a parasitoid mediated by volatiles informing on host and intraguild predator densities. *Oecologia*, 179, 151–162.
- Cox, J.G. & Lima, S.L. (2006). Naiveté and an aquatic-terrestrial dichotomy in the effects of introduced predators. *Trends Ecol. Evol.*, 21, 674–680.
- Creel, S. & Christianson, D. (2008). Relationships between direct predation and risk effects. *Trends Ecol. Evol.*, 23, 194–201.
- Crowder, D.W., Li, J., Borer, E.T., Finke, D.L., Sharon, R., *et al.* (2019). Species interactions affect the spread of vector-borne plant pathogens independent of transmission mode. *Ecology*, 100, 1–10. <https://doi.org/10.1002/ecy.2782>
- Cuny, M.A.C., Trainee, J., Bustos-Segura, C. & Benrey, B. (2019). Host density and parasitoid presence interact and shape the outcome of a tritrophic interaction on seeds of wild lima bean. *Sci. Rep.*, 9, <https://doi.org/10.1038/s41598-019-55143-5>
- Däder, B., Moreno, A., Viñuela, E. & Fereres, A. (2012). Spatio-temporal dynamics of viruses are differentially affected by parasitoids depending on the mode of transmission. *Viruses*, 4, 3069–3089.
- Deas, J.B. & Hunter, M.S. (2013). Delay, avoidance and protection in oviposition behaviour in response to fine-scale variation in egg parasitism risk. *Anim. Behav.*, 86, 933–940.
- Delnat, V., Janssens, L. & Stoks, R. (2020). Effects of predator cues and pesticide resistance on the toxicity of a (bio)pesticide mixture. *Pest Manag. Sci.*, 76, 1448–1455.
- Denno, R.F. & Peterson, M.A. (1995). Density-dependent dispersal and its consequences for population dynamics. *Population Dynamics: New Approaches and Synthesis* (eds Cappuccino, N. & Price, P.W.). Academic Press, San Diego, CA, pp.113–130.
- Dias, C.R., Bernardo, A.M.G., Mencialha, J., Freitas, C.W.C., Sarmento, R.A., Pallini, A. *et al.* (2016). Antipredator behaviours of a spider mite in response to cues of dangerous and harmless predators. *Exp. Appl. Acarol.*, 69, 263–276.
- Dicke, M. & Grostal, P. (2001). Chemical detection of natural enemies by arthropods: An ecological perspective. *Annu. Rev. Ecol. Syst.*, 32, 1–23.
- Duffy, M.A., Housley, J.M., Penczykowski, R.M., Caceres, C.E. & Hall, S.R. (2011). Unhealthy herds: indirect effects of predators enhance two drivers of disease spread. *Funct. Ecol.*, 25, 945–953.
- Dumont, F., Lucas, E. & Brodeur, J. (2015). Do furtive predators benefit from a selfish herd effect by living within their prey colony? *Behav. Ecol. Sociobiol.*, 69, 971–976.
- Dupuy, M.M. & Ramirez, R.A. (2019). Consumptive and non-consumptive effects of predatory arthropods on billbug (Coleoptera: Dryophthoridae) pests in turfgrass. *Biol. Control*, 129, 136–147.
- Ehlman, S.M., Trimmer, P.C. & Sih, A. (2019). Prey responses to exotic predators: Effects of old risks and new cues. *Am. Nat.*, 193, 575–587.
- Eilenberg, J., Hajek, A. & Lomer, C. (2001). Suggestions for unifying the terminology in biological control. *Biocontrol*, 46, 387–400.
- Elliott, K.H., Betini, G.S., Dworkin, I. & Norris, D.R. (2016). Experimental evidence for within- and cross-seasonal effects of fear on survival and reproduction. *J. Anim. Ecol.*, 85, 507–515.
- Feener, D.H. (1981). Competition between ant species: outcome controlled by parasitic flies. *Science*, 214, 815–817.
- Feener, D.H. Jr. & Brown, B.V. (1992). Reduced foraging of *Solenopsis geminata* (Hymenoptera: Formicidae) in the presence of parasitic *Pseudacteon* spp. (Diptera: Phoridae). *Ann. Entomol. Soc. Am.*, 85, 80–84.
- Ferrari, M.C., Wisenden, B.D. & Chivers, D.P. (2010). Chemical ecology of predator-prey interactions in aquatic ecosystems: a review and prospectus. *Can. J. Zool.*, 88, 698–724.

- Ferrari, M.C.O., McCormick, M.I., Meekan, M.G. & Chivers, D.P. (2015). Background level of risk and the survival of predator-naive prey: can neophobia compensate for predator naivety in juvenile coral reef fishes? *Proc. R. Soc. B Biol. Sci.*, 282, 20142197.
- Fievet, V., Lhomme, P. & Outreman, Y. (2008). Predation risk cues associated with killed conspecifics affect the behavior and reproduction of prey animals. *Oikos*, 117, 1380–1385.
- Fill, A., Long, E.Y. & Finke, D.L. (2012). Non-consumptive effects of a natural enemy on a non-prey herbivore population. *Ecol. Entomol.*, 37, 43–50.
- Finke, D.L. (2012). Contrasting the consumptive and non-consumptive cascading effects of natural enemies on vector-borne pathogens. *Entomol. Exp. Appl.*, 144, 45–55.
- Finke, D.L. & Snyder, W.E. (2008). Niche partitioning increases resource exploitation by diverse communities. *Science*, 321, 1488–1490.
- Fischhoff, I.R., Burtis, J.C., Keesing, F. & Ostfeld, R.S. (2018). Tritrophic interactions between a fungal pathogen, a spider predator, and the blacklegged tick. *Ecol. Evol.*, 8, 7824–7834.
- Folgarait, P.J. & Gilber, L.E. (1999). Phorid parasitoids affect foraging activity of *Solenopsis richteri* under different availability of food in Argentina. *Ecol. Ent.*, 24, 163–173.
- Fouzai, N., Opdal, A.F., Jørgensen, C. & Fiksen, Ø. (2019). Dying from the lesser of three evils: facilitation and non-consumptive effects emerge in a model with multiple predators. *Oikos*, 128, 1307–1317.
- Frago, E. (2016). Interactions between parasitoids and higher order natural enemies: intraguild predation and hyperparasitoids. *Curr. Opin. Insect Sci.*, 14, 81–86.
- Frago, E. & Godfray, H.C.J. (2014). Avoidance of intraguild predation leads to a long-term positive trait-mediated indirect effect in an insect community. *Oecologia*, 174, 943–952.
- Fraker, M.E. & Luttbeg, B. (2012). Predator–prey space use and the spatial distribution of predation events. *Behaviour*, 149, 555–574.
- Francesena, N., Rocca, M., Rizzo, E., Arneodo, J.D. & Greco, N.M. (2019). Potential of predatory Neotropical ladybirds and minute pirate bug on strawberry aphid. *Anais da Academia Brasileira de Ciências*, 91, 1–11.
- Furlong, M.J. (2015). Knowing your enemies: integrating molecular and ecological methods to assess the impact of arthropod predators on crop pests. *Insect Sci.*, 22, 6–19.
- García, A.G., Ferreira, C.P., Cónsoli, F.L. & Godoy, W.A. (2016). Predicting evolution of insect resistance to transgenic crops in within-field refuge configurations, based on larval movement. *Ecol. Complex.*, 28, 94–103.
- Gish, M., Dafni, A. & Inbar, M. (2011). Avoiding incidental predation by mammalian herbivores: accurate detection and efficient response in aphids. *Naturwissenschaften*, 98, 731–738.
- Godfray, H.C.J. & Waage, J.K. (1991). Predictive modelling in biological control: The mango mealy bug (*Rastrococcus invadens*) and its parasitoids. *J. Appl. Ecol.*, 28, 434.
- Gonçalves-Souza, T., Omena, P.M., Souza, J.C. & Romero, G.Q. (2008). Trait-mediated effects on flowers: artificial spiders deceive pollinators and decrease plant fitness. *Ecology*, 89, 2407–2413.
- Goodale, E. & Nieh, J.C. (2012). Public use of olfactory information associated with predation in two species of social bees. *Anim. Behav.*, 84, 919–924.
- Griffin, C.A.M. & Thaler, J.S. (2006). Insect predators affect plant resistance via density- and trait-mediated indirect interactions. *Ecol. Lett.*, 9, 335–343.
- Gruner, D.S. (2005). Biotic resistance to an invasive spider conferred by generalist insectivorous birds on Hawai'i Island. *Biol. Invasions*, 7, 541–546.
- Gyuris, E., Szép, E., Kontschán, J., Hettyey, A. & Tóth, Z. (2017). Behavioural responses of two-spotted spider mites induced by predator-borne and prey-borne cues. *Behav. Processes*, 144, 100–106.
- Hájek, A.E., Hurlley, B.P., Kenis, M., Garnas, J.R., Bush, S.J., Wingfield, M.J. *et al.* (2016). Exotic biological control agents: a solution or contribution to arthropod invasions? *Biol. Invasions*, 18, 953–969.
- Hamburg, H.V. & Hassell, M.P. (1984). Density dependence and the augmentative release of egg parasitoids against graminaceous stalk borers. *Ecol. Entomol.*, 9, 101–108.
- Hammill, E., Fitzjohn, R.G. & Srivastava, D.S. (2015). Conspecific density modulates the effect of predation on dispersal rates. *Oecologia*, 178, 1149–1158.
- Hassell, M.P. & Varley, G.C. (1969). New inductive population model for insect parasites and its bearing on biological control. *Nature*, 223, 1133–1137.
- Havel, J.E. & Dodson, S.I. (1984). Chaoborus predation on typical and spined morphs of *Daphnia pulex*: Behavioral observations. *Limnol. Oceanogr.*, 29, 487–494.
- Hawkins, B.A. & Cornell, H.V. (1994). Maximum parasitism rates and successful biological control. *Science*, 266, 1886–1887.
- Hawkins, B.A., Thomas, M.B. & Hochberg, M.E. (1993). Refuge theory and biological control. *Science*, 262, 1429–1432.
- Hawlena, D. & Schmitz, O.J. (2010). Physiological stress as a fundamental mechanism linking predation to ecosystem functioning. *Am. Nat.*, 176, 537–556.
- Head, G., Campbell, L.A., Carroll, M., Clark, T., Galvan, T., Hendrix, W.M. *et al.* (2014). Movement and survival of corn rootworm in seed mixtures of SmartStax® insect-protected corn. *Crop Prot.*, 58, 14–24.
- Heimpel, G.E. & Mills, N.J. (2017). *Biological Control: Ecology and Applications*. Cambridge University Press, Cambridge.
- Henry, L.M., Bannerman, J.A., Gillespie, D.R. & Roitberg, B.D. (2010). Predator identity and the nature and strength of food web interactions. *J. Anim. Ecol.*, 79, 1164–1171.
- Hentley, W.T., Vanbergen, A.J., Beckerman, A.P., Brien, M.N., Hails, R.S., Jones, T.H. *et al.* (2016). Antagonistic interactions between an invasive alien and a native coccinellid species may promote coexistence. *J. Anim. Ecol.*, 85, 1087–1097.
- Hermann, S.L. & Landis, D.A. (2017). Scaling up our understanding of non-consumptive effects in insect systems. *Curr. Opin. Insect Sci.*, 20, 54–60.
- Hermann, S.L. & Thaler, J.S. (2014). Prey perception of predation risk: volatile chemical cues mediate non-consumptive effects of a predator on a herbivorous insect. *Oecologia*, 176, 669–676.
- Hermann, S.L. & Thaler, J.S. (2018). The effect of predator presence on the behavioral sequence from host selection to reproduction in an invulnerable stage of insect prey. *Oecologia*, 188, 945–952.
- Hik, D. (1995). Does risk of predation influence population dynamics? Evidence from the cyclic decline of snowshoe hares. *Wildl. Res.*, 22, 115–129.
- Hlivko, J.T. & Rypstra, A.L. (2003). Spiders reduce herbivory: Nonlethal effects of spiders on the consumption of soybean leaves by beetle pests. *Ann. Entomol. Soc. Am.*, 96, 914–919.
- Hodde, M.S. & Pandey, R. (2014). Host range testing of *Tamarixia radiata* (Hymenoptera: Eulophidae) sourced from the Punjab of Pakistan for classical biological control of *Diaphorina citri* (Hemiptera: Liviidae: Euphyllurinae: Diaphorini) in California. *J. Econ. Entomol.*, 107, 125–136.
- Hodge, S., Hardie, J. & Powell, G. (2011). Parasitoids aid dispersal of a nonpersistently transmitted plant virus by disturbing the aphid vector. *Agric. For. Entomol.*, 13, 83–88.
- Hogg, B.N., Wang, X., Mills, N.J. & Daane, K.M. (2014). Resident spiders as predators of the recently introduced light brown apple moth, *Epiphyas postvittana*. *Entomol. Exp. Appl.*, 151, 65–74.
- Hoki, E., Losey, J. & Ugine, T.A. (2014). Comparing the consumptive and non-consumptive effects of a native and introduced lady beetle on pea aphids (*Acyrtosiphon pisum*). *Biol. CONTROL*, 70, 78–84.
- Hokkanen, H.M.T. (1991). Trap cropping in pest management. *Annu. Rev. Entomol.*, 36, 20.
- Höller, C., Micha, S.G., Schulz, S., Francke, W. & Pickett, J.A. (1994). Enemy-induced dispersal in a parasitic wasp. *Experientia*, 50, 182–185.
- Houston, A.I., McNamara, J.M. & Hutchinson, J.M.C. (1993). General results concerning the trade-off between gaining energy and avoiding predation. *Philos. Trans. R. Soc. B-Biol. Sci.*, 341, 375–397.

- Hufbauer, R.A. & Roderick, G.K. (2005). Microevolution in biological control: Mechanisms, patterns, and processes. *Biol. Control*, 35, 227–239.
- Hulthén, K., Chapman, B.B., Nilsson, P.A., Hollander, J. & Brönmark, C. (2014). Express yourself: bold individuals induce enhanced morphological defences. *Proc. R. Soc. B Biol. Sci.*, 281, 20132703.
- Humphreys, R.K. & Ruxton, G.D. (2019). Dropping to escape: a review of an under-appreciated antipredator defence: Dropping to escape. *Biol. Rev.*, 94, 575–589.
- Ims, R.A. (1990). On the adaptive value of reproductive synchrony as a predator-swamping strategy. *Am. Nat.*, 136, 15.
- Ingerslev, K.S. & Finke, D.L. (2017). Mechanisms underlying the nonconsumptive effects of parasitoid wasps on aphids. *Environ. Entomol.*, 46, 75–83.
- Jacobsen, S.K., Alexakis, I. & Sigsgaard, L. (2016). Antipredator responses in *Tetranychus urticae* differ with predator specialization. *J. Appl. Entomol.*, 140, 228–231.
- Jallow, M.F. & Hoy, C.W. (2005). Phenotypic variation in adult behavioral response and offspring fitness in *Plutella xylostella* (Lepidoptera: Plutellidae) in response to permethrin. *J. Econ. Entomol.*, 98, 2195–2202.
- Jandricic, S.E., Schmidt, D., Bryant, G. & Frank, S.D. (2016). Non-consumptive predator effects on a primary greenhouse pest: Predatory mite harassment reduces western flower thrips abundance and plant damage. *Biol. Control*, 95, 5–12.
- Janssens, L. & Stoks, R. (2013). Synergistic effects between pesticide stress and predator cues: Conflicting results from life history and physiology in the damselfly *Enallagma cyathigerum*. *Aquat. Toxicol.*, 132–133, 92–99.
- Jensen, K. & Toft, S. (2020). Fly disturbance suppresses aphid population growth. *Ecol. Entomol.*, 45, 901–903.
- Jonsson, M., Kaartinen, R. & Straub, C.S. (2017). Relationships between natural enemy diversity and biological control. *Curr. Opin. Insect Sci.*, 20, 1–6.
- Jouvenaz, D.P., Lofgren, C.S. & Banks, W.A. (1981) Biological control of imported fire ants: A review of current knowledge. *Bull. ESA*, 27, 203–209.
- Kaplan, I., McArt, S.H. & Thaler, J.S. (2014). Plant defenses and predation risk differentially shape patterns of consumption, growth, and digestive efficiency in a guild of leaf-chewing insects. *PLoS One*, 9, e93714.
- Kaplan, I. & Thaler, J.S. (2010). Plant resistance attenuates the consumptive and non-consumptive impacts of predators on prey. *Oikos*, 119, 1105–1113.
- Kaplan, I. & Thaler, J.S. (2012). Phytohormone-mediated plant resistance and predation risk act independently on the population growth and wing formation of potato aphids. *Macrosiphum euphorbiae*. *Arthropod-Plant Interact.*, 6, 181–186.
- Kats, L.B. & Dill, L.M. (1998). The scent of death: Chemosensory assessment of predation risk by prey animals. *Écoscience*, 5, 361–394.
- Kerfoot, W.C. & Sih, A. (1987). *Predation: Direct and Indirect Impacts on Aquatic Communities*. University Press of New England, Lebanon, NH.
- Kersch-Becker, M.F., Kessler, A. & Thaler, J.S. (2017). Plant defences limit herbivore population growth by changing predator-prey interactions. *Proc. R. Soc. B Biol. Sci.*, 284, 20171120.
- Kersch-Becker, M.F. & Thaler, J.S. (2015). Plant resistance reduces the strength of consumptive and non-consumptive effects of predators on aphids. *J. Anim. Ecol.*, 84, 1222–1232.
- Kiflawi, M., Blaustein, L. & Mangel, M. (2003). Oviposition habitat selection by the mosquito *Culiseta longiareolata* in response to risk of predation and conspecific larval density. *Ecol. Entomol.*, 28, 168–173.
- Koch, R.L. (2003). The multicolored Asian lady beetle, *Harmonia axyridis*: A review of its biology, uses in biological control, and non-target impacts. *J. Insect Sci.*, 3, 1–16.
- Kopta, T., Pokluda, R. & Psota, V. (2012). Attractiveness of flowering plants for natural enemies. *Horticultural Science*, 39, 8.
- Kraus, J.M. & Vonesh, J.R. (2010). Feedbacks between community assembly and habitat selection shape variation in local colonization. *J. Anim. Ecol.*, 79, 795–802.
- Krushelnicky, P.D., Ogura-Yamada, C.S., Kanegawa, K.M., Kaneshiro, K.Y. & Magnacca, K.N. (2017). Quantifying the effects of an invasive thief ant on the reproductive success of rare Hawaiian picture-winged flies. *Biol. Conserv.*, 215, 254–259.
- Kunert, G. & Weisser, W.W. (2003). The interplay between density- and trait-mediated effects in predator-prey interactions: A case study in aphid wing polymorphism. *Oecologia*, 135, 304–312.
- LaManna, J.A. & Martin, T.E. (2016). Costs of fear: behavioural and life-history responses to risk and their demographic consequences vary across species. *Ecol. Lett.*, 19, 403–413.
- Landis, D. & Van der Werf, W. (1997). Early-season predation impacts the establishment of aphids and spread of beet yellows virus in sugar beet. *Entomophaga*, 42, 499–516.
- Larsen, A.E. (2012). Modeling multiple nonconsumptive effects in simple food webs: a modified Lotka – Volterra approach. *Behav. Ecol.*, 23, 1115–1125.
- La-Spina, M., Jandricic, S.E. & Buitenhuis, R. (2019). Short-term increases in aphid dispersal from defensive dropping do not necessarily affect long-term biological control by parasitoids. *J. Econ. Entomol.*, 112, 1552–1559.
- Laundré, J.W., Hernández, L. & Altendorf, K.B. (2001). Wolves, elk, and bison: reestablishing the “landscape of fear” in Yellowstone National Park, U.S.A. *Can. J. Zool.*, 79, 1401–1409.
- Lawson-Balagbo, L.M. Jr, Gondim, M.G.C. & Moraes, G.J.D. (2007). Refuge use by the coconut mite *Aceria guerreronis*: Fine scale distribution and association with other mites under the perianth, 43, 102–110.
- Lee, D.H., Nyrop, J.P. & Sanderson, J.P. (2011). Avoidance of natural enemies by adult whiteflies, *Bemisia argentifolii*, and effects on host plant choice. *Biol. Control*, 58, 302–309.
- Lee, D.H., Nyrop, J.P. & Sanderson, J.P. (2014). Non-consumptive effects of the predatory beetle *Delphastus catalinae* (Coleoptera : Coccinellidae) on habitat use patterns of adult whitefly *Bemisia argentifolii* (Hemiptera : Aleyrodidae). *Appl. Entomol. Zool.*, 49, 599–606.
- Letourneau, D. & van Bruggen, A. (2006). Crop protection in organic agriculture. In: *Organic Agriculture: A Global Perspective* (eds Kristiansen, P., Taji, A., & Reganold, J.). CABI, Wallingford, pp. 93–121.
- Lima, S.L. (1998). Nonlethal effects in the ecology of predator-prey interactions. *Bioscience*, 48, 25–34.
- Livingston, G., Fukumori, K., Provete, D.B., Kawachi, M., Takamura, N. & Leibold, M.A. (2017). Predators regulate prey species sorting and spatial distribution in microbial landscapes. *J. Anim. Ecol.*, 86, 501–510.
- Lommen, S.T.E., Middendorp, C.W., Luijten, C.A., van Schelt, J., Brakefield, P.M. & de Jong, P.W. (2008). Natural flightless morphs of the ladybird beetle *Adalia bipunctata* improve biological control of aphids on single plants. *Biol. Control*, 47, 340–346.
- Long, E.Y. & Finke, D.L. (2015). Predators indirectly reduce the prevalence of an insect-vectored plant pathogen independent of predator diversity. *Oecologia*, 177, 1067–1074.
- Losey, J.E. & Denno, R.F. (1998). Positive predator-predator interactions: enhanced predation rates and synergistic suppression of aphid populations. *Ecology*, 79, 2143–2152.
- Losey, J.E. & Vaughan, M. (2006). The economic value of ecological services provided by insects. *Bioscience*, 56, 311.
- Lóvei, G.L. & Ferrante, M. (2017). A review of the sentinel prey method as a way of quantifying invertebrate predation under field conditions. *Insect Sci.*, 24, 528–542.
- Lucas, É., Coderre, D. & Brodeur, J. (2000). Selection of molting and pupation sites by *Coleomegilla maculata* (Coleoptera: Coccinellidae): avoidance of intraguild predation. *Environ. Entomol.*, 29, 454–459.
- Lundgren, J.G. & Fergen, J.K. (2006). The oviposition behavior of the predator orius insidiosus: acceptability and preference for different plants. *Biocontrol*, 51, 217–227.
- Maanak, V., Nordenhem, H., Bjorklund, N., Lenoir, L. & Nordlander, G. (2013). Ants protect conifer seedlings from feeding damage by the pine weevil *Hyllobius abietis*. *Agric. For. Entomol.*, 15, 98–105.

- Macfadyen, S., Davies, A.P. & Zalucki, M.P. (2015). Assessing the impact of arthropod natural enemies on crop pests at the field scale. *Insect Sci.*, 22, 20–34.
- Magalhães, S., Tudorache, C., Montserrat, M., van Maanen, R., Sabelis, M.W. & Janssen, A. (2004). Diet of intraguild predators affects antipredator behavior in intraguild prey. *Behav. Ecol.*, 16, 364–370.
- Mallet, J. & Porter, P. (1992). Preventing insect adaptation to insect-resistant crops: are seed mixtures or refugia the best strategy? *Proc. R. Soc. Lond. B Biol. Sci.*, 250, 165–169.
- Mappes, J., Mappes, T. & Lappalainen, T. (1997). Unequal maternal investment in offspring quality in relation to predation risk. *Evol. Ecol.*, 11, 7.
- Martini, X., Kincy, N. & Nansen, C. (2012). Quantitative impact assessment of spray coverage and pest behavior on contact pesticide performance. *Pest Manag. Sci.*, 68, 1471–1477.
- Matsumoto, T., Itioka, T. & Nishida, T. (2003). Rapid change in the settling behavior of the arrowhead scale *Unaspis yanonenis* as an avoidance mechanism against introduced parasitoids, *Aphytis yanonenis* and *Coccobius fulvus*. *Entomol. Exp. Appl.*, 107, 105–113.
- McArthur, C., Orlando, P., Banks, P.B. & Brown, J.S. (2012). The foraging tightrope between predation risk and plant toxins: a matter of concentration. *Funct. Ecol.*, 26, 74–83.
- McMurtry, J.A., Huffaker, C.B. & van de Vrie, M. (1970). Ecology of tetranychid mites and their natural enemies: a review. *Hilgardia*, 40, 391–458.
- Meadows, A.J., Owen, J.P. & Snyder, W.E. (2017). Keystone nonconsumptive effects within a diverse predator community. *Ecol. Evol.*, 7, 10315–10325.
- Meisner, M., Harmon, J.P., Harvey, C.T. & Ives, A.R. (2011). Intraguild predation on the parasitoid *Aphidius ervi* by the generalist predator *Harmonia axyridis*: The threat and its avoidance. *Entomol. Exp. Appl.*, 138, 193–201.
- Meresman, Y., Ben-ari, M. & Inbar, M. (2017). Turning in mid-air allows aphids that flee the plant to avoid reaching the risky ground. *Integr. Zool.*, 12, 409–420.
- Michaud, J. & Belliure, B. (2001). Impact of syrphid predation on production of migrants in colonies of the brown citrus aphid, *Toxoptera citricida* (Homoptera: Aphididae). *Biol. Control*, 21, 91–95.
- Michaud, J.P., Barbosa, P.R.R., Bain, C.L. & Torres, J.B. (2016). Extending the “Ecology of Fear” Beyond Prey: Reciprocal nonconsumptive effects among competing aphid predators. *Environ. Entomol.*, 45, 1398–1403.
- Miner, B.G., Sultan, S.E., Morgan, S.G., Padilla, D.K. & Relyea, R.A. (2005). Ecological consequences of phenotypic plasticity. *Trends Ecol. Evol.*, 20, 685–692.
- Mondor, E.B., Rosenheim, J.A. & Addicott, J.F. (2005). Predator-induced transgenerational phenotypic plasticity in the cotton aphid. *Oecologia*, 142, 104–108.
- Moore, G.G., Singh, R., Horn, B.W. & Carbone, I. (2009). Recombination and lineage-specific gene loss in the aflatoxin gene cluster of *Aspergillus flavus*. *Mol. Ecol.*, 18, 4870–4887.
- Murdoch, W.W., Chesson, J. & Chesson, P.L. (1985). Biological control in theory and practice. *Am. Nat.*, 125, 344.
- Nachman, G. (2006). The effects of prey patchiness, predator aggregation, and mutual interference on the functional response of *Phytoseiulus persimilis* Feeding on *Tetranychus urticae* (Acari: Phytoseiidae, Tetranychidae). *Exp. Appl. Acarol.*, 38, 87–111.
- Nakashima, Y. & Senoo, N. (2003). Avoidance of ladybird trails by an aphid parasitoid *Aphidius ervi*: active period and effects of prior oviposition experience. *Entomol. Exp. Appl.*, 109, 163–166.
- Naranjo, S.E., Ellsworth, P.C. & Frisvold, G.B. (2015). Economic value of biological control in integrated pest management of managed plant systems. *Annu. Rev. Entomol.*, 60, 621–645.
- Nelson, E.H. (2007). Predator avoidance behavior in the pea aphid: Costs, frequency, and population consequences. *Oecologia*, 151, 22–32.
- Nelson, E.H. & Rosenheim, J.A. (2006). Encounters between aphids and their predators: the relative frequencies of disturbance and consumption. *Entomol. Exp. Appl.*, 118, 211–219.
- Ninkovic, V., Feng, Y., Olsson, U. & Pettersson, J. (2013). Ladybird footprints induce aphid avoidance behavior. *Biol. Control*, 65, 63–71.
- Northfield T.D., Barton, B.T., & Schmitz, O.J. (2017). A spatial theory for emergent multiple predator-prey interactions in food webs. *Ecol. Evol.*, 7, 6935–6948. <https://doi.org/10.1002/ece3.3250>
- Northfield, T.D., Snyder, G.B., Ives, A.R. & Snyder, W.E. (2010). Niche saturation reveals resource partitioning among consumers. *Ecol. Lett.*, 13, 338–348.
- Oi, D., Porter, S. & Valles, S. (2015). A review of the biological control of fire ants. *Myrmecol. News*, 21, 101–116.
- Oi, D., Valles, S., Porter, S., Cavanaugh, C., White, G. & Henke, J. (2019). Introduction of fire ant biological control agents into the coachella valley of california. *Fla. Entomol.*, 102, 284–286.
- Okada, J. & Akamine, S. (2012). Behavioral response to antennal tactile stimulation in the field cricket *Gryllus bimaculatus*. *J. Comp. Physiol. A*, 198, 557–565.
- Op de Beeck, L., Janssens, L. & Stoks, R. (2016). Synthetic predator cues impair immune function and make the biological pesticide *Bti* more lethal for vector mosquitoes. *Ecol. Appl.*, 26, 355–366.
- Orr, M., Seike, S., Benson, W. & Gilbert, L.E. (1995). Flies suppress fire ants. *Nature*, 373, 292.
- Orrock, J.L., Preisser, E.L., Grabowski, J.H. & Trussell, G.C. (2013). The cost of safety: refuges increase the impact of predation risk in aquatic systems. *Ecology*, 94, 573–579.
- Otsuki H., & Yano S. (2014a). Functionally different predators break down antipredator defenses of spider mites. *Entomol. Exp. Appl.*, 151, 27–33. <https://doi.org/10.1111/eea.12164>
- Otsuki, H. & Yano, S. (2014b). Potential lethal and non-lethal effects of predators on dispersal of spider mites. *Exp. Appl. Acarol.*, 64, 265–275.
- Pallini, A., Janssen, A. & Sabelis, M.W. (1999). Spider mites avoid plants with predators. *Exp. Appl. Acarol.*, 23, 803–815.
- Pappas, M.L., Broekgaarden, C., Broufas, G.D., Kant, M.R., Messelink, G.J., Steppuhn, A. et al. (2017). Induced plant defences in biological control of arthropod pests: a double-edged sword. *Pest Manag. Sci.*, 73, 1780–1788.
- Paterson, R.A., Pritchard, D.W., Dick, J.T.A., Alexander, M.E., Hatcher, M.J. & Dunn, A.M. (2013). Predator cue studies reveal strong trait-mediated effects in communities despite variation in experimental designs. *Anim. Behav.*, 86, 1301–1313.
- Peacor, S.D., Barton, B.T., Kimbro, D.L., Sih, A. & Sheriff, M.J. (2020). A framework and standardized terminology to facilitate the study of predation-risk effects. *Ecology*.
- Pearce, S. & Zalucki, M.P. (2006). Do predators aggregate in response to pest density in agroecosystems? Assessing within-field spatial patterns. *J. Appl. Ecol.*, 43, 128–140.
- Peckarsky, B.L., Abrams, P.A., Bolnick, D.I. & Dill, L.M. (2008). Revisiting the classics: Considering nonconsumptive effects in textbook examples of predator – prey interactions. *Ecology*, 89, 2416–2425.
- Penfold, S., Dayananda, B. & Webb, J.K. (2017). Chemical cues influence retreat-site selection by flat rock spiders. *Behaviour*, 154, 149–161.
- Pepi, A.A., Broadley, H.J. & Elkinton, J.S. (2016). Density-dependent effects of larval dispersal mediated by host plant quality on populations of an invasive insect. *Oecologia*, 182, 499–509.
- Polis, G.A. (1981). The evolution and dynamics of intraspecific predation. *Annu. Rev. Ecol. Syst.*, 12, 225–251.
- Polis, G.A. (1999). Why are parts of the world green? Multiple factors control productivity and the distribution of biomass. *Oikos*, 86, 3–15.
- Polis, G.A., Myers, C.A. & Holt, R.D. (1989). The ecology and evolution of intraguild predation: potential competitors that eat each other. *Annu. Rev. Ecol. Syst.*, 20, 297–330.
- Porter, S.D. & Gilbert, L.E. (2004). Assessing host specificity and field release potential of fire ant decapitating flies (Phoridae: Pseudacteon). *Assess. Host Ranges Parasit. Predat. Used Class. Biol. Control Guide Best Pract. For. Health Technol. Enterp. Team FHTET Publ.*, 3, 152–176.
- Porter, S.D., Meer, R.K.V., Pesquero, M.A., Campiolo, S. & Fowler, H.G. (1995). Solenopsis (Hymenoptera: Formicidae) fire ant reactions

- to attacks of Pseudacteon flies (Diptera: Phoridae) in southeastern Brazil. *Ann. Entomol. Soc. Am.*, 88, 570–575.
- Prasad, R.P., Snyder, W.E., Prasad, R.P. & Snyder, W.E. (2018). A non-trophic interaction chain links predators in different spatial niches. *Oecologia*, 162(3), 747–753.
- Preisser, E.L. & Bolnick, D.I. (2008). The many faces of fear: comparing the pathways and impacts of nonconsumptive predator effects on prey populations. *PLoS One*, 3, 5–8.
- Preisser, E.L., Bolnick, D.I. & Benard, M.F. (2005). Scared to death? The effects of intimidation and consumption in predator-prey interactions. *Ecology*, 86, 501–509.
- Preisser, E.L., Orrock, J.L. & Schmitz, O.J. (2007). Predator hunting mode and habitat domain alter nonconsumptive effects in predator-prey interactions. *Ecology*, 88(11), 2744–2751.
- Southwood, T.R.E. & Henderson, P. (2000). *Ecological Methods*, 3rd edn.
- Rabus, M. & Laforsch, C. (2011). Growing large and bulky in the presence of the enemy: *Daphnia magna* gradually switches the mode of inducible morphological defences. *Funct. Ecol.*, 25, 1137–1143.
- Ramirez, R.A., Crowder, D.W., Snyder, G.B., Strand, M.R. & Snyder, W.E. (2010). Antipredator behavior of Colorado potato beetle larvae differs by instar and attacking predator. *Biol. Control*, 53, 230–237.
- Raymond, B., Darby, A. & Douglas, A. (2000). Intraguild predators and the spatial distribution of a parasitoid. *Oecologia*, 124, 367–372.
- Reddy, G.V.P. (2002). Plant volatiles mediate orientation and plant preference by the predator *Chrysoperla carnea* Stephens (Neuroptera: Chrysopidae). *Biol. Control*, 25, 49–55.
- Relyea, R.A. (2007). Getting out alive: how predators affect the decision to metamorphose. *Oecologia*, 152, 389–400.
- Relyea, R.A., Stephens, P.R., Barrow, L.N., Blaustein, A.R., Bradley, P.W., Buck, J.C. *et al.* (2018). Phylogenetic patterns of trait and trait plasticity evolution: Insights from amphibian embryos. *Evolution*, 72, 663–678.
- Rendon, D., Whitehouse, M.E.A. & Taylor, P.W. (2016). Consumptive and non-consumptive effects of wolf spiders on cotton bollworms. *Entomol. Exp. Appl.*, 158, 170–183.
- Roberts, D. (2014). Mosquito larvae change their feeding behavior in response to kairomones from some predators. *J. Med. Entomol.*, 51, 368–374.
- Rosenheim, J.A., Kaya, H.K., Ehler, L.E., Marois, J.J. & Jaffee, B.A. (1995). Intraguild predation among biological control agents – Theory and evidence. *Biol. Control*, 5, 303–335.
- Rosenheim, J.A. (1998). Higher-order predators and the regulation of insect herbivore populations. *Annu. Rev. Entomol.*, 43, 421–447.
- Rypstra, A.L. & Buddle, C.M. (2012). Spider silk reduces insect herbivory. *Biol. Lett.*, 9, 20120948.
- Saul, W.-C. & Jeschke, J.M. (2015). Eco-evolutionary experience in novel species interactions. *Ecol. Lett.*, 18, 236–245.
- Schausberger, P. (2003). Cannibalism among phytoseiid mites: a review. *Exp. Appl. Acarol.*, 29, 173–191.
- Schmitz, O.J. (1998). Direct and indirect effects of predation and predation risk in old-field interaction webs. *Am. Nat.*, 151, 327–342.
- Schmitz, O.J., Beckerman, A.P. & O'Brien, K.M. (1997). Behaviorally mediated trophic cascades: Effects of predation risk on food web interactions. *Ecology*, 78, 1388–1399.
- Schmitz, O.J., Grabowski, J.H., Peckarsky, B.L., Preisser, E.L., Trussell, G.C. & Vonesh, J.R. (2008). From individuals to ecosystem function: towards an integration of evolutionary and ecosystem ecology. *Ecology*, 89, 2436–2445.
- Schmitz, O.J., Krivan, V. & Ovadia, O. (2004). Trophic cascades: The primacy of trait-mediated indirect interactions. *Ecol. Lett.*, 7, 153–163.
- Schoeppner, N.M. & Relyea, R.A. (2005). Damage, digestion, and defence: the roles of alarm cues and kairomones for inducing prey defences: Damage, digestion, and defence. *Ecol. Lett.*, 8, 505–512.
- Seiter, M. & Schausberger, P. (2015). Maternal intraguild predation risk affects offspring anti-predator behavior and learning in mites. *Sci. Rep.*, 5, 15046.
- Shang, G.-Z., Zhu, Y.-H., Wu, Y., Cao, Y.-F. & Bian, J.-H. (2019). Synergistic effects of predation and parasites on the overwinter survival of root voles. *Oecologia*, 191, 83–96.
- Sih, A. (1992). Prey uncertainty and the balancing of antipredator and feeding. *Am. Nat.*, 139, 1052–1069.
- Sih, A., Bolnick, D.I., Luttbeg, B., Orrock, J.L., Peacor, S.D., Pintor, L.M. *et al.* (2010). Predator-prey naivete, antipredator behavior, and the ecology of predator invasions. *Oikos*, 119, 610–621.
- Sih, A., Englund, G. & Wooster, D. (1998). Emergent impacts of multiple predators on prey. *Trends Ecol. Evol.*, 13, 350–355.
- Sih, A. & Wooster, D.E. (1994). Prey behavior, prey dispersal, and predator impacts on stream prey. *Ecology*, 75, 1199–1207.
- Silberbush, A. & Blaustein, L. (2011). Mosquito females quantify risk of predation to their progeny when selecting an oviposition site. *Funct. Ecol.*, 25, 1091–1095.
- Silberbush, A., Markman, S., Lewinsohn, E., Bar, E., Cohen, J.E. & Blaustein, L. (2010). Predator-released hydrocarbons repel oviposition by a mosquito. *Ecol. Lett.*, 13, 1129–1138.
- Silberbush, A., Tsurim, I., Margalith, Y. & Blaustein, L. (2014). Interactive effects of salinity and a predator on mosquito oviposition and larval performance. *Oecologia*, 175, 565–575.
- Simberloff, D. & Stiling, P. (1996). How risky is biological control? *Ecology*, 77, 1965–1974.
- Sitvarin, M.I. & Rypstra, A.L. (2012). Sex-specific response of *Pardosa milvina* (Araneae: Lycosidae) to experience with a chemotactile predation cue. *Ethology*, 118, 1230–1239.
- Skals, N. (2005). Her odours make him deaf: crossmodal modulation of olfaction and hearing in a male moth. *J. Exp. Biol.*, 208, 595–601.
- Sloggett, J.J. & Weisser, W.W. (2002). Parasitoids induce production of the dispersal morph of the pea aphid, *Acyrtosiphon pisum*. *Oikos*, 98, 323–333.
- Snyder, W.E. & Ives, A.R. (2008). Behavior influences whether intra-guild predation disrupts herbivore suppression by parasitoids. *Behavioral Ecology of Insect Parasitoids: From Theoretical Approaches to Field Applications* (eds Wajnberg, E., Bernstein, C. & van Alphen, J.). Blackwell Publishing, Malden, MA, pp. 71–91.
- Snyder, W.E. & Wise, D.H. (2000). Antipredator behavior of spotted cucumber beetles (Coleoptera: Chrysomelidae) in response to predators that pose varying risks. *Environ. Entomol.*, 29, 35–42.
- Staats, E.G., Agosta, S.J. & Vonesh, J.R. (2016). Predator diversity reduces habitat colonization by mosquitoes and midges. *Biol. Lett.*, 12, 20160580.
- Stamps, J.A. (2007). Growth-mortality tradeoffs and 'personality traits' in animals. *Ecol. Lett.*, 10, 355–363.
- Stankowich, T. & Blumstein, D.T. (2005). Fear in animals: a meta-analysis and review of risk assessment. *Proc. R. Soc. B Biol. Sci.*, 272, 2627–2634.
- Stastny, M. & Sargent, R.D. (2017). Evidence for rapid evolutionary change in an invasive plant in response to biological control. *J. Evol. Biol.*, 30, 1042–1052.
- Stav, G., Blaustein, L. & Margalit, Y. (2000). Influence of nymphal *Anax imperator* (Odonata: Aeshnidae) on oviposition by the mosquito *Culiseta longiareolata* (Diptera: Culicidae) and community structure in temporary pools. *J. Vector Ecol.*, 25, 190–202.
- Stav, G., Kotler, B.P. & Blaustein, L. (2010). Foraging response to risks of predation and competition in artificial pools. *Isr. J. Ecol. Evol.*, 56, 9–20.
- Steffan, S.A. & Snyder, W.E. (2010). Cascading diversity effects transmitted exclusively by behavioral interactions. *Ecology*, 91, 2242–2252.
- Stephan, J.G., Stenberg, J.A. & Björkman, C. (2017). Consumptive and nonconsumptive effect ratios depend on interaction between plant quality and hunting behavior of omnivorous predators. *Ecol. Evol.*, 7, 2327–2339.
- Straub, C.S. & Snyder, W.E. (2008). Increasing enemy biodiversity strengthens herbivore suppression on two plant species. *Ecology*, 89, 1605–1615.
- Suh, C.-P.-C., Orr, D.B. & Van Duyn, J.W. (2000). Trichogramma releases in north carolina cotton: Why releases fail to suppress heliothine pests. *J. Econ. Entomol.*, 93, 1137–1145.
- Tabashnik, B.E., Brévault, T. & Carrière, Y. (2013). Insect resistance to Bt crops: lessons from the first billion acres. *Nat. Biotechnol.*, 31, 510.

- Tamaki, G., Eric, J.E. & Hathaway, D.O. (1970). Dispersal and reduction of colonies of pea aphids by *Aphidius smithi* (Hymenoptera: Aphidiidae). *Ann Entomol Soc Am*, 63, 973–980.
- Thaker, M., Vanak, A.T., Owen, C.R., Ogden, M.B., Niemann, S.M. & Slotow, R. (2011). Minimizing predation risk in a landscape of multiple predators: effects on the spatial distribution of African ungulates. *Ecology*, 92, 398–407.
- Thaler, J.S., Contreras, H. & Davidowitz, G. (2014). Effects of predation risk and plant resistance on *Manduca sexta* caterpillar feeding behaviour and physiology. *Ecol. Entomol.*, 39, 210–216.
- Thaler, J.S. & Griffin, C.A.M. (2008). Relative importance of consumptive and non-consumptive effects of predators on prey and plant damage: the influence of herbivore ontogeny. *Entomol. Exp. Appl.*, 128, 34–40.
- Thaler, J.S., McArt, S.H. & Kaplan, I. (2012). Compensatory mechanisms for ameliorating the fundamental trade-off between predator avoidance and foraging. *Proc. Natl Acad. Sci.*, 109, 12075–12080.
- Tholt, G., Kis, A., Medzihradsky, A., Szita, É., Tóth, Z., Havelda, Z. *et al.* (2018). Could vectors' fear of predators reduce the spread of plant diseases? *Sci. Rep.*, 8.
- Tollrian, R. (1995). Predator-induced morphological defenses: Costs, life history shifts, and maternal effects in *daphnia pulex*. *Ecology*, 76, 1691–1705.
- Trimmer, P.C., Ehlman, S.M. & Sih, A. (2017). Predicting behavioural responses to novel organisms: state-dependent detection theory. *Proc. R. Soc. B Biol. Sci.*, 284, 20162108.
- Tschamtko, T., Bommarco, R., Clough, Y., Crist, T.O., Kleijn, D., Rand, T.A. *et al.* (2007). Conservation biological control and enemy diversity on a landscape scale. *Biol. Control*, 43, 294–309.
- Tschamtko, T., Karp, D.S., Chaplin-Kramer, R., Batáry, P., DeClerck, F., Gratton, C. *et al.* (2016). When natural habitat fails to enhance biological pest control – Five hypotheses. *Biol. Cons.*, 204, 449–458.
- Tyndale-Biscoe, M. & Vogt, W.G. (1996). Population status of the bush fly, *Musca vetustissima* (Diptera: Muscidae), and native dung beetles (Coleoptera: Scarabaeinae) in south-eastern Australia in relation to establishment of exotic dung beetles. *Bull. Entomol. Res.*, 86, 183.
- Uesugi, A. (2015). The slow-growth high-mortality hypothesis: direct experimental support in a leafmining fly. *Ecol. Entomol.*, 40, 221–228.
- Ugine, T.A. & Thaler, J.S. (2020). Insect predator odors protect herbivore from fungal infection. *Biol. Control*, 143, 104186.
- Valente, C., Afonso, C., Gonçalves, C.I., Alonso-Zarazaga, M.A., Reis, A. & Branco, M. (2017). Environmental risk assessment of the egg parasitoid *Anaphes inexpectatus* for classical biological control of the Eucalyptus snout beetle, *Gonipterus platensis*. *Biocontrol*, 62, 457–468.
- Van Driesche, R.G. (2016). Methods for evaluation of natural enemy impacts on invasive pests of wildlands. *Integrating Biological Control into Conservation Practice* (eds Van Driesche, R.G., Simberloff, D., Blossey, B., Causton, C., Hoddle, M.S., Wagner, D.L., Marks, C.O., Heinz, K.M. & Warner, K.D.). Wiley, West Sussex, UK, pp. 189–207.
- Van Veen, F.J.F., Rajkumar, A., Muller, C.B. & Godfray, H.C.J. (2001). Increased reproduction by pea aphids in the presence of secondary parasitoids. *Ecol. Entomol.*, 26, 425–429.
- Vance-Chalcraft, H.D., Rosenheim, J.A., Vonesh, J.R., Osenberg, C.W. & Sih, A. (2007). The influence of intraguild predation on prey suppression and prey release: a meta-analysis. *Ecology*, 88, 2689–2696.
- Vance-Chalcraft, H.D. & Soluk, D.A. (2005). Estimating the prevalence and strength of non-independent predator effects. *Oecologia*, 146, 452–460.
- Vandermoten, S., Mescher, M.C., Francis, F., Haubruge, E. & Verheggen, F.J. (2012). Aphid alarm pheromone: an overview of current knowledge on biosynthesis and functions. *Insect Biochem. Mol. Biol.*, 42, 155–163.
- Velasco-Hernández, M.C., Ramirez-Romero, R., Cicero, L., Michel-Rios, C. & Desneux, N. (2013). Intraguild predation on the whitefly parasitoid *Eretmocerus eremicus* by the generalist predator *Geocoris punctipes*: a behavioral approach. *PLoS One*, 8, e80679.
- Venzon, M., Janssen, A., Pallini, A. & Sabelis, M.W. (2000). Diet of a polyphagous arthropod predator affects refuge seeking of its thrips prey. *Anim. Behav.*, 60, 369–375.
- Verdolin, J.L. (2006). Meta-analysis of foraging and predation risk trade-offs in terrestrial systems. *Behav. Ecol. Sociobiol.*, 60, 457–464.
- Vonesh, J.R. & Blaustein, L. (2010). Predator-induced shifts in mosquito oviposition site selection: A meta-analysis and implications for vector control. *Isr. J. Ecol. Evol.*, 56, 263–279.
- de Vos, M., Cheng, W.Y., Summers, H.E., Raguso, R.A. & Jander, G. (2010). Alarm pheromone habituation in *Myzus persicae* has fitness consequences and causes extensive gene expression changes. *Proc. Natl Acad. Sci.*, 107, 14673–14678.
- Walzer, A., Lepp, N. & Schausberger, P. (2015). Compensatory growth following transient intraguild predation risk in predatory mites. *Oikos*, 124, 603–609.
- Walzer, A. & Schausberger, P. (2009). Non-consumptive effects of predatory mites on thrips and its host plant. *Oikos*, 118, 934–940.
- Wanger, T.C., Wielgoss, A.C., Motzke, I., Clough, Y., Brook, B.W., Sodhi, N.S. *et al.* (2011). Endemic predators, invasive prey and native diversity. *Proc. R. Soc. B Biol. Sci.*, 278, 690–694.
- Warburg, A., Faiman, R., Shtern, A., Silberbush, A., Markman, S., Cohen, J.E. *et al.* (2011). Oviposition habitat selection by *Anopheles gambiae* in response to chemical cues by *Notonecta maculata* oviposition habitat selection by *Anopheles gambiae* in response to chemical cues by *Notonecta maculata*. *J. Vector Ecol.*, 36, 421–425.
- Wasserberg, G., White, L., Bullard, A., King, J. & Maxwell, R. (2013). Oviposition site selection in *Aedes albopictus* (Diptera: Culicidae): are the effects of predation risk and food level independent? *J. Med. Entomol.*, 50, 1159–1164.
- Weber, D.C., Rowley, D.L., Greenstone, M.H. & Athanas, M.M. (2006). Prey preference and host suitability of the predatory and parasitoid carabid beetle, *Lebia grandis*, for several species of *Leptinotarsa* beetles. *J. Insect Sci.*, 6, 1–14.
- Weissburg, M. & Beauvais, J. (2015). The smell of success: the amount of prey consumed by predators determines the strength and range of cascading non-consumptive effects. *PeerJ*, 3, e1426.
- Weissburg, M., Smees, D.L. & Ferner, M.C. (2014). The sensory ecology of nonconsumptive predator effects. *Am. Nat.*, 184, 141–157.
- Weisser, W.W., Braendle, C. & Minoretti, N. (1999). Predator-induced morphological shift in the pea aphid. *Proc. R. Soc. B Biol. Sci.*, 266, 1175–1181.
- Welch, K.D. & Harwood, J.D. (2014). Temporal dynamics of natural enemy-pest interactions in a changing environment. *Biol. Control*, 75, 18–27.
- Werner, E.E. & Anholt, B.R. (1996). Predator-induced behavioral indirect effects: consequences to competitive interactions in anuran larvae. *Ecology*, 77, 157–169.
- Werner, E.E. & Peacor, S.D. (2003). A review of trait-mediated indirect interactions in ecological communities. *Ecology*, 84, 1083–1100.
- Wiedenmann, R.N. & Smith, J.W. (1997). Attributes of natural enemies in ephemeral crop habitats. *Biol. Control*, 10, 16–22.
- Wilson, E.E., Mullen, L.M. & Holway, D.A. (2009). Life history plasticity magnifies the ecological effects of a social wasp invasion. *Proc. Natl Acad. Sci.*, 106, 12809–12813.
- Wilson, M.R. & Leather, S.R. (2012). The effect of past natural enemy activity on host-plant preference of two aphid species. *Entomol. Exp. Appl.*, 144, 216–222.
- Winder, L., Alexander, C.J., Holland, J.M., Woolley, C. & Perry, J.N. (2001). Modelling the dynamic spatio-temporal response of predators to transient prey patches in the field. *Ecol. Lett.*, 4, 568–576.
- Wise, D.H. (2006). Cannibalism, food limitation, intraspecific competition, and the regulation of spider populations. *Annu. Rev. Entomol.*, 51, 441–465.
- Wuellner, A.C.T., Aglio-Holvorcem, C.G.D., Benson, W.W. & Gilbert, E. (2002). Phorid Fly (Diptera: Phoridae) oviposition behavior and fire ant (Hymenoptera: Formicidae) reaction to attack differ according to phorid species phorid fly (Diptera: Phoridae) oviposition behavior

- and fire ant (Hymenoptera : Formicidae) reactio. *Ann. Entomol. Soc. Am.*, 95, 257–266.
- Xiong, X., Michaud, J. P., Li, Z., Wu, P., Chu, Y., *et al.* (2015). Chronic, predator-induced stress alters development and reproductive performance of the cotton bollworm, *Helicoverpa armigera*. *BioControl*, 60, 827–837. <https://doi.org/10.1007/s10526-015-9689-9>
- Zaguri, M. & Hawlena, D. (2019). Beardng the scorpion in his den: desert isopods take risks to validate their ‘landscape of fear’ assessment. *Oikos*, 128, 1458–1466.
- Zhang, W. & Swinton, S.M. (2012). Optimal control of soybean aphid in the presence of natural enemies and the implied value of their ecosystem services. *J. Environ. Manage.*, 96, 7–16.

SUPPORTING INFORMATION

Additional supporting information may be found online in the Supporting Information section at the end of the article.

Editor, Jonathan Chase
Manuscript received 12 May 2020
First decision made 30 June 2020
Manuscript accepted 13 August 2020

RESEARCH ARTICLE

Agent-based and continuous models of hopper bands for the Australian plague locust: How resource consumption mediates pulse formation and geometry

Andrew J. Bernoff¹, Michael Culshaw-Maurer², Rebecca A. Everett³, Maryann E. Hohn⁴, W. Christopher Strickland⁵, Jasper Weinburd¹*

1 Department of Mathematics, Harvey Mudd College, Claremont, California, United States of America, **2** Departments of Entomology and Nematology/Evolution and Ecology, University of California, Davis, Davis, California, United States of America, **3** Department of Mathematics and Statistics, Haverford College, Haverford, Pennsylvania, United States of America, **4** Mathematics Department, Pomona College, Claremont, California, United States of America, **5** Department of Mathematics and Department of Ecology & Evolutionary Biology, University of Tennessee, Knoxville, Tennessee, United States of America

☯ These authors contributed equally to this work.

* jweinburd@hmc.edu



OPEN ACCESS

Citation: Bernoff AJ, Culshaw-Maurer M, Everett RA, Hohn ME, Strickland WC, Weinburd J (2020) Agent-based and continuous models of hopper bands for the Australian plague locust: How resource consumption mediates pulse formation and geometry. *PLoS Comput Biol* 16(5): e1007820. <https://doi.org/10.1371/journal.pcbi.1007820>

Editor: Corina E. Tarnita, Princeton University, UNITED STATES

Received: November 1, 2019

Accepted: March 23, 2020

Published: May 4, 2020

Peer Review History: PLOS recognizes the benefits of transparency in the peer review process; therefore, we enable the publication of all of the content of peer review and author responses alongside final, published articles. The editorial history of this article is available here: <https://doi.org/10.1371/journal.pcbi.1007820>

Copyright: © 2020 Bernoff et al. This is an open access article distributed under the terms of the [Creative Commons Attribution License](https://creativecommons.org/licenses/by/4.0/), which permits unrestricted use, distribution, and reproduction in any medium, provided the original author and source are credited.

Data Availability Statement: All code and numerically generated data files are available from

Abstract

Locusts are significant agricultural pests. Under favorable environmental conditions flightless juveniles may aggregate into coherent, aligned swarms referred to as hopper bands. These bands are often observed as a propagating wave having a dense front with rapidly decreasing density in the wake. A tantalizing and common observation is that these fronts slow and steepen in the presence of green vegetation. This suggests the collective motion of the band is mediated by resource consumption. Our goal is to model and quantify this effect. We focus on the Australian plague locust, for which excellent field and experimental data is available. Exploiting the alignment of locusts in hopper bands, we concentrate solely on the density variation perpendicular to the front. We develop two models in tandem; an agent-based model that tracks the position of individuals and a partial differential equation model that describes locust density. In both these models, locust are either stationary (and feeding) or moving. Resources decrease with feeding. The rate at which locusts transition between moving and stationary (and vice versa) is enhanced (diminished) by resource abundance. This effect proves essential to the formation, shape, and speed of locust hopper bands in our models. From the biological literature we estimate ranges for the ten input parameters of our models. Sobol sensitivity analysis yields insight into how the band's collective characteristics vary with changes in the input parameters. By examining 4.4 million parameter combinations, we identify biologically consistent parameters that reproduce field observations. We thus demonstrate that resource-dependent behavior can explain the density distribution observed in locust hopper bands. This work suggests that feeding behaviors should be an intrinsic part of future modeling efforts.

a GitHub repository at https://github.com/mountainindus/Locusts_2020 which has been given the DOI [10.5281/zenodo.3738721](https://doi.org/10.5281/zenodo.3738721).

Funding: All authors were supported by the Mathematics Research Communities Program of the American Mathematical Society in 2018 under National Science Foundation grant DMS-1321794 (<http://www.ams.org/programs/research-communities/mrc>). All authors were supported by the Institute for Advanced Study Summer Collaborators Program (<https://www.math.ias.edu/summercollaborators>). JW is supported by an NSF Mathematical Sciences Postdoctoral Research Fellowship grant DMS-1902818 (https://www.nsf.gov/funding/pgm_summ.jsp?pims_id=5301). WCS was supported by a Simons Foundation Grant #585322. AJB was also supported by a Simons Foundation Grant #317319 (<https://www.simonsfoundation.org/grant/collaboration-grants-for-mathematicians/>). Funding for open access to this research was provided by the University of Tennessee's Open Publishing Support Fund. The funders had no role in study design, data collection and analysis, decision to publish, or preparation of the manuscript.

Competing interests: The authors have declared that no competing interests exist.

Author summary

Locusts aggregate in swarms that threaten agriculture worldwide. Initially these aggregations form as aligned groups, known as hopper bands, whose individuals alternate between marching and paused (associated with feeding) states. The Australian plague locust (for which there are excellent field studies) forms wide crescent-shaped bands with a high density at the front where locusts slow in uneaten vegetation. The density of locusts rapidly decreases behind the front where the majority of food has been consumed. Most models of collective behavior focus on social interactions as the key organizing principle. We demonstrate that the formation of locust bands may be driven by resource consumption. Our first model treats each locust as an individual agent with probabilistic rules governing motion and feeding. Our second model describes locust density with deterministic differential equations. We use biological observations of individual behavior and collective band shape to identify numerical values for the model parameters and conduct a sensitivity analysis of outcomes to parameter changes. Our models are capable of reproducing the characteristics observed in the field. Moreover, they provide insight into how resource availability influences collective locust behavior that may eventually aid in disrupting the formation of locust bands, mitigating agricultural losses.

Introduction

Locusts are a significant agricultural pest in parts of Africa, Asia, Central and South America, and Australia. They aggregate in large groups with as many as billions of individuals that move collectively, consuming large quantities of vegetation [1, 2]. Collective movement occurs in both nymphal and adult stages of development and is associated with an epigenetic phase change from a solitary to a gregarious social state which is mediated by conspecific density and abiotic factors [1, 3–6]. Flightless nymphs march along the ground in aligned groups, often through agricultural systems where they cause significant crop damage as they feed and advance [4, 7, 8]. Some species, such as the brown locust *Locustana pardalina*, form intertwining streams of relatively homogeneous density [1, 2, 8]. By contrast the Australian plague locusts *Chortoicetes terminifera* form wide, crescent-shaped bands that contain a high density in front and a rapidly decreasing density behind [4, 9, 10]. Clark [4] notes:

The structure of bands varies according to the type of pasture through which they are passing. In areas of low cover containing plenty of green feed, bands develop well-marked fronts in which the majority of hoppers may be concentrated. In areas lacking green feed, bands lose their dense fronts and extend to form long streams, frequently exhibiting marked differences in density throughout.

As bands of *C. terminifera* move through a field of low pasture, they create a sharp transition from undamaged vegetation in front of the band to significant defoliation immediately behind the band, see a schematic in Fig 1 or aerial photographs such as Figure 2 in [10], Figure 1 in [11], Figure 9 in [12], and multiple images in [13]. In natural systems, *C. terminifera* tend to consume one of several species of grasses; in agricultural systems, they tend to eat primarily pasture and sometimes early stage winter cereals [14].

The Australian plague locust *C. terminifera* is the most common locust species on the Australian continent. For ease, we henceforth refer to *C. terminifera* simply as “locust”. Outbreaks of locust nymphs emerge as the result of a pattern of rainfall, vegetation growth, and drought

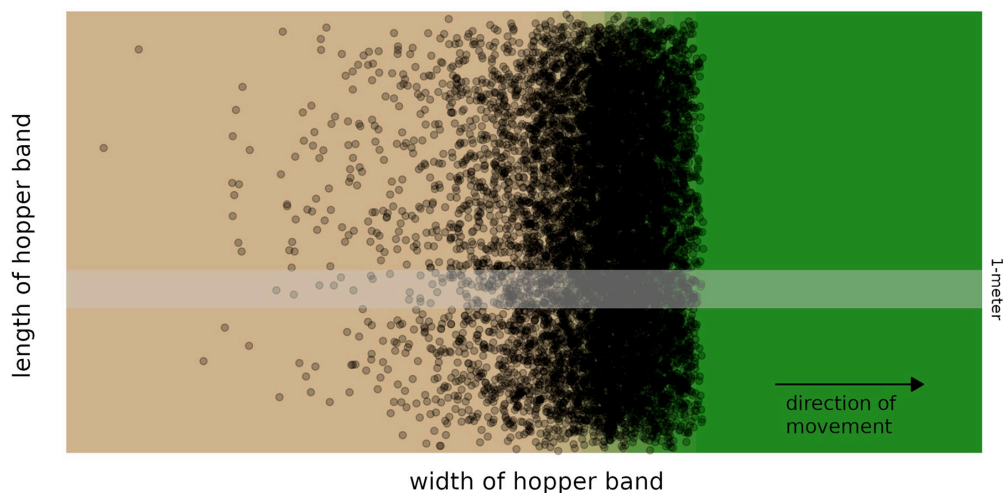


Fig 1. Schematic of a traveling pulse of locusts. The Australian plague locust forms broad hopper bands that propagate through vegetation in the direction perpendicular to the aggregate structure [4, 9, 10]. The cross-sectional density profile is a *traveling pulse*, with a steep leading edge (right) and shallower decay behind (left) that is roughly exponentially decreasing in density [9]. Aerial photographs, for instance Figure 2 in [10], show a notable contrast between the verdant green of the unperturbed crops in front of the band and the lifeless brown in the pulse's wake. The one meter wide strip above represents the dimensions we use to model locust movement in a single dimension, as described below.

<https://doi.org/10.1371/journal.pcbi.1007820.g001>

[11, 15] which promotes breeding, hatching, crowding, and gregarization [3]. Gregarious nymphs form *hopper bands* of aligned individuals, which march distances from tens to hundreds of meters in a single day [4]. Locusts proceed through five nymphal stages, called *instars*, with marching behavior beginning during the second instar [4]. Throughout these phases of life, hoppers consume large quantities of green biomass with an individual eating one third to one half of its body weight per day [14]. Approximately four weeks after eggs hatch, locusts reach adulthood and are then capable of forming even more destructive and highly mobile flying swarms [16].

This study focuses on collective marching in hopper bands, which dominates the behavior of gregarious locust nymphs in the third and fourth instars. Temperature and sunlight dictate a daily cycle of behavior with basking in the morning, roosting at midday, and active periods of collective marching and feeding for up to nine hours when temperatures are in an optimal range ($\sim 25^\circ\text{C}$) [10]. During these periods of collective marching, individuals crawl and hop across the ground in nearly the same direction as their neighbors, due to social interactions [17, 18]. When individuals at the front of a band encounter available food resources, they stop and feed (see [4, 10] for qualitative observations and [19] for quantitative experimental results). Immediately after feeding, locusts exhibit a post-prandial quiescent period whose duration increases with the amount consumed [19–21]. Locusts farther back in the band may continue to move forward, eventually passing those that stopped. This creates a “leap-frogging” type motion with a cycling of individuals in the dense front of the band. Clark [4] describes this behavior:

Those hoppers behind the front were in places which had been partly or wholly eaten out, and thus lacked the same stimulus of food to stop them. As their average rate of progress was

greater than that of the hoppers in the front, they tended to overtake them, becoming in turn slowed down in their progress by the presence of food.

Thus, individual motion during marching depends on individuals stopping to feed and consequently on local resource density. We hypothesize that this effect mediates the coherence and persistence of hopper bands with a dense front [4, 10] as well as the characteristic cross-sectional density distribution documented in [9].

To test our hypothesis we conduct an in-depth modeling study concentrating on the interaction of pause-and-go motion with food resources. We assume that hoppers march in an aligned band through a field of finite resources, which is depleted as the locusts stop to feed. We develop a model for the probability of movement or stopping as a function of resource availability. We construct and analyze in tandem an agent-based model (ABM), which tracks individual locusts, and a partial differential equation (PDE) model, which considers mean-field densities. Both models produce traveling pulse type solutions that are consistent with the detailed field observations of Buhl et al [9]. The ABM is easily simulated, allows us to track individuals within the swarm, and captures the natural stochasticity of a biological process. In contrast, the PDE produces smooth solutions and lends itself to analysis and a detailed characterization of how observable outcomes, such as mean band speed, cross-sectional density profile, and density of resources left unconsumed in the wake, are related to the model's parameters.

Previous modeling efforts have considered both agent-based and continuous models, see [1] for an excellent overview of locust models. The majority of these have focused on social behavior—notably alignment, attraction, and repulsion with respect to conspecifics [18, 22–27]. Many of the agent-based models consider the pause-and-go behavior of locusts [18, 26, 27], and other insects [28]. Continuous models have been used to study transitions between stationary and moving states [29, 30] and gregarization [31]. Foraging has been modeled in an agent-based framework [32] and resource distribution effects on peak density has been posed as an energy minimization problem [33]. Other continuous models explicitly include food resources having animal movement depend on a combination of aggregation and gradient sensing (chemotaxis in many, starting with [34], or “herbivory-taxis” in [35, 36], for instance). These studies find that traveling animal bands are the result of a balance between attraction to food and inter-animal dispersal, bearing some qualitative resemblance to the results presented here. However, locusts in the present model do not sense resource gradients (instead, direction is prescribed implicitly by social alignment) and the corresponding mathematical equations are distinct from the well-studied equations of chemotaxis.

We are aware of no models of locust band movement that incorporate foraging behavior or food resources. Previous studies such as [23, 27] suggest that the formation of sharp asymmetric fronts may be explained solely by social forces. By contrast, our main conclusion is that foraging and resource-mediated stationary/moving transitions produce pulse-shaped density profiles, supporting the observations of hopper bands with dense fronts and the inferences on foraging of Clark [4] and Hunter et al. [10]. A further strength of our model is that it quantitatively reproduces the observed density profiles of [9] from biologically realistic parameters.

In Models and methods we construct our two models beginning with biological and simplifying assumptions, and ending with parameter identification from empirical field data in Table 2. Our Results describe how both models produce a traveling pulse in locust density precisely when the locusts' stationary/moving transitions are dependent upon the amount of nearby resources. Evidence consists of numerical simulations for the ABM, mathematical traveling wave analysis for the PDE, and a robust sensitivity analysis of the models to changes in the input parameters. In our Discussion we revisit our main findings and outline extensions of

this work incorporating more biological complexity. [S1](#), [S2](#) and [S3](#) Appendices each contain mathematical analysis and proofs substantiating results for the PDE. Finally, [S1 Video](#) shows a typical simulation of our agent-based model.

Models and methods

Basic assumptions

We outline our assumptions for the modeling framework. Our models are minimal in the sense that we include only the effects necessary to investigate the main question: *Can resource-dependent locust behavior drive the formation of a dense front and the propagation of hopper bands?*

- We assume that resources (food) can only decrease, since locusts feed much more quickly than vegetation grows. Moreover, resources are identical so that they can be characterized by a single variable. Prior to locust arrival, we assume available resources have a spatially uniform density.
- We model only the part of the daily cycle dominated by collective movement. During a typical day, a hopper band has one or two periods of collective movement (marching) totaling up to nine hours. The remainder of the day is spent resting (basking and roosting) [1, 4, 8–10].
- We assume hopper bands consist of flightless nymphs that are behaviorally identical in all regards. Bands often include a mix of two instars (e.g. II and III instars or III and IV instars) which behave qualitatively similarly with later instars being larger, eating more, and moving more quickly.
- We assume individuals move parallel to one another, creating a constant direction of movement for the entire band. Locusts are known to align their direction of movement with their nearest neighbors and may align with environmental cues such as wind or the location of the sun [2, 4, 8].
- We model behavior in a narrow strip aligned to the direction of movement, as shown in [Fig 1](#). For dimensional consistency of the model, we assume the transverse width to be 1 meter.
- We assume that each individual is either stationary or moving. Further, only stationary locusts feed while moving locusts propagate forward with a constant speed that represents an average of crawling and hopping.
- We assume that locusts feed continuously when they are stationary. In fact, locusts eat a meal and then remain sedentary during a post-prandial period [19–21]. While biologically different, these processes are mathematically analogous and we believe including such a delay in the model is unlikely to significantly alter our results.

Furthermore, we make additional assumptions on the rate of transitions between moving and stationary that are supported by empirical observation, although they combine and simplify multiple locust behaviors.

- We assume that locusts transition back and forth between stationary and moving states at a rate depending solely on the resources nearby.

Notably, we have not included any explicit social interaction between locusts; interaction is mediated solely through the consumption of resources. Social interaction plays a well-documented role in the aggregation, alignment, and marching of hopper bands, see [1] for instance. By modeling one spatial dimension only, we implicitly include the social tendency of locusts to

align their direction of motion with neighbors as demonstrated in [17]. We do not focus on social interactions simply because our primary goal is to investigate the effect of linking resource consumption with pause-and-go motion on hopper band morphologies.

- We assume the transition rate from moving to stationary is positive and increases as the resource density increases.

Field observations [4, 10] and laboratory experiments [19] have shown that individuals stop marching to eat when they encounter resources in their path. While we assume resources have a uniform local density, the reality on the ground is that a locust is more likely to encounter an edible plant, and thus stop to feed, when the resource density is high.

- We assume the transition rate from stationary to moving is positive and decreasing with resource density.

This behavior is consistent with foraging theories, such as the simple mechanisms illustrated in [37] where insects are likely to leave a patch of resources before the point of diminishing returns. The *Marginal Value Theorem* [38] quantifies this behavior: if an energy cost assigned to foraging is proportional to resource density, then when local resource densities drop below a critical level it costs less energy per unit resource to move on in search of higher density resources. Additionally, there is a second, more subtle behavior behind this assumption. Locusts that become stationary are assumed to have consumed resources. After feeding, locusts exhibit a post-prandial period of inactivity which extends in proportion with the amount consumed [19–21]. Our assumption about this transition rate reflects a longer period of inactivity when resources are plentiful and larger amounts are therefore consumed.

Foreshadowing our results, only one of these two transition rates must depend strictly on local resource availability for our model to produce coherent traveling pulse-type density profiles akin to observed hopper bands with dense fronts.

- These transition processes are completely memoryless, which implies that locusts experience neither hunger nor satiation.

The biological reality is that feeding behavior is complex, see [39] for a review. Locust hunger has been well documented in other species [19, 40]. Since, in our model, locusts are traveling through a field of relatively plentiful resources we suggest that most locusts do not experience starvation (i.e. no sustenance for 24 hours as in some experiments).

We remind the reader that our goal in this study is to demonstrate that resource-dependent behavior is sufficient for the formation and propagation of hopper bands with a coherent dense front. We acknowledge that the efficacy of this model may be improved by adding social interactions—such as alignment, attraction, and repulsion. Additionally, we believe these additions, particularly that of alignment, would play a pivotal role when modeling locust behavior in two-dimensions, as in [23, 27].

General model formulation

Within the framework described above, we build two models: an agent-based model (ABM) which tracks individual locusts and a partial differential equation model (PDE) that determines locust density. These models share much in their basic structure. Table 1 compares their independent and state variables and Table 2 lists their common model parameters.

Table 1. Independent and dependent variables appearing in the agent-based and partial differential equation models. Units are L = length [meters], T = time [seconds], C = number of locusts, P = locust density [number/(meter)²], and Q = resource density [grams/(meter)²].

Agent-Based Model	Units	Continuous Model	Units	Description
x_n	L	x	L	position (along direction of motion)
t_m	T	t	T	time
$S_{n,m}$	C	$S(x, t)$	P	number/density of stationary locusts
$M_{n,m}$	C	$M(x, t)$	P	number/density of moving locusts
$R_{n,m}$	Q	$R(x, t)$	Q	edible resource density

<https://doi.org/10.1371/journal.pcbi.1007820.t001>

In the ABM, space and time lie on a discrete, evenly spaced lattice (x_n, t_m) while in the PDE space and time (x, t) are continuous. In both models, S and M denote the number or density of stationary and moving locusts respectively. For the ABM, the number of stationary (moving) locusts at x_n, t_m is denoted $S_{n,m}$ ($M_{n,m}$). For the PDE, the analogous continuous quantities for the density of locusts are $S(x, t)$ and $M(x, t)$.

Resources edible by locusts are measured by the non-negative scalar density variable R ; specifically, the resource density in the agent-based model is $R_{n,m}$, and the resource density in the continuous model is $R(x, t)$.

We assume that the group rate of feeding is proportional to the product of the stationary locust density and the resource density; that is,

$$(\text{rate of change of resources at a given location}) = -\lambda SR \tag{1}$$

where λ is a positive rate constant that describes how quickly individual locusts consume resources. This implies that an individual locust’s foraging efficiency decreases as resources become scarcer at their location. This is not an explicit implementation of the Marginal Value Theorem but fits the general concept of foraging efficiency within a patch decreasing due to searching time, not satiation by the forager [38]: as the resources at a location are eaten, locusts have difficulty locating the next unit to consume, reducing the overall rate of resource consumption at that location. We will refer to λ as the *foraging rate*, as it reflects both feeding and foraging efficiency.

We model the stationary-moving transitions as a Markov (memoryless) process. For the PDE model, this yields a rate at which the population of stationary locusts transitions to moving, and vice versa. This assumption ignores the transition history and hunger (as discussed above) of any individual locust, which is justifiable on the timescale of the collective motion

Table 2. Estimates of biological parameters for both models. Parameters above the horizontal line are estimated from empirical observations, with explanations in text. Parameters below the horizontal line are estimated from collective information and model behavior. Units are L = length [meters], T = time [seconds], C = number of locusts, P = locust density [number/(meter)²], and Q = resource density [grams/(meter)²].

	Description	Units	Min	Max	Example	Source
N	total number locusts in strip	C/L	5000	30000	7000	[9]
R^*	resource density in front of band	Q	120	250	200	[44]
v	individual marching speed	L/T	0.003	0.1	0.04	[27, 45]
α	$S \rightarrow M$ transition rate for $R = 0$	$1/T$	η	1	0.0045	[27]
β	$M \rightarrow S$ transition rate for $R = 0$	$1/T$	0.01	θ	0.02	[26]
η	$S \rightarrow M$ transition rate, large R	$1/T$	0	α	0.0036	
θ	$M \rightarrow S$ transition rate, large R	$1/T$	β	12.5	0.14	
γ	exponent of $S \rightarrow M$ transition	$1/Q$	0.0004	0.08	0.03	
δ	exponent of $M \rightarrow S$ transition	$1/Q$	0.0004	0.08	0.005	
λ	individual foraging rate	$1/TP$	10^{-10}	10^{-4}	10^{-5}	[46]

<https://doi.org/10.1371/journal.pcbi.1007820.t002>

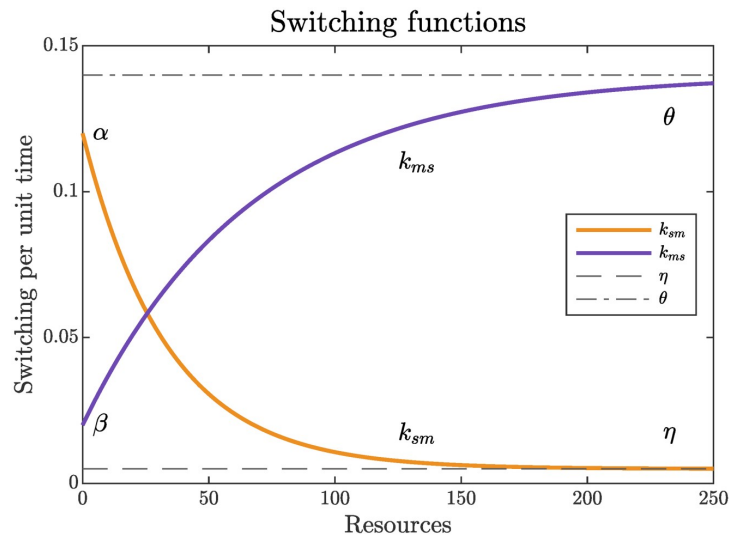


Fig 2. Transition rates for stationary to moving k_{sm} (gold) and moving to stationary k_{ms} (purple) with $\alpha = 0.12$, $\beta = 0.02$, $\gamma = 0.03$, $\delta = 0.015$, $\eta = 0.005$, and $\theta = 0.14$.

<https://doi.org/10.1371/journal.pcbi.1007820.g002>

(hours). We use exponentially saturating functions of resources as illustrated in Fig 2. The stationary to moving rate is denoted k_{sm} while the moving to stationary rate is called k_{ms} . Specifically,

$$k_{sm}(R) = \eta - (\eta - \alpha)e^{-\gamma R}, \quad k_{ms}(R) = \theta - (\theta - \beta)e^{-\delta R}, \quad (2)$$

where $\gamma, \delta > 0$, $0 \leq \beta \leq \theta$, and $0 < \eta \leq \alpha$. The conditions on the parameters guarantee that $k_{sm}(R)$ is a decreasing function and $k_{ms}(R)$ is an increasing function of R . (Most of the analytical results concerning the PDE model hold for any choice of monotone switching rates—see S2 Appendix for details).

This functional form derives from the assumption that the transition rate’s sensitivity to changes in resources is proportional to the resource availability [38]. Biologically, this implies that when encountering excess resources, there will be a high proportion of stationary locusts, and doubling the excess resources will do little to change the proportion of stationary locusts. Similarly, when resources are scarce, locusts are most likely to transition from stationary to moving and least likely to stop. Mathematically, this functional form preserves the positivity of the transition rates and means that the transition rates are constant in the limit of abundant resources.

In the PDE model, the transition rates k_{sm} , k_{ms} appear as coefficients in growth and decay terms in the differential equations. In the ABM we use a stochastic version of these transitions. At each time step, locusts switch from stationary to moving via a transition probability p_{sm} and from moving to stationary via p_{ms} , both of which are functions of $R_{n,m}$. The smooth transition rates k_{ms} and k_{sm} can be understood to be derived from these probabilities as the time step Δt approaches zero. Assuming Δt is small yields the following approximations,

$$p_{sm}(R_{n,m}) \approx k_{sm}(R_{n,m})\Delta t, \quad p_{ms}(R_{n,m}) \approx k_{ms}(R_{n,m})\Delta t. \quad (3)$$

This is equivalent to assuming that each locust undergoes only a single transition in any given time step. Biologically, these transition probabilities can be estimated from intermittent motion observed in the laboratory [26, 41] or the field [18, 27]. These observations suggest that transitions occur on a timescale of a few second. Additionally locusts also exhibit a post-prandial quiescence which may last several minutes, particularly after a large meal [19–21]. These timescales are much shorter than the period of collective marching (hours) which justifies our original approximation that the process is Markovian (memoryless).

Agent-Based Model (ABM): Pause-and-go motion on a space-time grid

We now describe the details and implementation of our agent-based model (ABM) which encodes the behavior of each individual locust. The temporal evolution of the ABM may be thought of as a probabilistic cellular automaton. The model is one dimensional in space, representing a 1-meter-wide cross section of the locust hopper band.

Our ABM tracks the position of each locust, their states (stationary or moving), and the spatial availability of resources (food). Locust position and the spatial distribution of resources are confined to a discrete lattice of points given by $x_n = n\Delta x$ and time $t_m = m\Delta t$, for $n, m \in \mathbb{N}$. We fix $\Delta x = v\Delta t$ so that a moving locust moves forward one step on the lattice per each time step.

Let $X_i(t_m)$ be the position of the i^{th} locust at time t_m . Let $\sigma_i(t_m)$ be a binary state variable where $\sigma_i = 1$ when the locust is moving and 0 otherwise. The motion of the locusts can now be expressed succinctly as

$$X_i(t_{m+1}) = X_i(t_m) + \sigma_i(t_m)v\Delta t = X_i(t_m) + \sigma_i(t_m)\Delta x, \tag{4}$$

where we have applied the value of the state variable at t_m throughout the interval of length Δt . Note this artifice ensures that the values X_i remain on the lattice for all time t_m .

We model transitions between stationary and moving states with a discrete-time Markov process given via the probabilities in Eq (3). Thus, at time t_m , each locust at position x_n has a probability $p_{sm}(R_{n,m})$ to switch from stationary $\sigma_i = 0$ to moving $\sigma_i = 1$ or a probability $p_{ms}(R_{n,m})$ to switch from moving to stationary.

We define the histogram variables mentioned above by simply counting the number of locusts in each state at each space-time grid point:

$$M_{n,m} = \sum X_n(t_m)\sigma_n(t_m) = \# \text{ of moving } (\sigma_i = 1) \text{ locusts at } (x_n, t_m) \tag{5}$$

$$S_{n,m} = \sum X_n(t_m)(1 - \sigma_n(t_m)) = \# \text{ of stationary } (\sigma_i = 0) \text{ locusts at } (x_n, t_m). \tag{6}$$

We model the resources with a scalar variable $R_{n,m}$ which is defined as available food, measured in grams, at time t_m in the interval of width Δx centered at x_n . Following Eq (1) and converting $S_{n,m}$ to a density, we have

$$\frac{dR_{n,m}}{dt} = -\lambda \frac{S_{n,m}}{\Delta x} R_{n,m}. \tag{7}$$

Solving Eq (7) (assuming $S_{n,m}$ is constant between t_m and t_{m+1}) yields

$$R_{n,m+1} = R_{n,m} e^{-\lambda S_{n,m} \frac{\Delta t}{\Delta x}}. \tag{8}$$

Biologically, this evolution implies that the resources in a patch of vegetation infested by a group of stationary, feeding locusts will decrease by approximately half in an amount of time inversely proportional to λ times the number of locusts in the patch. That is, the half-life of

resources in the patch is $\ln(2)\Delta x/(\lambda \cdot \# \text{ locusts})$. We initialize each simulation with $R_{n,1} = R^+$, indicating an initially constant field of resources.

Together with initial conditions, Eqs (3), (4) and (8) specify the evolution completely. Our agent-based model then takes the form of three sequential, repeating steps for each locust agent:

1. Update state S or M according to the Markov process.
2. If in state M , move to the right Δx .
3. If in state S , decrease resources in current location.

Each locust performs each of these steps simultaneously with all other locusts, and resources in each location are also updated simultaneously according to Eq (8).

PDE model: A conservation law for locusts

We construct a continuous-time, mean-field model for the density of locusts. As outlined in General model formulation, we write a continuous function of space and time $R(x, t)$ for the density of available resources. Similarly, we write $S(x, t)$ and $M(x, t)$ for the density of stationary and moving locusts, respectively. See Table 1 for comparison with the variables of the agent-based model.

These densities are governed by the partial differential equations

$$\begin{aligned} R_t &= -\lambda SR \\ S_t &= -k_{sm}S + k_{ms}M \\ M_t &= k_{sm}S - k_{ms}M - vM_x \end{aligned} \quad x \in \mathbb{R}, \quad t \in [0, \infty), \quad (9)$$

which describe the feeding, switching, and movement behaviors on the scale of the aggregate band. The rate of decrease of R is proportional to the density of stationary locusts and available resources as established in General model formulation. The constant of proportionality is given by the foraging rate λ . As in the ABM, locust foraging efficiency decreases as resources decrease. Note that the food R is decreasing in time at each spatial point x . The rate of change of S is determined wholly by the switching behavior. Here, the decrease of S represents the switching of locusts from stationary to moving with a rate dependent on R through $k_{sm}(R)$. Similarly, S increases as locusts switch from moving to stationary with rate $k_{ms}(R)$. See Eq (2) for the functional forms of k_{sm} , k_{ms} . The same terms with opposite signs contribute to changes in M . The term vM_x in the equation for M represents the marching of moving locusts to the right with the individual speed v . This spatial derivative makes the third equation into a standard transport equation. A full list of all parameters appears in Table 2.

We consider initial conditions with resources that are a positive constant R^+ for large x ; that is, $R(x, 0)$ has $\lim_{x \rightarrow \infty} R(x, 0) = R^+$. We assume initial locust densities $S(x, 0)$, $M(x, 0)$ are non-negative and smooth (continuous with continuous derivative). For biologically reasonable choices of such initial conditions, all solutions are guaranteed to remain non-negative, continuous, and finite by standard quasilinear hyperbolic PDE [42].

Finally, since the switching terms are of opposite signs in the S and M equations, we have mathematically guaranteed a conservation law. In particular, the total number of locusts in our 1-meter cross section $N = \int_{-\infty}^{\infty} (S + M) dx$ is conserved.

Numerical simulations. For direct numerical simulations of the PDE, we use a 4th-order Runge-Kutta method for the temporal derivative with step dt . By choosing $dx = v \cdot dt$ we approximate the spatial derivative by a simple shift of the discretized M on the spatial grid.

Table 3. Collective observables with ranges based on field research. Units are L = length [meters], T = time [seconds], C = number of locusts, P = locust density [number/(meter)²], and Q = resource density [grams/(meter)²]. Note that skewness (Σ) is nondimensional.

Symbol	Description	Units	Min	Max	Example Output	Citation
c	speed of collective band	L/T	0.0005	0.009	0.0053	[4, 10]
R^+	remaining resource density	Q	0	100	0.002	[44]
P	maximum locust density	P	950	4280	1296	[9, 10, 47]
W	threshold width of profile	L	30	500	18.6	[9, 10, 47]
Σ	skewness of locust profile	1	1	2	1.78	[9]

<https://doi.org/10.1371/journal.pcbi.1007820.t003>

This is equivalent to a first-order upwind scheme because

$$\frac{M(x_n, t_{m+1}) - M(x_n, t_m)}{dt} = -v \frac{M(x_n, t_m) - M(x_{n-1}, t_m)}{dx} \Rightarrow M(x_n, t_{m+1}) = M(x_{n-1}, t_m).$$

For additional accuracy, we implement these schemes using a split-step method, as in [43] for instance. All simulations of the PDE used Matlab.

Parameter identification

We identify a range of values for biological parameters from a variety of sources including research papers, Australian government guides and reports (particularly the Australian Plague Locust Commission), and agricultural organizations. A list of input parameters and ranges can be found in Table 2. A list of observable outcomes can be found in Table 3.

Input parameters.

Empirical estimates. We estimate five parameters directly from empirical observations: the total number of locusts N in the cross section, the initial resource density R^+ , the speed v of an individual locust, and the two switching rates when no resources are present $k_{sm}(R=0)$, $k_{ms}(0)$. We provide ranges for these parameters in the first five rows of Table 2.

The total number of locusts N in our model is the number of locusts in a 1-meter cross section as shown in Fig 1. We rely on Buhl et al [9] to estimate N . In Figure 1 of [9], the authors present three profiles of locust density computed by counting locusts in frames of video of a marching locust band taken during field experiments. The authors fit exponential curves to these data, see Figure 2 in [9], which yield exponential rates of decay of density in time. We use these rates to estimate the area under the density profiles by integrating a corresponding exponential function. This provides three estimates for the total number of locusts who passed under the camera, which range from 9300 to 15000. Rather than a precise measurement, we consider this an estimate and acknowledge that it may be improved by more direct analysis of the underlying data in [9]. We believe it does capture the correct order of magnitude and so include only a modestly larger range in our table.

Typical resource densities R^+ come from Meat and Livestock Australia [44]. This resource indicates that pasture with vegetation between 4 – 10cm high is desirable for livestock grazing. It also converts this range to a vegetation density measured in units of kilograms green Dry Matter per hectare. (Note that this measure discounts the mass of water in the vegetation, sometime up to 80%. While locusts typically feed on live non-dry vegetation, its water content does not provide energy or nutrients. As a result our variable R reflects not the harvestable greenery but instead represents the locust-edible resources.) We convert units and arrive at the range given in our table.

We obtained the speed v of an individual marching locust from experimental measurements in [45] and field data reported in [27]. The experiments were conducted with the desert

locust, *Schistocerca gregaria*, and results in a range of 0.0339 – 0.0532 m/sec. This range contains the estimate from field data for the Australian plague locust collected by Buhl and reported by Bach [27]. The latter source also provides a second (higher) estimate that accounts for hopping, a common behavior of the Australian plague locust. Buhl's observations also show an increase in an individual's speed (averaged over crawling and hopping) with increasing temperature. Our range in Table 2 spans all of these estimates. Most other recorded observations of speed represent collective information—the speed of the aggregate band—which we discuss in the subsection Collective observables—model outcomes. below.

Constants α and β represent the proportion of locusts that switch from stationary to moving (and vice versa) on bare ground, $R \approx 0$. One laboratory study [26] with *S. gregaria* provides data from which we draw out a single estimate for β as follows. The authors record the probability of these transitions in a laboratory area with no food present. They construct probability distributions (depending on time) for these transitions and fit curves to these distributions, see Figure 1 in [26]. They find an exponential best fit for the probability that a locust transitions from moving to stationary. The exponential rate represents a reasonable value for β , so we gather that $\beta \approx 0.368 \text{ sec}^{-1}$. We use this estimate to set a minimum value of $0.01 < \beta$ and provide an upper limit below. The same source does not provide an estimate for α because the authors find that the probability distribution for stationary to moving transitions is best described by a power law.

Instead, for α we rely on the field data of Buhl appearing in [27] for *C. terminifera*. A similar procedure as above yields an estimate of $\alpha \approx 0.56 \text{ sec}^{-1}$. We use this to set a maximal value of $1 > \alpha$ and provide a lower limit below. In using ranges for α and β , we aim to allow for natural variation between the two species for which there is data.

Additional parameters. The parameters below the horizontal line in Table 2 do not all have readily available estimates in the literature; likely because the individual information encoded in these parameters is difficult to measure empirically amid the chaos of the swarm. We discuss the effects each in our Parameter sensitivity analysis.

Constants η and θ represent the proportion of locusts that begin/restart or stop marching in a resource-rich environment, $R \approx R^+$. To empirically measure these would require a detailed examination of locusts marching in natural plant cover. We are not aware of a situation where such a study of marching has been conducted in a setting with abundant food.

To choose a range for η we rely on our biological assumption that a locust is more likely to begin moving when there are fewer resources nearby; that is, $\eta < \alpha$. (In our Parameter sensitivity analysis, this results in the bound $\eta/\alpha < 1$.) This assumption provides a lower bound for α and an upper bound for η . We choose 0 as a lower bound for η , since it seems conceivable that a hungry locust might be satisfied to remain near food indefinitely. The converse biological assumption, that a locust is less likely to stop moving when there are fewer resources nearby, leads us to conclude that $\beta < \theta$. (In our sensitivity analysis of, this results in the bound $1 < \theta/\beta$.) This provides our upper limit for β and our lower bound for θ . We choose our upper limit for θ to be significantly larger than η , the comparable transition rate with nearby food. This encodes an assumption that the attraction of nearby food is stronger than its absence. Note that these bounds are contained in the conditions we listed after introducing k_{sm} , k_{ms} in Eq (2). Namely, these choices force the transition rates to be decreasing and increasing respectively.

The parameters γ and δ determine how sharply the transition rates $k_{sm}(R)$ and $k_{ms}(R)$ depend on resources R . Specifically, they are the rate of exponential decrease and increase, respectively. One of our primary claims is that γ and δ must be positive, otherwise the transition rates k_{sm} and k_{ms} would be constant. More specifically, one may deduce that γ , δ should be of the same magnitude as $1/R^+$, since the functions $k_{sm}(R)$ and $k_{ms}(R)$ are defined on the

interval $[0, R^+]$. Using our range of R^+ values above, we obtain the ranges appearing in the table for γ and δ .

The individual foraging rate λ is difficult to estimate for two reasons. First, it represents an instantaneous rate of change while most data on locust consumption is averaged over days or weeks, as in [47]. We found finer measurements of feeding in [46], where rates are averaged over ten-minute intervals. After unit conversions, we estimated a range of consumption rates on the order of $10^{-8} - 10^{-6}$ grams/(locust-sec). However, these rates are measured in a laboratory setting where locusts are provided with abundant resources to feed. This highlights a second difficulty in estimating λ ; the lab data does not account for search times and so may represent a “consumption rate” rather than a foraging rate. To explain, recall that our ABM places a locust at a grid point which represents a rectangle of physical space with dimensions $\Delta x \times 1 \text{ m}^2$. A locust may need to move within this small rectangle to find an individual plant suitable for feeding. Since we track only the resource density in that local rectangle, this search time is simply accounted for in the foraging rate. Other factors such as digestion times and the post-prandial rest period complicate the matter further. With such persistent uncertainty, we allow a large range for λ and explore it thoroughly in our Parameter sensitivity analysis.

Example values. Throughout the remainder of the text we illustrate our results using the set of example parameter values appearing in the second column from the right in Table 2. These values produce in both models a density profile consistent with observed locust bands. We selected these values using insight gleaned from our parameter sensitivity analysis, for details see the end of our Parameter sensitivity analysis.

Collective observables—Model outcomes. We consider five measures of collective behavior. Table 3 provides an empirical range for each, estimated in the following paragraphs from data in the literature.

We approximated the collective speed c of the band from observations in [4, 10]. Authors of [10] observed that bands moved between 36 – 92 meters per day (in “green grass”). Table 4 in [10] estimates the times of day during which marching was observed, with a range of 3 to 7 total hours per day. We computed averages over these time intervals and converted units to obtain a range. In Clark [4], bands of locusts were observed for periods of an hour during daily marching and reports a range of average band speeds overlapping with the range computed above. Our Table 2 shows the union of all three ranges with rounding. Measuring this observable in our models is straightforward. In simulations of either the ABM or PDE we compute the mean position (or center of mass) of the locust band. Tracking the speed of the center of mass gives us the mean speed of the band. Additionally, analysis of the PDE model yields an explicit formula of for c with no need for simulations, details in Theoretical results for the PDE: Hopper bands as traveling waves.

The density of locust-edible food resources left behind by a band R^- does not appear to be well studied. Wright [47] makes a careful study of leftover grain fit for human consumption; however, data are reported after threshing and processing and does not describe the amount of remaining green matter edible by locusts. An alternative approach to understanding R^- could be to use [44] which suggests that a low range of green dry matter in pastures is 40 – 100 grams per square meter. This low range of green dry matter inhibits vegetation regrowth, increases erosion hazards, and is insufficient for grazing livestock. We emphasize that there is no data suggesting that a marching locust band leaves a field with leftover vegetation in this range. In particular, this provides us with an upper range only since some of the vegetation left behind may be inedible, even for voracious locusts. Thus we arrive at a lower bound of zero for R^- . To measure the resources left behind in our models, we take a spatial average over the part of our domain to the left of the band of locusts.

The maximum locust density $P = \max(S+M)$ in a band is taken from Table 1 in [10]. We used the range of estimates observed for III and IV instars. This range is in line with the data of [47] who estimated a maximum density of 4000 locusts per square meter. In [9], the authors observed maximum densities ranging from 600 – 1200 locusts per square meter. We expect that these densities lie in (and just out of) the lower end of our range because the studies of [9] were conducted on bare ground with no vegetation while, typically, locusts aggregate into denser bands in lush vegetation, as observed in [4] for instance. The maximum density of a band in our models is measured simply by adding the components S and M and taking the maximal value.

The width W of the band, measured parallel to the direction of motion, is taken primarily from Hunter et al [10]. Hunter et al measured the widths of bands by walking from the front into the band until “marching was no longer seen”. Estimates from other sources fall in line with part of the range found in Hunter. For instance, 30 – 140 meters in [47] or 50 – 200 meters in [9]. We attribute the large range of band widths in [10] to the fact that these observations come from bands with a variety of sizes, as can also be seen by the large range for maximum densities in the same data set.

Measuring band width W in our model is not entirely straightforward as we cannot simply observe where “marching [is] no longer seen”, as in [10]. Marching refers to a consistent movement of locusts with a preferred direction determined by alignment with their nearby neighbors. Since our models assume that locusts are always highly aligned, we rely on the locust density to determine where marching occurs. Experimental data and modeling work in [17] suggest that locusts in a group with a density greater than 20 locusts per square meter are likely to be highly aligned. We thus take W to be the length of the spatial interval where our density profile measures above the threshold of 20 locusts/m².

This threshold definition of width W is biological and observable but it is not a good quantitative measure of the shape of a density distribution. For instance, consider a distribution with a maximum density less than the threshold density. This distribution will always measure $W = 0$ regardless of if it is very wide with a large total mass or if it is narrow with a much smaller mass. In other words, W does not scale with the total number of locusts in our band. We therefore introduce a second notion of width for use in comparing the shapes of bands with different total masses. A natural choice is the standard deviation of locust positions. We denote our standard deviation width by W_σ and use it particularly in our Parameter sensitivity analysis. Unfortunately, there is no general correspondence between our two notions of width W and W_σ . Even for a fixed mass, one can construct distributions with different shapes and broad ranges of W_σ while keeping W constant. For a given parameter set and varying mass we do compute W and make some a posteriori comparisons below.

The skewness Σ of a distribution is the third central moment (nondimensionalized by W_σ^3) and measures the distribution’s symmetry about its mean. When $\Sigma = 0$ the distribution is symmetric while $\Sigma > 0$ suggests the distribution is leaning to the right with a longer tail on the left. (We acknowledge that this is the opposite of the standard convention.) Any exponential distribution e^{-Ax} has skewness $\Sigma = 2$. Since [9] has demonstrated that an exponential fits well the locust density behind the peak, we consider 2 as a physically realistic upper bound. Including the sharp increase and maximum density at the front of the band will decrease skewness suggesting that we might expect values in the range $1 < \Sigma < 2$.

Collective observables for example values. The example parameter values produce rather realistic collective outcomes; each of them is very nearly in the range obtained from the literature, see Table 3. A small exception is the threshold width W , which is less than twelve units outside a large range of several hundred units. Secondly, we remind the reader of our

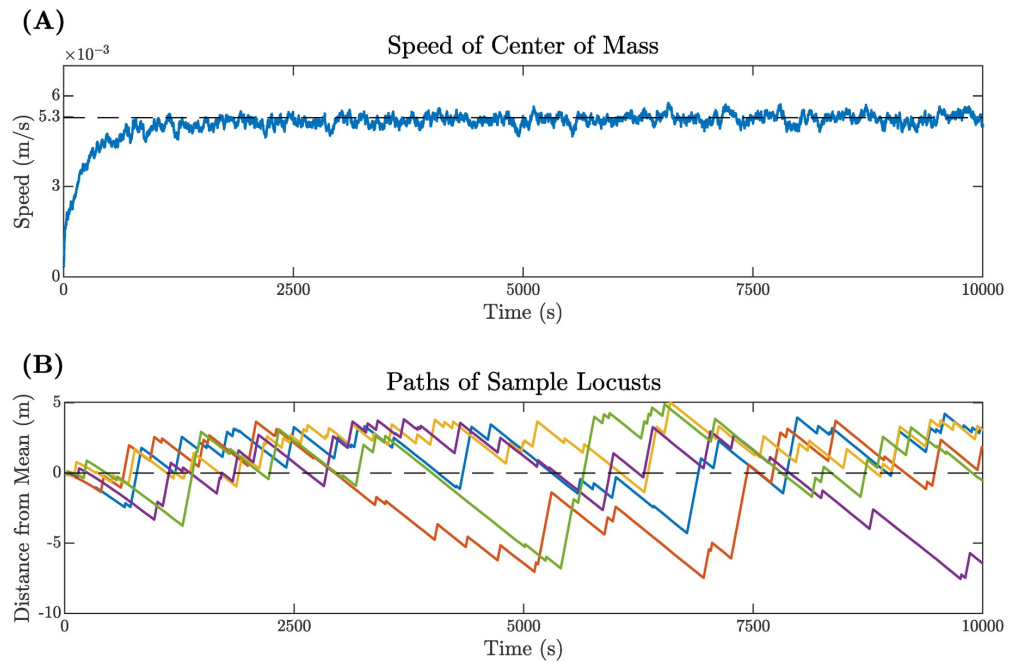


Fig 3. (A) Speed of the mean position of all locusts (center of mass of the swarm). Note the initial increase followed by a sustained period of variation around the average $c = 5.3 \times 10^{-3}$ m/sec. The standard deviation around c is 0.16×10^{-3} m/sec after transients. (B) Paths of five sample locusts, each shown in a different color. Note the initial transients appearing as curves near $t = 0$, after which all each path appears piece-wise linear with either positive or negative slope corresponding to when the given locust was in a moving or stationary state. Each locust spends some time ahead of the mean and some time behind it, reminiscent of the “leap-frogging” behavior noted in [4].

<https://doi.org/10.1371/journal.pcbi.1007820.g003>

difficulty in estimating the remaining resources. We interpret the small value $R^- = 0.002 \text{ g/m}^2$ to mean that in our models bands of locusts eat essentially all of the edible vegetable matter. We do not claim that they leave behind no vegetation at all.

Results

Numerical results for the ABM

Typical behavior for the agent-based model is a transient period followed by a traveling pulse shape, see [S1 Video](#) for a typical simulation. During the transient period, the locust histogram variables $S_{n,m}$ and $M_{n,m}$ evolve to an equilibrium profile that moves with constant speed, each with stochastic variation at each time step. The duration of the transient period and shape of the equilibrium profile vary depending on biological input parameters, while the level of stochastic noise depends primarily on the size of Δt . We explored a refinement of Δt from 1 sec to 0.1 sec and observed similar behavior with decreasing levels of noise. In all results presented in this section we use $\Delta t = 1$ sec and our example values from [Table 2](#) for all biological parameters.

[Fig 3A](#) shows the instantaneous speed of the mean position of all locusts over the course of 10000 sec. After an initial increase, the speed stabilizes around an average $c = 5.3 \times 10^{-3}$ m/sec with a standard deviation of 0.16×10^{-3} m/sec. Individual locusts move according to a biased

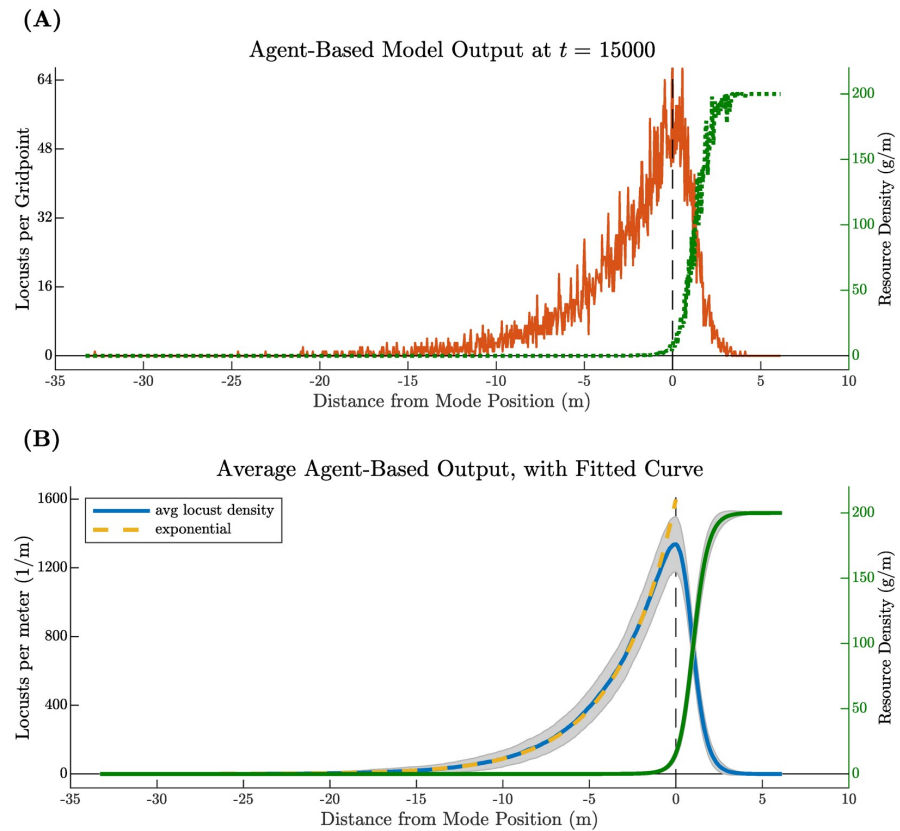


Fig 4. Output of the agent-based model with $N = 7000$ locust agents at time $t = 15000$ sec, re-centered so that the mean position of all locusts occurs at zero. (A) Shows the final state of the model including the number of locusts at each spatial grid point (orange) and the remaining resource density at each spatial grid point (dotted, green). Compares well with previously published data, see Figure 1 in [9]. (B) Displays a time-average of model outputs taken after an amount of time to account for transients (in this case, approximately $t = 7500$). Gray shading indicates \pm one standard deviation from the average locust density (blue) and resources (green). The tail of the pulse agrees well with an exponential least squares fit (gold). *S1 Video* shows a full, time-dependent simulation of the ABM.

<https://doi.org/10.1371/journal.pcbi.1007820.g004>

random walk around the mean position, as illustrated by the paths of five sample locusts in Fig 3B. Note the brief period of transients visible as arcing curves near $t = 0$, after which the distance to the mean is given by a piece-wise linear function for each locust. Intervals with positive slope $v - c$ correspond to periods where the individual was moving, while negative slope $-c$ indicates periods where the individual was stationary and the mean position marched on ahead.

The shape of the traveling pulse may be seen in Fig 4. The final histogram of locusts per spatial grid point at time $t = 15000$ appears in Fig 4A. A time-averaged pulse shape appears in Fig 4B. We construct this smooth density profile by averaging histograms for all time steps after the end of transients, in this case approximately $t = 7500$. Both plots show corresponding resource levels. The resources left behind R^- after the pulse has completely passed depends primarily on the foraging rate constant λ . Shape of the traveling pulse profile also depends on λ but also on a complex combination of parameters in the stationary-moving transition

probabilities p_{sm}, p_{ms} . For more detail on how the model depends upon parameters, see Parameter sensitivity analysis.

Qualitative and quantitative observations suggest that the tail of the density distribution of a hopper band is roughly exponential in shape [4, 9, 10]. Results from our agent-based model agree. We fit an exponential curve e^{a+bx} to the tail of our average traveling pulse and obtained $a = 4.11, b = 0.2831$ and a root-mean squared error of 15.94, see the gold curve in Fig 4B. These data are within an order of magnitude of those observed in the field from Figures 1 and 2 in [9]. (To make this comparison, one must convert the independent variable in the exponential from space in our numerical data to time in the empirical data. Since the pulse travels with constant speed c , we have $x = ct$ and our converted exponential is e^{a+bct} with $bc = 1.50 \times 10^{-3}$, compared with exponential rates on the order of 10^{-2} in [9]).

Theoretical results for the PDE: Hopper bands as traveling waves

Hopper bands require R-dependent switching. To demonstrate the importance of the R-dependence in the switching rates k_{sm}, k_{ms} , we first consider a simplification of our model. Suppose that these switching rates are constant ($k_{sm} \equiv \alpha, k_{ms} \equiv \beta$). We mathematically determine the long-time behavior of solutions to this simplified problem in S1 Appendix. For any locust density solution $\rho = S + M$, the center of mass moves to the right with a speed that approaches $v \frac{\alpha}{\alpha+\beta}$ as $t \rightarrow \infty$. This is consistent with our search for traveling-wave solutions. However, we also find that the asymptotic standard deviation $W_\sigma \sim \sqrt{t}$ so that solutions spread diffusively for all time. In other words, no coherent hopper bands form in the long-time limit. Gray dashed lines in Fig 5A depict this behavior, illustrating the decay of a locust density profile with resource-independent switching rates.

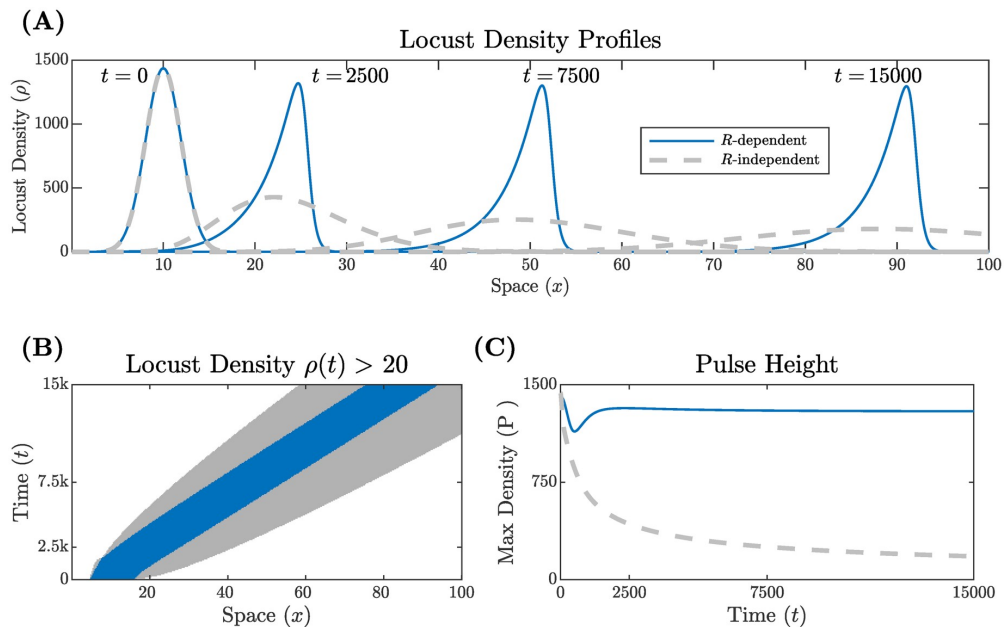


Fig 5. Locust density profiles with R-dependent (solid blue line) and R-independent (dashed gray line) switching rates. Each profile evolves from the same initial condition. (A) Shows snapshots of the density profiles over distance and time for both types of switching rates. (B) Illustrates the width of the bands where color represents a locust density greater than 20. (C) Displays the peak density of each pulse over time.

<https://doi.org/10.1371/journal.pcbi.1007820.g005>

Existence of traveling wave solutions. Returning to the main case with R -dependent switching, we show existence and development of hopper bands as traveling wave solutions to the PDE (9). A traveling wave is a solution with a fixed profile that propagates right or left with a constant speed c . Since locusts move only to the right in our model, we expect right-moving traveling waves and S2 Appendix includes a mathematical analysis of these solutions. Numerical simulations suggest that these traveling waves organize all long-time dynamics of the model. That is, all solutions with our initial condition appear to converge to a traveling wave. Biologically, we conclude that a typical initial distribution of locusts aggregates into a coherent hopper band. The solid blue curves in Fig 5A show snapshots of the asymmetrical traveling wave created by R -dependent switching rates.

Fig 5B and 5C compare the width and maximum density of the profiles for switching rates with and without resource dependence. In Fig 5B, colored regions correspond to a locust density greater than 20 locusts/m with gray and blue corresponding to R -independent and R -dependent switching rates, respectively. As the locust band without R -dependent switching progresses, the width of the gray region increases in time, showing diffusive spreading. On the other hand, the width of the locust band with R -dependent switching (blue) remains constant over time. Additionally, the locust band with R -dependent switching reaches a constant height as seen in Fig 5C (blue). In contrast, the maximum locust density with R -independent switching rates decreases over time as locusts spread out (dashed gray).

Traveling waves dynamically select collective observables. By viewing hopper bands as traveling waves, our existence proof also determines a relationship between the total number (or total mass) N of locusts in our 1-meter cross section, the average band speed c , and the initial and remaining resources R^+ and R^- . In S3 Appendix we show that these four variables must satisfy an explicit equation for any traveling wave. One consequence is that our model exhibits a selection mechanism whereby the average band velocity and the remaining resources are determined by the number of locusts in the band and the initial resource level.

These explicit equations are illustrated in Fig 6. Each subfigure shows curves on which R^+ is constant (level curves). Plotting these in the N, c -plane (mass vs. speed), we obtain Fig 6A. (Here each curve is parameterized by R^- .) Note that the curves appear monotone: speed c increases as a function of mass N . Biologically, this is what one expects; a larger swarm

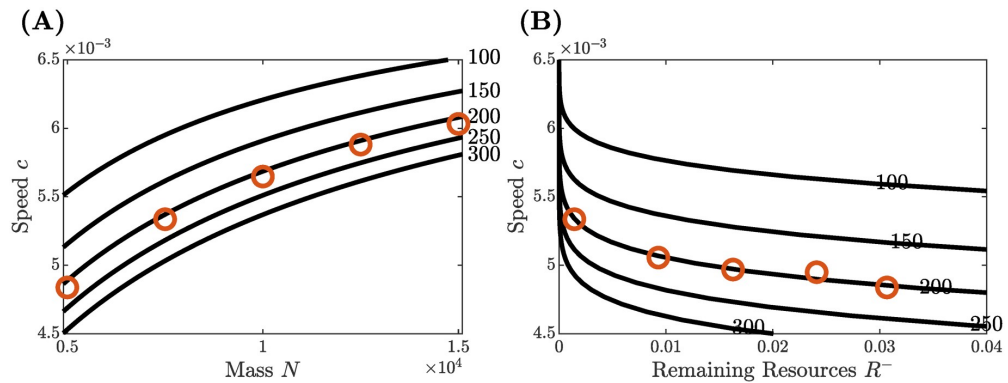


Fig 6. Level curves on which initial resources R^+ are constant (black curves) computed explicitly from the analytic formulas of the PDE model, and numerical data points (orange circle) generated by direct simulation of the ABM. (A) Illustrates that the average swarm speed c monotonically increases with the mass N and shows agreement with numerical data obtained for $N = 5000, 7500, 10000, 12500, 15000$. (B) Illustrates the inverse relationship between c and R^- and shows agreement with numerical data for $N = 5000, 5250, 5500, 6000, 7500$.

<https://doi.org/10.1371/journal.pcbi.1007820.g006>

consumes food more quickly and moves on at a faster average pace. In Fig 6B, we plot the same level curves in the R^- , c -plane (remaining resources vs. speed). (Now each curve is parameterized by N .) Again the curves are monotone but we now see that speed c decreases as a function of remaining resources R^- . Here we also observe that the speed is much more sensitive when the remaining resources are very small. In S3 Appendix, we use the explicit formulas to prove the monotonicity of speed as a function of input parameters.

Agreement between ABM and PDE

We evaluate agreement between our two models by comparing the collective observables of Table 3. We divide these into two groups: the shape of the band as characterized by maximum density P , width W , and skewness Σ ; and the mean speed c and remaining resources R^- , which we consider to be more agriculturally relevant.

ABM simulations and PDE analysis. The quantities c and R^- can be determined for the PDE model via the traveling wave analysis of the last section. This analysis results in explicit formulas in S3 Appendix. Substituting input parameters total mass N and initial resources R^+ , one can calculate exact results for c and R^- . These relationships are represented by level curves in Fig 6, for details see Theoretical results for the PDE: Hopper bands as traveling waves.

We ran direct numerical simulations of the ABM for selected values of the total mass $N = 5000, 5250, 5500, 6000, 7500, 10000, 12500, 15000$. In each simulation we used our example values for all other biological parameters. We ran each simulation for 2.5×10^4 time steps with $\Delta t = 1$ for a final end time of 25000 sec and confirmed that the simulation reached the end of transients. We measured the collective speed c and remaining resources behind the band R^- for each simulation. The resulting values agree with the explicit formulas to within 1% and are shown in Fig 6 (orange circle).

Direct simulation of both models. We used direct numerical simulation of both models to evaluate their agreement on the basis of the shape characteristics maximum density P , standard deviation width W_σ , and skewness Σ .

We ran both models for $nt = 2 \times 10^5$ time steps using our example parameters and a range for the foraging rate λ so that $-8 < \log(\lambda) < -4$. For each value of λ , we plot the shape characteristics in Fig 7. For the PDE, we measure the shape characteristics of the final output density profile. For the ABM, we measure the shape characteristics of a time-averaged density profile (as constructed in Fig 4B). The plots in Fig 7 are the result of continuation in the parameter $\log(\lambda)$. We begin with $\log(\lambda) = -4$ and chose initial conditions computed from independent simulations of each model. For each value of $\log(\lambda)$ the algorithm proceeds as follows: We run both models for nt time steps; measure P , W_σ , and Σ ; choose new spatial grids for each model based on the value of W_σ ; increase $\log(\lambda)$ by 0.1; and use the current output as the next initial condition. Practically speaking, the interval $-8 < \log(\lambda) < -4$ is in fact covered by three such continuations originating at -4 and -7 . Note that our numerical scheme begins to reach its limits as $\log(\lambda)$ approaches -8 because there the evolution of the profile shape is so slow that it requires very long computation times to reach equilibrium. This is also why we do not cover the full range of $\log(\lambda)$ explored in the next section.

To visually compare the profiles, see Fig 8. These six profiles are the result of running each model for $nt = 10^6$ time steps with our example parameter values and selected $\log(\lambda) = -7.4, -6.3, -4.2$. First, note the strong agreement along each row. Second, a data point (gold dot and x) from each of these $\log(\lambda)$ values is included in the plots of Fig 7. Since there is little difference between these data points and the rest in the figure, which are the result of only 2×10^5 time steps, we can conclude that the shape characteristics have reached near-equilibrium values. The gold x at $\log(\lambda) = -6.3$ demonstrates the stochasticity of the ABM—the maximum of a

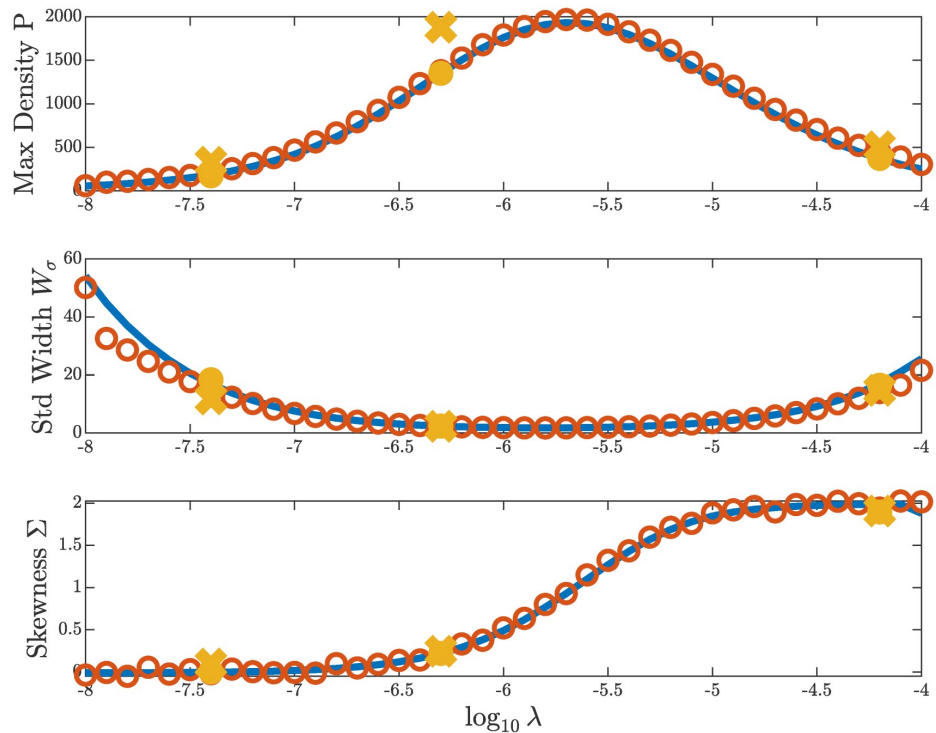


Fig 7. Comparison of the peak, width, and skewness of profiles from the PDE (blue line) and the ABM (orange circle), both obtained through direct numerical simulation for 2×10^5 time steps. Each shape observable is measured from the final numerical output for the PDE and from a time-averaged output the ABM. Longer simulations with 10^6 time steps, for ABM (gold x) and PDE (gold dot) show little evolution in the profile for longer times. Note that the maximum density is higher for long simulations of the ABM (gold x) because these represent a single instance, rather than an average.

<https://doi.org/10.1371/journal.pcbi.1007820.g007>

single distribution is larger than the maximum of the time-averaged profile, see Fig 8 (right, center).

Finally, these profiles also provide insight into the possible shapes of density profiles far from our example value of $\log(\lambda) = -5$. Immediately, we notice that the remaining resources R^- behind the pulse decrease quickly as foraging rate λ grows, confirming intuition. Next, the shape also varies dramatically as can be seen by noting that the horizontal axes in each row have vastly different scales. In particular, the profiles in the top row are short and wide while the middle row is narrow and tall, all having the same total number of locusts. The bottom row reveals a transition where the resources are nearly all depleted behind the pulse, leading to wide asymmetrical profile as observed in the field [10].

We carry out a more rigorous study of how the model responds to changes in the input parameters in the next section.

Parameter sensitivity analysis

The sensitivity of the model to its parameters was examined by computing Sobol indices [48] for several biologically observable quantities (see Table 3) with samples from the parameter

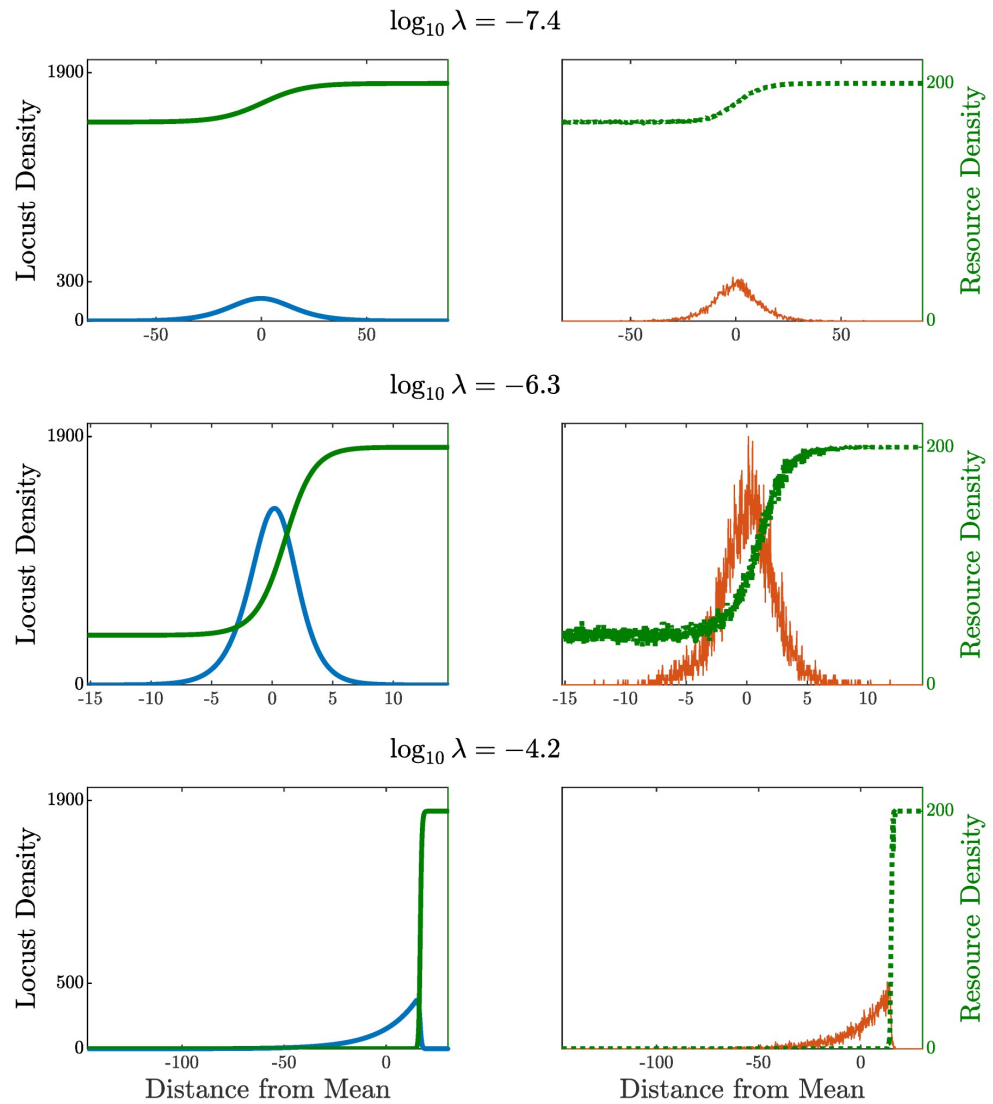


Fig 8. Model outputs from direct numerical simulation for 10^6 time steps. Density profiles from the PDE (blue, left) and histograms from the ABM (orange, right) for selected foraging rates $\log_{10}(\lambda) = -7.4, -6.3, -4.2$. For quick visual shape comparison, all outputs shifted so that center of mass is $x = 0$. Each plot corresponds to a data point in Fig 7 (gold x for ABM, gold dot for PDE). Note the differences in scale on the horizontal axes in each plot.

<https://doi.org/10.1371/journal.pcbi.1007820.g008>

space chosen via Saltelli’s extension of the Sobol sequence [49, 50]. Sobol indices represent a global, variance-based sensitivity analysis for nonlinear models that has become extremely popular in recent years for examining the performance of mathematical models in the context of data (e.g., [51, 52]). One of its strengths is the ability to calculate not just first-order (one-at-a-time) parameter sensitivity, but also second-order (two-at-a-time) and total-order (all possible combinations of parameters that include the given parameter) indices [50]. All indices are

normalized by the variance of the output variable. Here, we will focus on the first-order and total-order indices, and note that the presence of higher-order interactions between the parameters can be inferred by comparing differences between these two.

Scalar output quantities for our model (our collective observables) were all chosen with respect to the asymptotic traveling wave solution of the PDE model and are calculated by solving analytically for this solution. The observables chosen are the speed of the traveling wave c , the density of remaining resources R^- , the peak (maximum) density of the wave profile, the width of the profile measured by its standard deviation W_σ , and the skewness Σ of the profile. [Table 3](#) provides physically relevant ranges for these observables from empirical studies.

In the case of switching parameters α , β , θ , and η , sensitivity to the ratios θ/β and η/α and the ratio difference $\Delta = \alpha/\beta - \eta/\theta$ were used rather than the parameters themselves. One reason for this choice is to guarantee existence of a traveling wave solution; existence is guaranteed whenever $\Delta > 0$. Note that we also would like $\eta/\alpha < 1$ and $\theta/\beta > 1$ so that k_{sm} is a decreasing function of resources R and k_{ms} is an increasing function of resources. Additionally, these two conditions imply that $\Delta > 0$ so there is consistency between these constraints. Another reason for using these ratios lies in mathematical interpretation: Δ is a measure of the difference in asymptotic switching rates behind the pulse (small R , α/β) and ahead of the pulse (large R , η/θ), and the two other ratios η/α (θ/β) describe how much the stationary to moving (moving to stationary) switching rates depend on R . More specifically, as these ratios approach 1 the switching rate changes little as R increases, while η/α close to zero or θ/β large implies a relatively large change in the switching rate. With these ratios and a value for β (chosen because we have some biological data for β), all four parameters in the ratios are uniquely determined.

Results are shown in [Fig 9](#). All bars are stacked with each color corresponding to a different observable; reading across the parameters, the length of like colors can be compared. Critically, the parameter sensitivity is with respect to the range of parameter values given in the table included with [Fig 9](#). These ranges were chosen to represent both biologically expected values (when information about these values could be obtained) and the necessary conditions for a traveling wave solution.

One immediate observation concerning the Sobol sensitivity analysis in [Fig 9](#) is that $\log_{10}(\lambda)$ and $\log_{10}(\Delta)$ have a large effect on the collective observables of the pulse. Recall that λ is the parameter encoding the foraging rate; Δ is discussed in detail earlier in this section. The bottom row of [Fig 9](#) shows the impact of these parameters on the density of resources asymptotically left behind the locust band as a fraction of the starting density (R^-/R^+) and the ratio of the traveling wave velocity to the marching speed of a locust (c/v) respectively. Max density, pulse width as measured by standard deviation, and skewness also depend heavily on these two parameters as seen in the top row of [Fig 9](#). This is in fact unsurprising since λ and Δ have by far the largest sample space range in terms of order of magnitude, and for this reason are the only ones examined on a log scale while all other parameters are on a linear scale. To explain this discrepancy, we remind the reader that our chosen sampling ranges represent our uncertainty about the value that the parameters should take on in nature given all the information we were able to find in the biological literature. Our conclusion with this analysis then is that the model is in fact sensitive to this level of uncertainty in $\log_{10}(\lambda)$ and $\log_{10}(\Delta)$, and we should seek to narrow down the possibilities given what we know about observable, biological characteristics of the traveling locust band generated by our parameter choices ([Table 3](#)). Through the following numerical analysis of our sample data, we do just that.

To begin, we further illustrate the effect of varying $\log_{10}(\lambda)$ and $\log_{10}(\Delta)$ on the fraction of resources remaining R^-/R^+ (in [Fig 10A](#)) and on the ratio of the average pulse speed compared to the speed of a moving locust c/v (in [Fig 10B](#)). In each figure, we plot a uniform random subset of the sample points used in the Sobol sensitivity analysis for the purpose of down-sampling

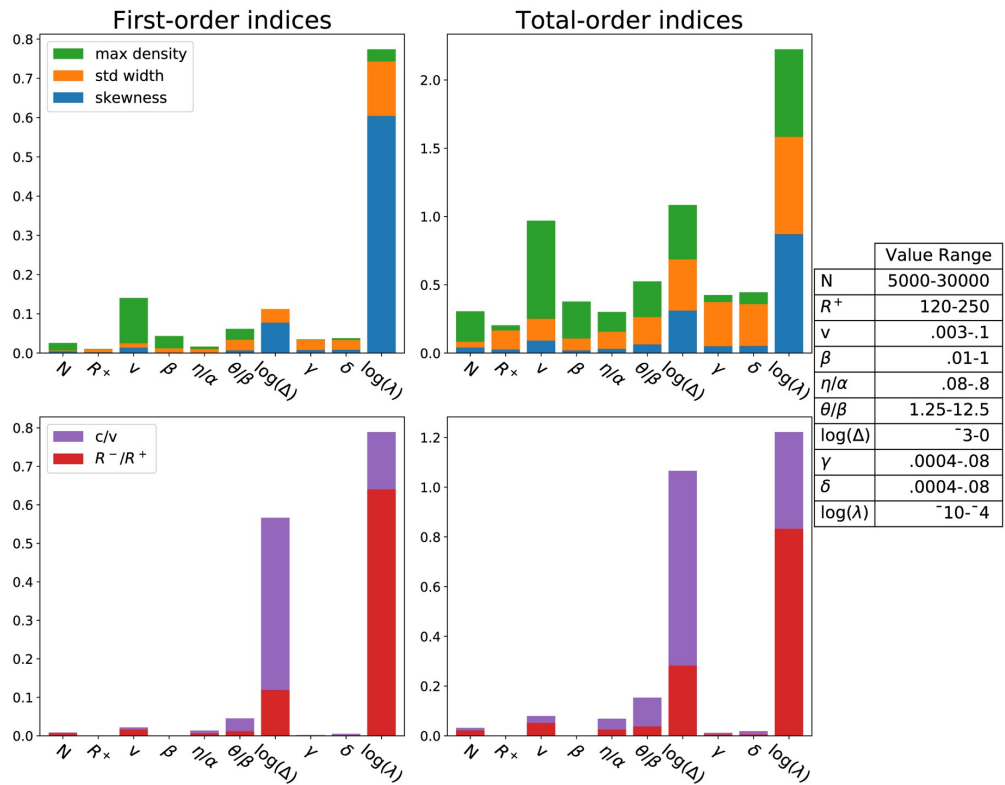


Fig 9. Sensitivity of various traveling wave observables to model parameters (bars are stacked). See Table 2 for parameter definition and ranges; this analysis was run using 4,400,000 samples from the given ranges. All log functions are base-10. First-order indices neglect all interactions with other parameters while total-order indices measure sensitivity through all higher-order interactions. Max 95% confidence intervals for the response variables was 0.01 for the first-order indices, 0.049 for total-order.

<https://doi.org/10.1371/journal.pcbi.1007820.g009>

the image and better visualizing sparse regions in the parameter space—it is qualitatively the same when using all sample points from the Sobol analysis.

Inspecting Fig 10A we note that, generally, at small λ a majority of resources persist after the locust front has passed while at large λ , the majority of resources are consumed. The red dot on the λ axis represents the example parameter set described in Table 2 which we believe to be a relatively feasible choice of parameter values in the context of the biological data about the observables in Table 3. We acknowledge that this appears to suggest the locusts leave behind no vegetation at all, but remember that our variable R represents locust-edible resources—there may be dry plant matter left behind that even locusts would not consume.

Locust swarms observed in the field have a characteristic sharp rise at the beginning of the front and an exponential decay in the tail, see [9] for a quantitative analysis. This observation suggests that the skewness Σ is positive and less than or approximately equal to 2 (see Table 3). Fig 11 investigates the relationship between skewness Σ , foraging rate λ , and the difference of ratios Δ . For $\lambda < 10^{-7}$, most values of Σ are negative, indicating an unrealistic density profile leaning to the left. As λ increases from 10^{-7} to 10^{-4} , Σ increases and clusters around 2. A smattering of points appear with $\Sigma > 2$ but these all correspond to profiles with unbiologically large

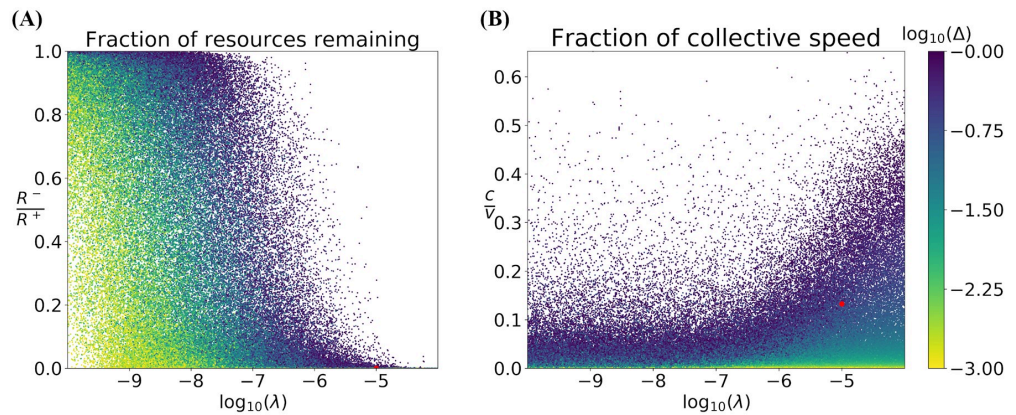


Fig 10. Scatter plot of (A) remaining resource fraction R^-/R^+ and (B) fraction of the traveling wave speed c over individual locust speed v as a function of the foraging rate λ and colored by Δ , the difference in asymptotic switching rates behind and ahead of the pulse. Points are taken from the parameter ranges in Table 2 and represent 5% of all the points sampled for the Sobol analysis, chosen randomly. The red dots represent the example parameter set described in Table 2.

<https://doi.org/10.1371/journal.pcbi.1007820.g010>

maximum locust densities, as demonstrated by Fig 11B which only shows profiles with maximum locust density <10,000.

To identify a set of parameter inputs that would produce a density profile with observable quantities matching those found in the literature (see Collective observables—model outcomes), we finally sorted the data underlying these figures and conditioned on desirable observable properties as specified in Table 3. This resulted in the example parameters specified in Table 2, with context provided by Figs 10 and 11. The results of the model run with these parameters can be seen in the figures included within the previous results sections.

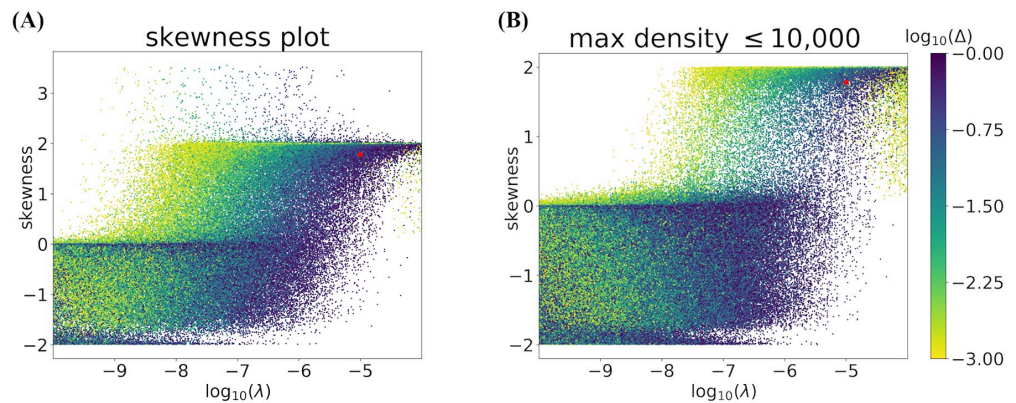


Fig 11. Skewness as a function of foraging rate (λ) and colored by Δ . Fig 11A is representative of the entire sampled parameter space while Fig 11B shows only the points with peak wave amplitudes less than 10,000 locusts per square meter. Points are taken from the parameter ranges in Table 2 and represent 5% (in the case of Fig 11A) and 50% (in the case of Fig 11B) of all the points sampled for the Sobol analysis, chosen randomly. The red dot represents the example parameter set described in Table 2.

<https://doi.org/10.1371/journal.pcbi.1007820.g011>

Discussion

We present two minimal models for hopper bands of the Australian plague locust and demonstrate that resource consumption can mediate pulse formation. In these models all locusts are aligned and are either stationary (and feeding) or moving. Our agent-based model (ABM) tracks the locations, state, and resource consumption of individuals. In tandem, our partial differential equation (PDE) model represents the mean-field of the ABM. Both models generically form pulses as long as the transition rate from stationary to moving states is diminished by the presence of resources and/or the transition from moving to stationary states is enhanced by the presence of resources.

The ABM and the PDE each allow us to examine different facets of the problem. The ABM is easy to simulate and directly relates to observations at the scale of individual locusts. It captures pulse formation and propagation, reproduces the stochastic variation seen in the field, and lets us track individual locusts which perform random walks within the band. The PDE model provides a theoretical framework for proving the existence of traveling pulses. This framework facilitates analysis of the collective behavior of the band including mean speed, total resource consumption, maximum locust density, pulse width, and pulse skewness. In turn, this theory enables us to conduct an in-depth sensitivity analysis of the pulse's characteristics with respect to the input parameters. The two models are consistent in the following sense: the characteristics of pulses in the ABM, when averaged over many realizations, correlate precisely with the densities in the PDE model.

We are fortunate that there is a healthy literature addressing the behavior of the Australian plague locust, notably the shape and speed of observed bands [4, 9, 10, 16, 46]. We have used these studies to estimate ranges for the organism-level parameters in our models. Some of these parameters (such as individual marching speed) have been carefully measured yielding narrow ranges. Others (notably the individual foraging rate) can only be deduced to lie within a range of several orders of magnitude. Using these biologically plausible ranges, we analyze the sensitivity of a pulse's characteristics to changes in the input parameters. Sampling parameter values from within these ranges, we examine the resulting speed, remaining resources, and pulse peak, width, and skewness of over 4.4×10^6 traveling pulse profiles. Sobol sensitivity analysis quantifies the change in these characteristics as a function of the change in each input parameter. Guided by this analysis, we are able to identify a set of parameters that produces pulses concordant with those observed in the field. We conclude that resource-dependent transitions are a consistent explanation for the formation and geometry of traveling pulses in locust hopper bands.

A reasonable question is whether a different mechanism can drive pulse formation or if the formation of pulses is enhanced by a combination of behaviors. Prior works, both for the Australian plague locust and for other locust species, investigate a variety of social mechanisms for collective movement in hopper bands. In two agent-based modeling studies [23, 27], pulses are among a handful of aggregate band structures obtained by varying the parameters that model individual locust behavior. A continuum approach in [30] finds traveling pulses in a PDE similar to our Eq (9) but without accounting for resources. Instead, social behavior is encoded via dependence on locust density of both the transition rates and the speed. This is coarsely akin to our model where resource-dependent transitions between moving and stationary states is necessary for pulse formation, see S1 Appendix. However, a model with social behavior as the only driving factor does not account for the observations of Clark [4] and Hunter [10] that *C. terminifera* manifests pulse-shaped bands with varying shapes based on the surrounding vegetation. We believe that incorporating both social and resource-dependent behaviors will better reproduce field observations.

Further experiments and field observations could help to elucidate the combined roles of resources and social behavior in the formation of hopper bands. While there is a considerable literature on the social [3, 9] and feeding [15, 46] behavior of *C. terminifera*, less progress has been made in quantifying the effect of food on individuals in dense bands exhibiting collective motion. One notable exception is the recent study of Dkhili et al. [19]. Looking ahead, field data could be collected as video while a hopper band moved through lush vegetation, see the methods in [9]. With continuing advances in motion tracking, for instance as employed in [28], one could collect time-series data on each individual moving through the frame. From such data one could draw out the effects of nearby vegetation, satiation or hunger, and local locust density on pause-and-go motion. In turn these processes could be modeled more thoroughly.

We see our present models as a testbed upon which one may develop extensions that capture more of the complexity in locust hopper behavior. The most natural of these extensions is to consider locusts' social behavior, as discussed above. A second is to include stochastic, individual, and environmental variation. This could be incorporated into the agent-based model in order to examine the robustness of pulse characteristics with respect to a distribution of individual marching speeds, or even large hops, as in [27]. For the PDE model, random variations in locust movement could naturally be represented by a linear diffusion term. Thirdly, we could incorporate motion of locusts transverse to the primary direction of propagation. This two-dimensional model might aim to capture the curving of the front of hopper bands often seen in the field. Lastly, large changes in resource density could be included to represent the band entering or exiting a lush field or pasture, with a view towards informing barrier control strategies as discussed in [11, 19]. These extensions could help explain the variety of morphologies and density profiles—including curving dense fronts, complex fingering, and lower-density columns—observed in hopper bands of the Australian plague locust and other species.

Supporting information

S1 Appendix. Resource-independence: The Telegrapher's Equation. Supposing that the stationary-moving transition rates k_{sm} , k_{ms} are independent of R , we construct an argument using moments of the resulting density distributions to show that solutions spread indefinitely with a gaussian shape. In particular, there are no coherent pulse solutions with a steep front. (PDF)

S2 Appendix. Traveling wave analysis. We prove the existence of traveling wave solutions to the PDE (9) using an invariant region argument. The existence result also provides a selection mechanism; that is, for a given set of parameter inputs there is only one traveling wave. (PDF)

S3 Appendix. Formulas for N , c , R^+ , R^- . In S2 Appendix we show existence of a traveling wave solution. We now characterize this solution with explicit formulas that relate N , c , R^+ , and R^- . Given any two of these variables and the remaining model parameter inputs, these formulas determine the other two exactly. (PDF)

S1 Video. Visualizations of the Agent-Based Model. Video showing timesteps from a simulation of our Agent-Based Model (ABM): Pause-and-go motion on a space-time grid with example parameter values from Table 2. The top panel shows a schematic of the 1-meter cross section represented by our one-dimensional model. Each locust (maroon and blue dots) has a unique horizontal lane in this schematic; there is no vertical motion. The bottom panel shows

a line plot (orange) reporting the number of locusts, both stationary and moving, at each spatial gridpoint and the resource density (green); compare to Fig 4B. (M4V)

Acknowledgments

This collaboration began as part of a Mathematics Research Community of the American Mathematical Society. We thank Tom Barr for his role in organizing this program and also to the leaders of our session on Agent-based Modeling in Biological and Social Systems including Maria R. D'Orsogna, Alan Lindsay, Chad Topaz, Alexandria Volkening, and Lori Ziegelmeier. We are also grateful to the Institute for Advanced Study which hosted our group for a subsequent research visit through their Summer Collaborators Program. We wish to thank Leah Edelstein-Keshet who brought this problem to our attention and for her thoughtful insights on this work. Andrew Bernoff also thanks Edward Green and Jerome Buhl and the hospitality of the University of Adelaide for supporting a visit which lead to many insightful conversations about this work. We are also deeply grateful to Jerome Buhl for his encyclopedic knowledge of locusts, notably the Australian plague locust, for sharing and confirming some of the biological estimates in this paper, and for his comments on an earlier draft of this work.

Author Contributions

Methodology: Andrew J. Bernoff, Michael Culshaw-Maurer, Rebecca A. Everett, Maryann E. Hohn, W. Christopher Strickland, Jasper Weinburd.

Writing – original draft: Andrew J. Bernoff, Michael Culshaw-Maurer, Rebecca A. Everett, Maryann E. Hohn, W. Christopher Strickland, Jasper Weinburd.

Writing – review & editing: Andrew J. Bernoff, Michael Culshaw-Maurer, Rebecca A. Everett, Maryann E. Hohn, W. Christopher Strickland, Jasper Weinburd.

References

1. Ariel G, Ayali A. Locust Collective Motion and Its Modeling. *PLOS Computational Biology*. 2015; p. 1–25.
2. Uvarov B. Grasshoppers and Locusts. vol. 2. London, UK: Cambridge University Press; 1977.
3. Gray LJ, Sword GA, Anstey ML, Clissold FJ, Simpson SJ. Behavioural Phase Polyphenism in the Australian Plague Locust (*Chortoicetes Terminifera*). *Biology Letters*. 2009; 5(3):306–309. <https://doi.org/10.1098/rsbl.2008.0764> PMID: 19324645
4. Clark LR. Behaviour of Swarm Hoppers of the Australian Plague locust *Chortoicetes terminifera* (Walker). Commonwealth Scientific and Industrial Research Organization, Australia. 1949; 245:5–26.
5. Simpson SJ, McCaffery AR, Hägele BF. A Behavioral Analysis of Phase Change in the Desert Locust. *Biol Rev*. 1999; 74(4):461–480. <https://doi.org/10.1111/j.1469-185X.1999.tb00038.x>
6. Pener MP, Simpson SJ. Locust Phase Polyphenism: An Update. In: *Advances in Insect Physiology*. vol. 36. Elsevier; 2009. p. 1–272.
7. Love G, Riwoe D. Economic costs and benefits of locust control in eastern Australia. Canberra: Australian Plague Locust Commission; 2005. 05.14.
8. Symmons PM, Cressman K. Desert Locust Guidelines. Rome: UNFAO; 2001.
9. Buhl J, Sword GA, Clissold FJ, Simpson SJ, Buhl J, Sword GA, et al. Group structure in locust migratory bands. *Behavioral Ecology and Sociobiology*. 2011; 65(2):265–273. <https://doi.org/10.1007/s00265-010-1041-x>
10. Hunter DM, McCulloch L, Spurgin PA. Aerial detection of nymphal bands of the Australian plague locust (*Chortoicetes terminifera* (Walker)) (Orthoptera: Acrididae). *Crop Protection*. 2008; 27:118–123. <https://doi.org/10.1016/j.cropro.2007.04.016>

11. Hunter DM. Advances in the Control of Locusts (Orthoptera: Acrididae) in Eastern Australia: From Crop Protection to Preventive Control. *Australian Journal of Entomology*. 2004; 43(3):293–303. <https://doi.org/10.1111/j.1326-6756.2004.00433.x>
12. Silliman BR, McCoy MW, Angelini C, Holt RD, Griffin JN, van de Koppel J. Consumer Fronts, Global Change, and Runaway Collapse in Ecosystems. *Annual Review of Ecology, Evolution, and Systematics*. 2013; 44(1):503–538. <https://doi.org/10.1146/annurev-ecolsys-110512-135753>
13. Spratt W. Risk management of a major agricultural pest in Australia—plague locusts. *The Australian Journal of Emergency Management*. 2004; 19(3):20–25.
14. Walton CS, Hardwick L, Hanson J. Locusts in Queensland: Pest status review series—Land protection. Queensland Government. 1994; 78(February 2003):1193.
15. Clissold FJ, Sanson GD, Read J. The paradoxical effects of nutrient ratios and supply rates on an outbreaking insect herbivore, the Australian plague locust. *Journal of Animal Ecology*. 2006; 75(4):1000–1013. <https://doi.org/10.1111/j.1365-2656.2006.01122.x> PMID: 17009763
16. Wright DE. Analysis of the development of major plagues of the Australian plague locust *Chortoicetes terminifera* (Walker) using a simulation model. *Australian Journal of Ecology*. 1987; 12(4):423–437. <https://doi.org/10.1111/j.1442-9993.1987.tb00959.x>
17. Buhl J, Sumpter DJT, Couzin ID, Hale JJ, Despland E, Miller ER, et al. From Disorder to Order in Marching Locusts. *Science*. 2006; 312:1402–1406. <https://doi.org/10.1126/science.1125142> PMID: 16741126
18. Buhl J, Sword GA, Simpson SJ. Using field data to test locust migratory band collective movement models. *Interface Focus*. 2012; 2:757–763. <https://doi.org/10.1098/rsfs.2012.0024> PMID: 24312729
19. Dkhili J, Maeno KO, Idrissi Hassani LM, Ghaout S, Piu C. Effects of starvation and Vegetation Distribution on Locust Collective Motion. *Journal of Insect Behavior*. 2019; 32(3):207–217. <https://doi.org/10.1007/s10905-019-09727-8>
20. Kennedy JS, Moorhouse JE. Laboratory observations on locust responses to wind-borne grass odour. *Entomologia Experimentalis et Applicata*. 1969; 12(5):487–503. <https://doi.org/10.1111/j.1570-7458.1969.tb02547.x>
21. Moorhouse JE. Experimental analysis of the locomotor behaviour of *Schistocerca gregaria* induced by odour. *Journal of Insect Physiology*. 1971; 17(5):913–920. [https://doi.org/10.1016/0022-1910\(71\)90107-7](https://doi.org/10.1016/0022-1910(71)90107-7)
22. Vicsek T, Czirok A, Ben Jacob E, Cohen I, Shochet O. Novel Type of Phase-Transition in a System of Self-Driven Particles. *Phys Rev Lett*. 1995; 75(6):1226–1229. <https://doi.org/10.1103/PhysRevLett.75.1226> PMID: 10060237
23. Dkhili J, Berger U, Idrissi Hassani LM, Ghaout S, Peters R, Piu C. Self-Organized Spatial Structures of Locust Groups Emerging from Local Interaction. *Ecological Modelling*. 2017; 361:26–40. <https://doi.org/10.1016/j.ecolmodel.2017.07.020>
24. Grégoire G, Chaté H, Tu Y. Moving and Staying Together Without a Leader. *Physica D*. 2003; 181(3–4):157–170. [https://doi.org/10.1016/S0167-2789\(03\)00102-7](https://doi.org/10.1016/S0167-2789(03)00102-7)
25. Romanczuk P, Couzin ID, Schimansky-Geier L. Collective Motion due to Individual Escape and Pursuit Response. *Physical Review Letters*. 2009; 010602:1–4.
26. Ariel G, Ophir Y, Levi S, Ben-Jacob E, Ayali A. Individual pause-and-go motion is instrumental to the formation and maintenance of swarms of marching locust nymphs. *PLOS One*. 2014; 9(7):e101636. <https://doi.org/10.1371/journal.pone.0101636> PMID: 24988464
27. Bach A. Exploring locust hopper bands emergent patterns using parallel computing. Université Paul Sabatier Toulouse III; 2018.
28. Nilsen C, Paige J, Warner O, Mayhew B, Sutley R, Lam M, et al. Social Aggregation in Pea Aphids: Experiment and Random Walk Modeling. *PLOS One*. 2013; 8(12):e83343. <https://doi.org/10.1371/journal.pone.0083343> PMID: 24376691
29. Navoret L. A two-species hydrodynamic model of particles interacting through self-alignment. *Mathematical Models and Methods in Applied Sciences*. 2013; 23(06):1067–1098. <https://doi.org/10.1142/S0218202513500036>
30. Edelstein-Keshet L, Watmough J, Grunbaum D. Do travelling band solutions describe cohesive swarms? An investigation for migratory locusts. *Journal of Mathematical Biology*. 1998; 36:515–549. <https://doi.org/10.1007/s002850050112>
31. Topaz CM, D'Orsogna MR, Edelstein-Keshet L, Bernoff AJ. Locust Dynamics: Behavioral Phase Change and Swarming. *PLOS Comp Bio*. 2012; 8(8):e1002642. <https://doi.org/10.1371/journal.pcbi.1002642>
32. Nonaka E, Holme P. Agent-Based Model Approach to Optimal Foraging in Heterogeneous Landscapes: Effects of Patch Clumpiness. *Ecography*. 2007; 30(6):777–788. <https://doi.org/10.1111/j.2007.0906-7590.05148.x>

33. Bernoff AJ, Topaz CM. Biological Aggregation Driven by Social and Environmental Factors: A Nonlocal Model and its Degenerate Cahn-Hilliard Approximation. *SIAM J Appl Dyn Sys*. 2016; 15(3):1528–1562. <https://doi.org/10.1137/15M1031151>
34. Keller EF, Segel LA. Traveling bands of chemotactic bacteria: A theoretical analysis. *Journal of Theoretical Biology*. 1971; 30(2):235–248. [https://doi.org/10.1016/0022-5193\(71\)90051-8](https://doi.org/10.1016/0022-5193(71)90051-8) PMID: 4926702
35. Gueron S, Liron N. A model of herd grazing as a travelling wave, chemotaxis and stability. *Journal of Mathematical Biology*. 1989; 27(5):595–608. <https://doi.org/10.1007/bf00288436> PMID: 2794805
36. Lewis MA. Spatial Coupling of Plant and Herbivore Dynamics: The Contribution of Herbivore Dispersal to Transient and Persistent “Waves” of Damage. *Theoretical Population Biology*. 1994; 45(3):277–312. <https://doi.org/10.1006/tpbi.1994.1014>
37. Bell WJ. Searching Behavior Patterns in Insects. *Annual Review of Entomology*. 1990; 35(1):447–467. <https://doi.org/10.1146/annurev.en.35.010190.002311>
38. Charnov EL. Optimal Foraging, the Marginal Value Theorem. *Theoretical Population Biology*. 1976; 9(2):129–136. [https://doi.org/10.1016/0040-5809\(76\)90040-x](https://doi.org/10.1016/0040-5809(76)90040-x) PMID: 1273796
39. Simpson SJ, Raubenheimer D. The Hungry Locust. *Advances in the Study of Behavior*. 2000; p. 1–44. [https://doi.org/10.1016/S0065-3454\(08\)60102-3](https://doi.org/10.1016/S0065-3454(08)60102-3)
40. Bernays EA, Chapman RF. Meal size in nymphs of *Locusta migratoria*. *Entomologia Experimentalis et Applicata*. 1972; 15(4):399–410. <https://doi.org/10.1111/j.1570-7458.1972.tb00227.x>
41. Bazazi S, Bartumeus F, Hale JJ, Couzin ID. Intermittent Motion in Desert Locusts: Behavioural Complexity in Simple Environments. *PLoS Computational Biology*. 2012; 8(5):e1002498. <https://doi.org/10.1371/journal.pcbi.1002498> PMID: 22589707
42. Evans LC. *Partial differential equations*. Providence, R.I.: American Mathematical Society; 2010.
43. Bernoff AJ. Slowly varying fully nonlinear wavetrains in the Ginzburg-Landau equation. *Physica D: Nonlinear Phenomena*. 1988; 30(3):363–381. [https://doi.org/10.1016/0167-2789\(88\)90026-7](https://doi.org/10.1016/0167-2789(88)90026-7)
44. Meat & Livestock Australia. Improving pasture use with the MLA Pasture Ruler; 2014. Available from: <https://mbfp.mla.com.au/pasture-growth/>.
45. Bazazi S, Buhl J, Hale JJ, Anstey ML, Sword GA, Simpson SJ, et al. Collective Motion and Cannibalism in Locust Migratory Bands. *Current Biology*. 2008; 18(10):735–739. <https://doi.org/10.1016/j.cub.2008.04.035> PMID: 18472424
46. Bernays EA, Chapman RF. The role of food plants in the survival and development of *Chortocetes terminifera* (Walker) under drought conditions. *Australian Journal of Zoology*. 1973; 21:575–592. <https://doi.org/10.1071/ZO9730575>
47. Wright DE. Damage and loss in yield of wheat crops caused by the Australian plague locust, *Chortocetes terminifera* (Walker). *Australian Journal of Experimental Agriculture*. 1986; 26(5):613–618. <https://doi.org/10.1071/EA9860613>
48. Sobol IM. Global sensitivity indices for nonlinear mathematical models and their Monte Carlo estimates. *Math and Comput in Simul*. 2001; 55(1-3):271–280. [https://doi.org/10.1016/S0378-4754\(00\)00270-6](https://doi.org/10.1016/S0378-4754(00)00270-6)
49. Saltelli A. Making best use of model evaluations to compute sensitivity indices. *Comp Phys Comm*. 2002; 145(2):280–297. [https://doi.org/10.1016/S0010-4655\(02\)00280-1](https://doi.org/10.1016/S0010-4655(02)00280-1)
50. Saltelli A, Annoni P, Azzini I, Campolongo F, Ratto M, Tarantola S. Variance based sensitivity analysis of model output. Design and estimator for the total sensitivity index. *Comp Phys Comm*. 2010; 18(2):259–270. <https://doi.org/10.1016/j.cpc.2009.09.018>
51. Aggarwal M, Hussaini MY, De La Fuente L, Navarrete F, Cogan NG. A framework for model analysis across multiple experiment regimes: Investigating effects of zinc on *Xylella fastidiosa* as a case study. *Journal of Theoretical Biology*. 2018; 457(14):88–100. <https://doi.org/10.1016/j.jtbi.2018.08.028> PMID: 30138631
52. Battista NA, Pearcy LB, Strickland WC. Modeling the prescription opioid epidemic. *Bulletin of Mathematical Biology*. 2019; 81(7):2258–2289. <https://doi.org/10.1007/s11538-019-00605-0> PMID: 31012032

An agent-based model of indirect virulence via pathogen-induced cannibalism

Michael Culshaw-Maurer

April 01, 2021

Introduction

While cannibalism is one of the simplest trophic interactions, involving only a single species, its effects on population dynamics can be complex and varied. Cannibalism can destabilize populations when it is the only density-dependent process or stabilize populations when there are other sources of density dependence (Claessen, de Roos, and Persson 2004). It is typically size-dependent, with larger individuals consuming smaller ones, which can alter the size or age structure of populations and induce population cycles via temporal lags in density dependence (Hastings and Costantino 1987; Costantino et al. 1997). In some species there is a genetic basis to cannibalism (Croft and Murray 1972; Englert and Raibley 1977; Radwan 1995) or specific morphological differences between cannibals and non-cannibals (Łukasik 2010; Vijendravarma, Narasimha, and Kawecki 2013), but the behavior is frequently a plastic response to resource scarcity (Fox 1975; Polis 1981; Wise 2006) or conspecific density (Manica 2004; Law and Rosenheim 2011, 2013). Resource limitation and cannibalism are so tightly linked that in some cases a single hormonal pathway links starvation and cannibalism expression (Zhou, Rao, and Rao 2008; El Husseiny et al. 2018; Yakovlev 2018). Because cannibalism is a common

phenomenon in the animal kingdom, documented across a wide array of taxa (Polis 1981), it is important to understand how variation in cannibalism expression impacts population dynamics.

Disease is another ubiquitous biological phenomenon that can affect host population dynamics, primarily through the induction of virulence, or negative impacts on infected host fitness (Smith, Acevedo-Whitehouse, and Pedersen 2009). Virulence is typically described as increased host mortality (Read 1994; McCallum and Dobson 1995; Day 2002; Bull 1994), but decreases in host fecundity (Jaenike 1996; O’Keefe and Antonovics 2002) and delayed development times can also occur (Reynolds, Thomson, and Hoffmann 2003). However, virulence that is too strong may reduce transmission, which is referred to as the virulence-transmission tradeoff (Bull 1994; Acevedo et al. 2019). The act of reproduction within a host is necessary to produce new pathogen individuals that can go on to infect other hosts, but reproduction is also costly to the host. If reproduction is too low, the pathogen may fail to spread. If reproduction is too high, the virulent effects on the host may kill or incapacitate the host before transmission can occur. For this reason, simple models of disease predict that pathogens will not drive the host population to extinction (Anderson and May 1992). In these models, as virulence drives population densities down, density-dependent transmission decreases, and the pathogen dies out before the host population can go extinct. However, here are several mechanisms by which a disease may drive a population extinct (reviewed in De Castro and Bolker 2004), including driving the host population to such a small size that it stochastically goes extinct, non-density dependent transmission such as sexual or vector transmission, and biotic or abiotic reservoirs that allow the pathogen to persist when host densities are low.

In some systems, infection with a pathogen can induce increased cannibalistic behavior. Diseases frequently impose energetic or nutritional stress on their hosts, a common trigger of cannibalism.

While the reduction of population density due to disease virulence (increased mortality, reduced fecundity) may increase resource availability, pathogen-induced energetic stress may still be enough to trigger the cannibalism behavior. There are several documented cases of elevated cannibalism expression linked to infection (Bunke et al. 2015; Yan, Stevens, and Schall 1994; Rosenheim et al. 2019), but pathogen-induced cannibalism is potentially more widespread than currently documented. While there is a growing body of literature investigating the effect of cannibalism on disease transmission (Rudolf and Antonovics 2007; Sadeh and Rosenheim 2016; Sadeh, Northfield, and Rosenheim 2016; Allen et al. 2017), the phenomenon of pathogen-induced cannibalism has been mostly overlooked.

One particularly striking example of increased cannibalism expression associated with a pathogen is that of *Geocoris pallens*, which was one of the primary motivations for the current study (Rosenheim et al. 2019). In the early to mid-2010s, a yet-unidentified pathogen was detected in California populations of *G. pallens* that was associated with greatly elevated cannibalism expression. Putatively infected females collected from the field and assayed in the laboratory consumed 80-100% of their own eggs, compared to 0-20% for uninfected females; the same pattern occurred in all laboratory colonies. Elevated cannibalism occurred regardless of conspecific density and food provisioning, indicating that cannibalism expression was not density-dependent. The detection of the pathogen coincided with dramatic collapses of *G. pallens* populations across California's Central Valley, with densities declining by an order of magnitude, suggesting that pathogen-induced cannibalism may greatly affect population size and dynamics.

If infection with a pathogen increases cannibalism expression, there is potential for an indirect effect of the pathogen on both infected and uninfected hosts via cannibalism. We call this effect

indirect virulence, referring to the negative fitness impact of the pathogen on other members of the host population, mediated by the behavior of infected hosts (Fig. 1). Indirect virulence may impact pathogen and host population dynamics differently from direct virulent effects.

Cannibalism is often stage-structured, and many diseases only impact a particular life stage (Briggs and Godfray 1995), which means a pathogen that does not infect juveniles could still affect them through indirect virulence, potentially causing large changes in the stage or age structure of a population. The indirect virulence pathway can also extend from a single infected host to many uninfected hosts, whereas direct virulence only occurs in currently infected hosts, meaning indirect virulence may persist even if pathogen prevalence is relatively low. Indirect virulence may also act on different temporal scales compared to direct virulence, since an infected host may immediately cannibalize another host, while direct virulence requires a successful transmission event to occur first. Finally, pathogen-induced cannibalism upsets the typical density-dependence of cannibalism, since the behavior is driven by the infection and not population density, which may allow cannibalism to persist even at small population sizes.

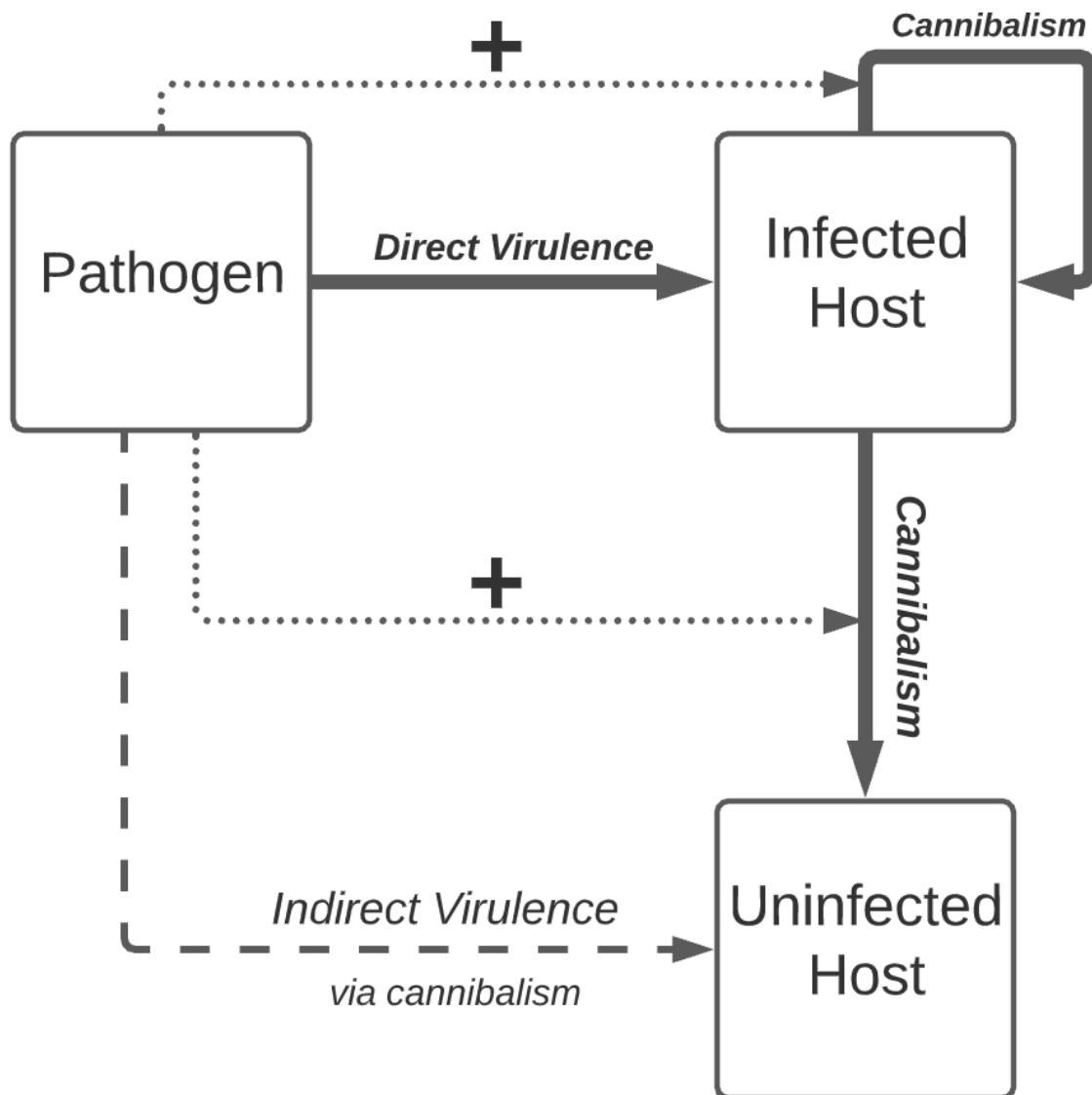


Figure 1: Interaction diagram depicting direct and indirect virulence pathways. Indirect virulence is defined as increased cannibalism expression by infected hosts, causing mortality in uninfected hosts, creating a behaviorally-mediated indirect effect of the pathogen on uninfected hosts. Note that if the victims of cannibalism may also be infected, some of the effects of indirect virulence may be directed back towards the infected host population.

Indirect virulence has the potential to upset the typical virulence-transmission tradeoff, since the effect is not experienced by the focal infected host. A pathogen that induces more moderate direct virulence but high indirect virulence may persist for longer, because the host does not die as quickly, allowing the indirect virulence pathway to be expressed for longer. This combination of high total virulence and relatively high infected host longevity has the potential to severely suppress host populations. Indirect virulence may also impact transmission by removing susceptible hosts from the population before transmission can occur, or through the cannibalism of infected juveniles.

Since cannibalism and disease can have a range of effects on population dynamics, their combined impacts may be complex and varied. To study the effects of pathogen-induced cannibalism and the indirect virulence pathway on population dynamics, we utilize a spatially explicit agent-based model. We use the model to investigate two primary questions: 1) how do direct and indirect virulence interact to affect host population and disease dynamics; and 2) does indirect virulence enable a pathogen to drive the host population extinct by removing the typical density-dependence of cannibalism? We use an *in silico* experiment to simulate host populations affected by pathogens with varying levels of direct and indirect virulence.

Methods

Agent-Based Model

To explore the dynamical consequences of different combinations of direct and indirect virulence pathways, we use a discrete-space and discrete-time agent-based model developed using NetLogo (Wilensky 1999) software. The model has four agent classes: uninfected juveniles,

uninfected adults, infected juveniles, and infected adults. Agents move between patches in a 12x12 grid. During each time step, agents go through a series of processes in the following order: mortality, cannibalism, movement, reproduction, maturation, and infection. The entire set of agents goes through each process asynchronously, with a random order of agents, before the next process begins.

First, there is a probability that any given agent dies in the current time step, modified by the number of agents of the same stage on the same patch, using the formula

$p = base_mortality * (neighbors + 1)^{dens_dep}$. Infected agents experiencing direct virulence may suffer increased mortality risk, which is parameterized as a modifier to the uninfected mortality, so infected agents would experience a 10% greater probability of mortality per time step if the infected mortality modifier is 1.1.

Next, infected adults have a probability of cannibalizing a juvenile, given that there is a juvenile present on its patch. Given the asynchronous updating of agents, if there are multiple infected adults on a patch and a single juvenile, only one adult will successfully cannibalize it. The probability of cannibalism is not density-dependent, as we assume that infection induces cannibalistic behavior regardless of population density. We also assume no baseline cannibalism for uninfected adults. Juveniles already suffer density-dependent baseline mortality, so the simplifying assumption allows us to more clearly investigate the effects of pathogen-induced cannibalism, particularly as population sizes decrease.

Next, each agent has a probability of moving. Given that they do move, a number is drawn from a Poisson distribution that is parameterized separately from the movement probability. They then take a random walk with this number of steps. For each step, they randomly move to one of the

patches to the north, south, east, or west of the current patch. The spatial grid has reflecting boundaries such that agents reaching the edge of the grid turn around and continue their random walk. Juveniles move less frequently and have shorter random walks than adults.

Next, there is a probability p that any given adult gives birth to an uninfected juvenile (no vertical transmission), modified by the density of conspecifics on the focal patch, using the formula $p = base_fecundity * (1/(neighbors + 1))^{dens_dep}$ (Hassell 1975).. Infected adults may suffer reduced baseline fecundity. Juveniles mature to adults after a number of time steps, which is drawn from a normal distribution, rounded up to the nearest integer. While the scale of the mean and standard deviation of the maturation times make negative values extremely unlikely, a negative value for maturation time would result in the immediate maturation of the juvenile. Infected juveniles mature into infected adults, and may experience an increase in the mean development time as a result of infection.

Finally, pathogen transmission occurs within a given patch. During each time step, each infected agent has a probability of infecting each uninfected agent on its patch. Therefore, the infection risk for an uninfected agent increases as the local density of infected agents increases, according to a Bernoulli distribution: $p = 1 - (1 - horizontal_infection_prob)^{n_infecteds}$ (Perez and Dragicevic 2009; Halloran, Longini, and Struchiner 2010; Tracey et al. 2014). Because the agents update asynchronously, each transmission event is independent. In other words, more infected agents on a patch means each uninfected agent faces a greater number of independent possible transmission events. Agents do not recover from infection (making this a susceptible/infected, or SI, model), and infected juveniles mature into infected adults. A complete description of the model according to the ODD protocol (Grimm et al. 2020) may be found in Appendix A.

***In Silico* Experiment**

In order to study the interacting effects of direct and indirect virulence on population dynamics, stage structure, and disease dynamics, we ran an *in silico* experiment with varying combinations of direct and indirect virulence. To determine baseline demographic parameter ranges that maintain a sufficiently stable host population and reasonable ranges of disease parameters, we conducted a global sensitivity analysis of the model. The ranges for baseline demographic parameters were derived from literature on *Geocoris pallens*, a motivating case study for the model. (see Appendix B for description and results). For the *in silico* experiment, we held all parameters constant except for direct virulence modifiers and the probability of cannibalism by infected adults.

Using the baseline parameter set, the model was run without introduction of the pathogen to determine the uninfected host population's quasi-stationary state, a stationary state when conditioned on non-extinction (Faure and Schreiber 2014). We ran the model for 5,000 time steps took the mean juvenile and adult population sizes for the last 4000 time steps, after the population has leveled off to a relatively stable state. The starting conditions for the *in silico* experiments were 80% of the number of adults and juveniles at this quasi-stationary state, which allowed the population to reach the quasi-stationary state by ~500 time steps. At 1,000 time steps, a single infected adult was introduced to a random patch, and the model continues to run until 10,000 time steps. For each treatment (a unique set of parameters), 100 simulations were run. At each time step, the number of agents of each class is recorded, allowing us to determine total population dynamics, changes in stage structure, and infection prevalence.

NetLogo simulations slow considerably as the number of agents grows; to reduce simulation time for large, stable populations, we set a ceiling on the number of total agents that enter the simulation. If the parameter set leads to a large, stable host population and the coexistence of host and pathogen, the simulation ends when the ceiling of total agents is reached. The effect can be seen in the upper left of Fig. 2, where low direct and indirect virulence allow the population to maintain a large, stable size.

The experiment involves twenty treatments, combining five levels of direct virulence (low, med-low, medium, med-high, and high) and four levels of indirect virulence (none, low, medium, high) (Table 1). For this experiment, all four components of direct virulence (adult mortality, fecundity, juvenile mortality, and development time) varied together. As previously described, all direct virulence parameters are expressed as modifiers to the base demographic parameters.

Table 1: Direct virulence parameters

Direct virulence level	Infected adult mortality	Infected juvenile mortality	Infected adult fecundity	Infected juvenile development time
low	1.1	1.1	0.900	1.1
med-low	2.0	2.0	0.500	2.0
medium	5.0	5.0	0.100	5.0
med-high	8.0	8.0	0.050	8.0
high	10.0	10.0	0.025	10.0

Table 1: Indirect virulence parameters

	Infected adult cannibalism
Indirect virulence level	rate
none	0.0
low	0.1
medium	0.5
high	0.9

Results

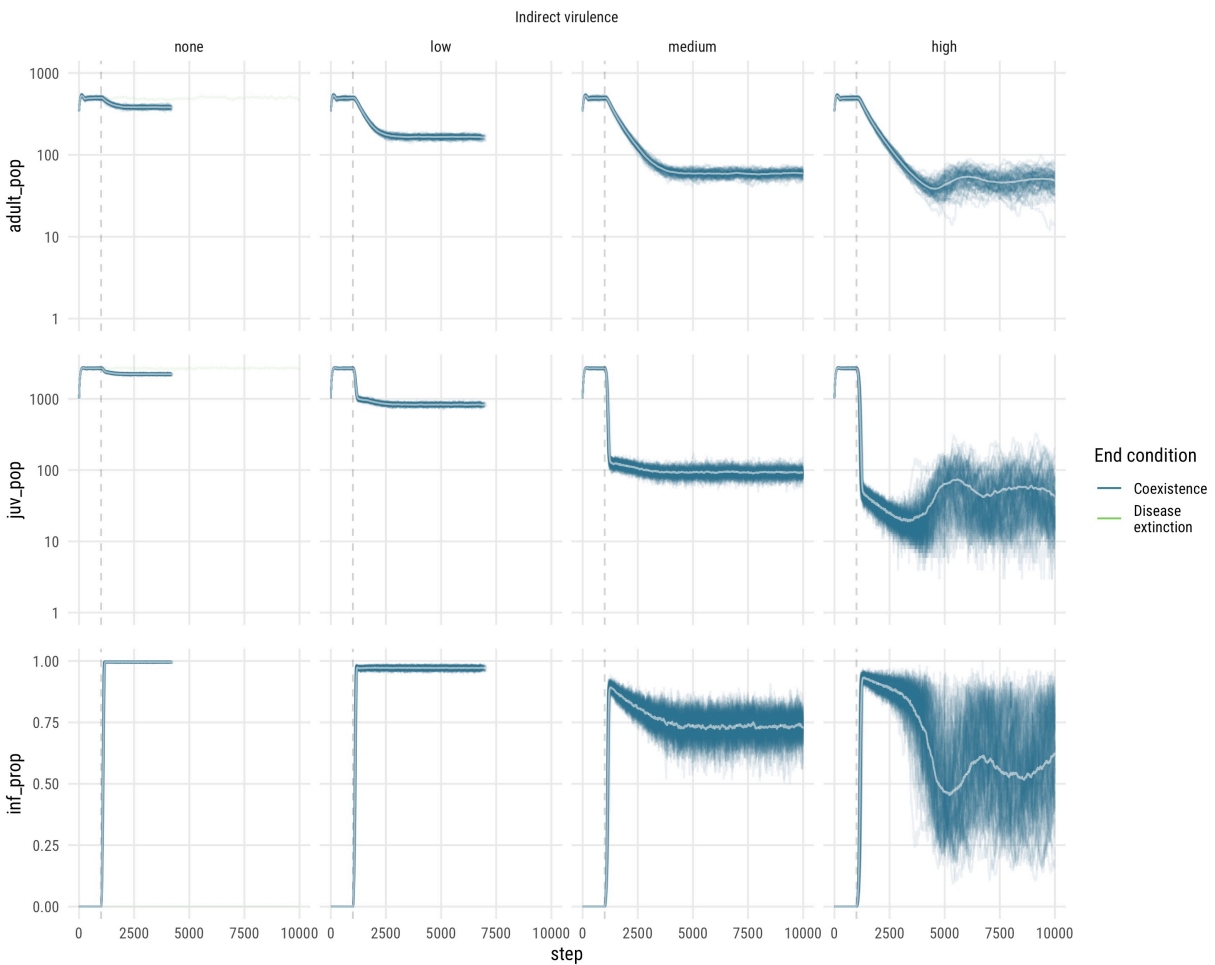


Figure 2: Total population size, juvenile proportion, and infection prevalence for all low direct virulence simulations. Columns represent increasing indirect virulence levels. Colors indicate simulation end condition, and the dashed vertical line denotes the introduction of the pathogen. The white line within the blue lines represents the mean time series for runs where coexistence occurs.

At low levels of direct virulence, increases in indirect virulence reduce mean population size and infection prevalence (see Fig. 2 and the leftmost side of Fig. 6A). When direct virulence is low,

infected adults suffer little added mortality, allowing them to live longer and cannibalize many juveniles over their lifespans. The high level of juvenile mortality via cannibalism drives both juvenile and adult population sizes down, to the point that the population is small enough that transmission rates decline, reducing mean infection prevalence.

A similar mechanism drives the instability of population dynamics as indirect virulence increases (see rightmost column of Fig. 2). As infection prevalence decreases, so does the overall level of cannibalism, which allows the juvenile population to rebound. The adult population also recovers due to the increase in reproductive recruitment, and the total population size increases. The larger population size allows the pathogen to spread more effectively, increasing infection prevalence and cannibalism, once more driving juvenile population size down, creating a cycle.

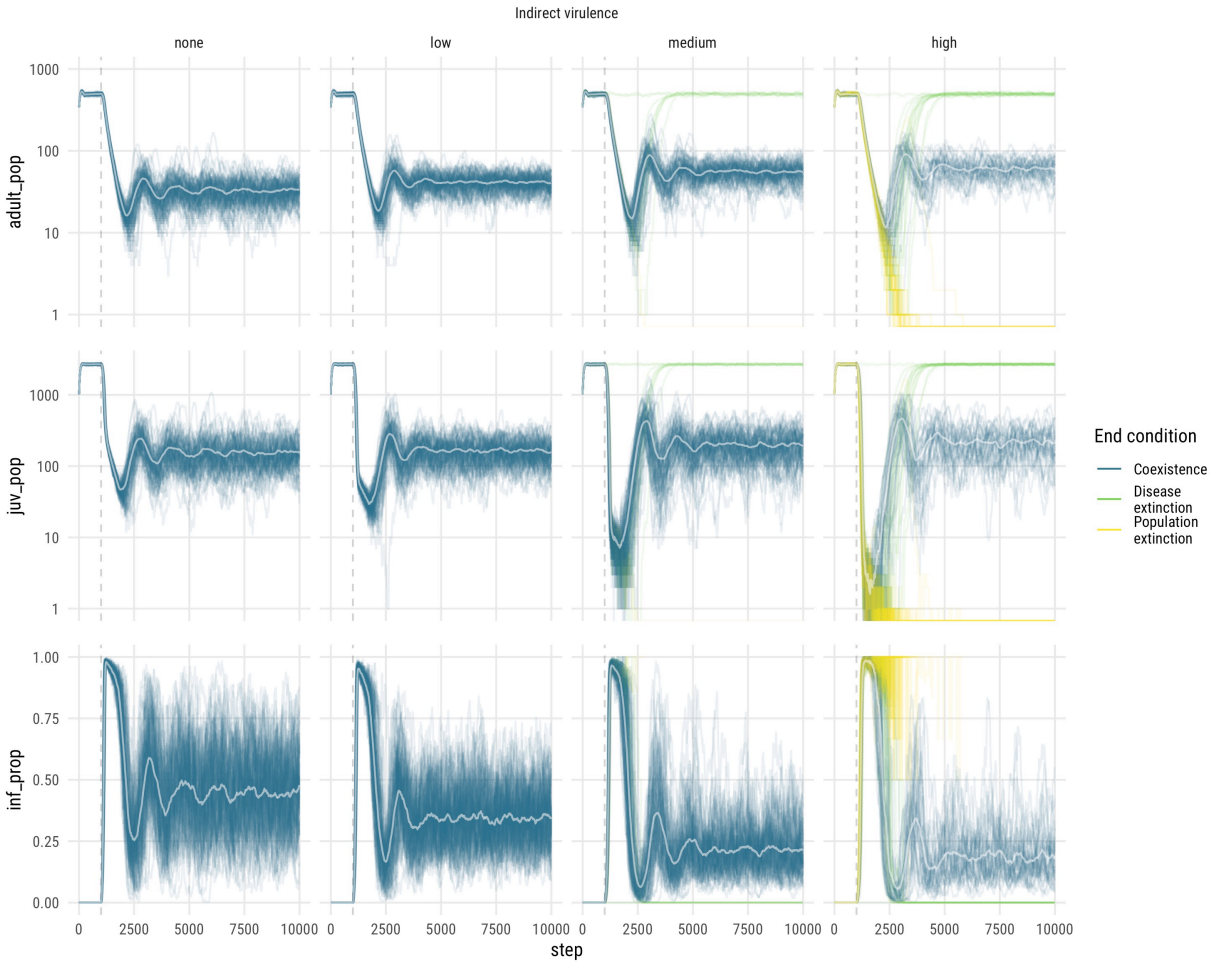


Figure 3: Total population size, juvenile proportion, and infection prevalence for all medium direct virulence simulations. Columns represent increasing indirect virulence levels. Colors indicate simulation end condition, and the dashed vertical line denotes the introduction of the pathogen. The white line within the blue lines represents the mean time series for runs where coexistence occurs.

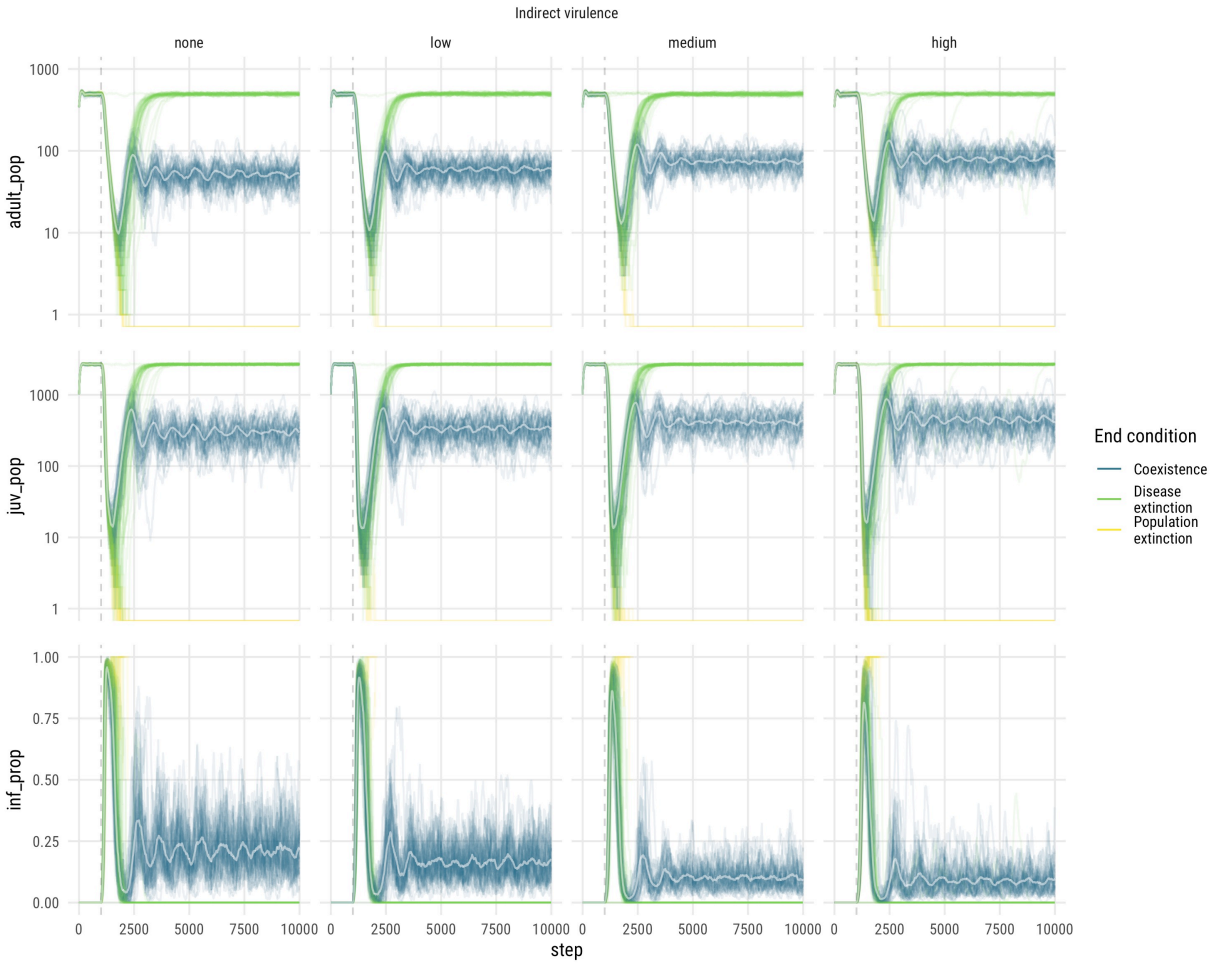


Figure 4: Total population size, juvenile proportion, and infection prevalence for all high direct virulence simulations. Columns represent increasing indirect virulence levels. Colors indicate simulation end condition, and the dashed vertical line denotes the introduction of the pathogen. The white line within the blue lines represents the mean time series for runs where coexistence occurs.

As medium direct virulence (Fig. 3), the host or pathogen can go extinct (yellow and green lines, respectively) and these extinction events become more frequent at high levels of direct virulence (Fig. 4). These extinction events occur because the initial wave of infection drives the host

populations to very small sizes resulting in high extinction risk. The combination of direct and indirect virulence levels shape which type of extinction is more likely (Fig. 5).

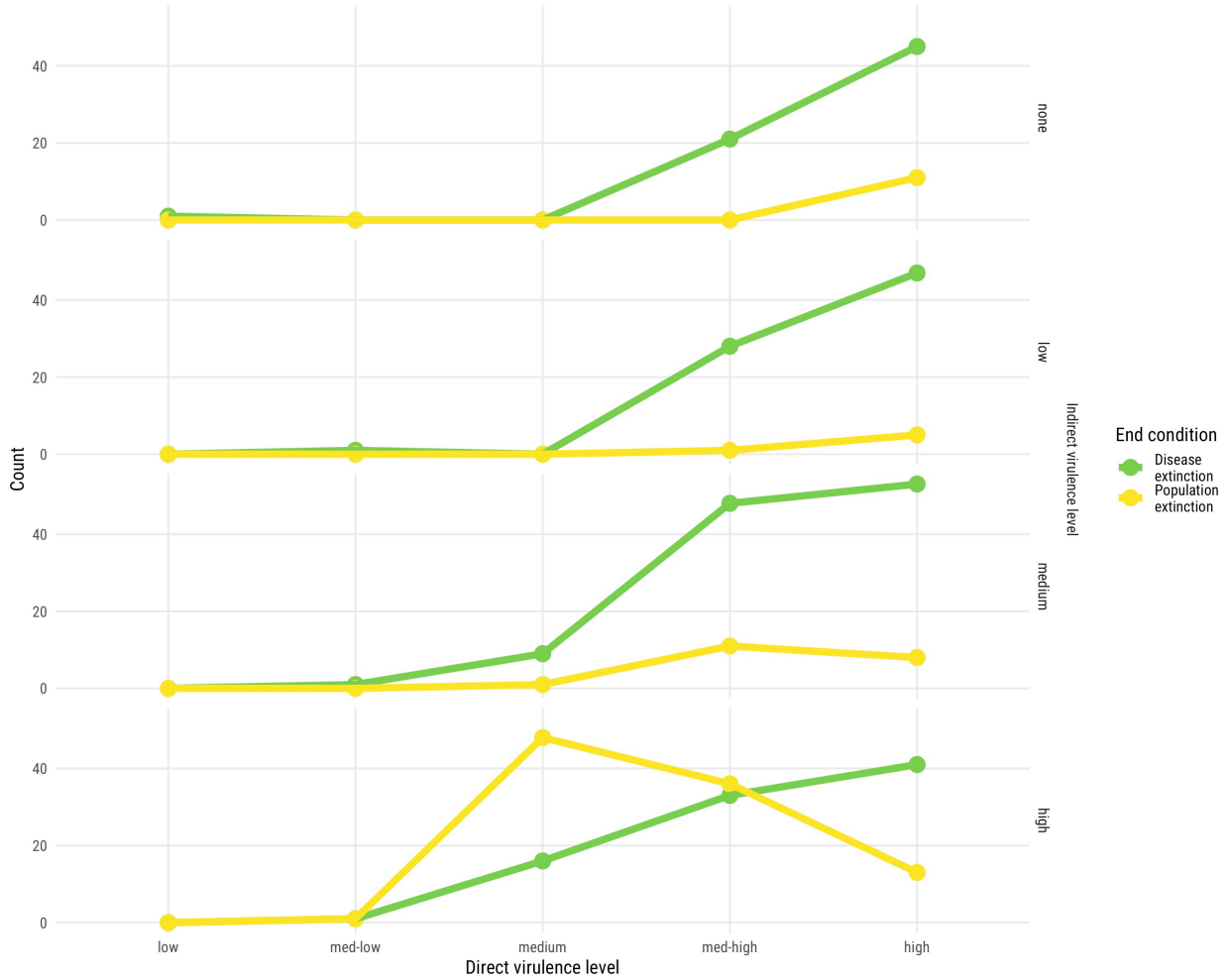


Figure 5: Number of simulations leading to host or pathogen extinction, with panels for each level of indirect virulence.

Host and Pathogen Extinction

When indirect virulence is low to medium, increasing direct virulence leads to greater rates of pathogen extinction (see top 3 panels of Fig. 5). As direct virulence increases, the disease drives the host population to lower densities, which results in transmission becoming rare and high

pathogen extinction risk spread. When the pathogen goes extinct, the host population rebounds to pre-infection levels (see green lines on Figs. 3 and 4).

At high levels of indirect virulence, a different pattern occurs (see bottom panel of Fig. 5). When indirect virulence is high and direct virulence is moderate, host extinction becomes more common. The combination of direct and indirect virulence can drive the juvenile population to very low densities (see far right column of Fig. 3). The lag between juvenile and adult population decline means some adults survive even as juvenile population drops to nearly zero. Because infection prevalence is high, these adults are infected, and because direct virulence is only moderate, they live long enough to cannibalize all the remaining juveniles. This reduces reproductive recruitment to zero and drives the host population extinct. If both direct and indirect virulence are high, host extinction becomes less frequent (bottom right of Fig. 5). When direct virulence is too high, the remaining adults die before they are able to cannibalize the last juveniles, so the host population is not driven extinct. Rather, the small population size leads to frequent pathogen extinction.

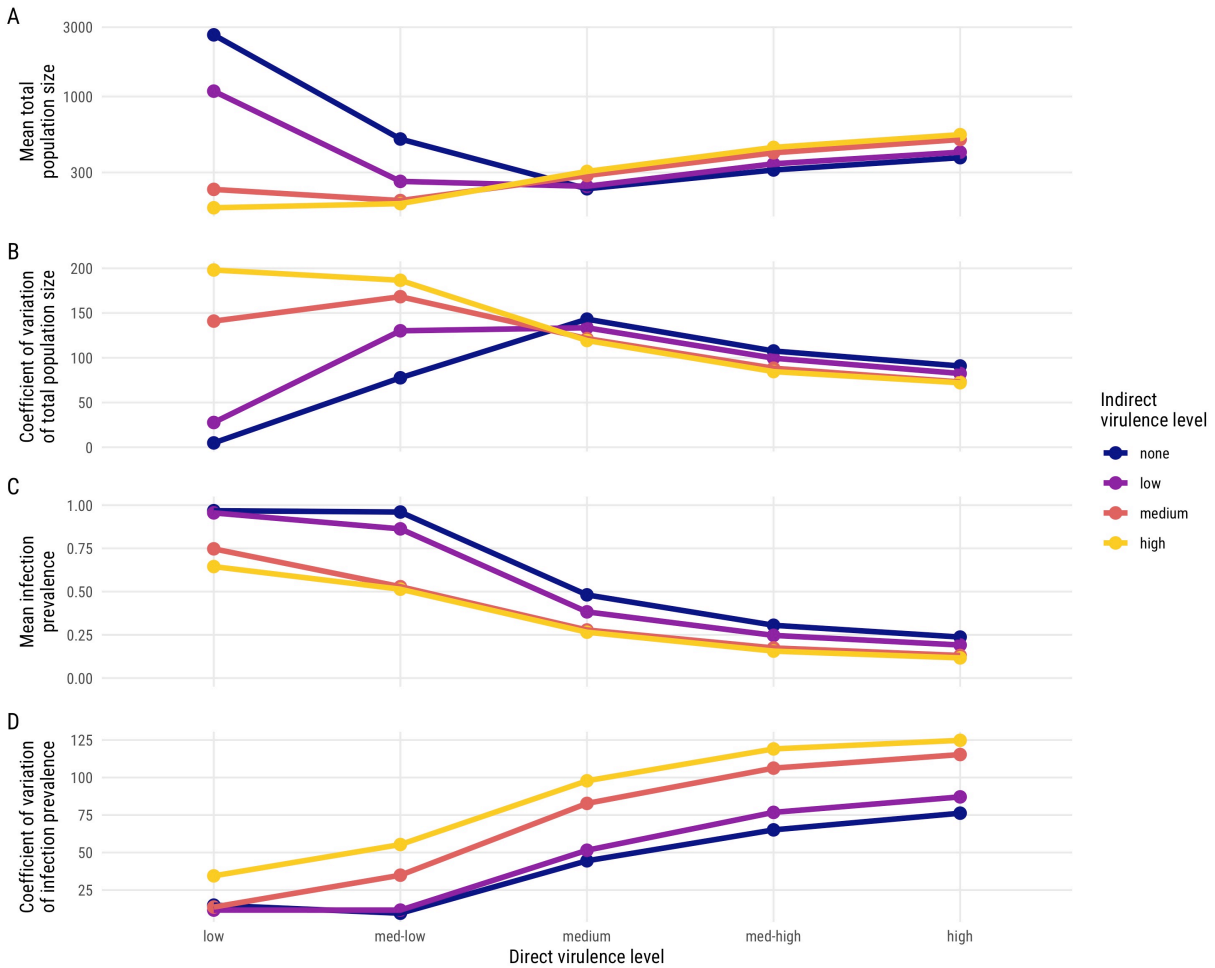


Figure 6: Total population metrics after pathogen introduction, for runs where coexistence occurs. (A) shows the mean population size, (B) shows the coefficient of variation of population size, (C) shows the mean infection prevalence, and (D) the coefficient of variation of infection prevalence.

Host and Pathogen Coexistence

When coexistence occurs, direct and indirect virulence have interacting effects on mean population size and fluctuation, and infection prevalence and fluctuation (Fig. 6). Both direct and indirect virulence have negative effects on infection prevalence. This is expected for direct

virulence, as infected hosts die before they can transmit the disease. For indirect virulence, the effect stems from reduced population size and the removal of infected juveniles via cannibalism. Since contact with infected adults is a source of both infection and cannibalism, infected juveniles are typically located in areas of high adult infection, so their cannibalism risk is high relative to uninfected juveniles near uninfected adults.

Direct and indirect virulence interact to affect population size and fluctuation. Mean population size and coefficient of variation are negatively correlated across all levels of direct and indirect virulence, as are mean infection prevalence and coefficient of variation. This is likely driven by cycles of population size and infection. When the pathogen drives populations to small sizes, the overall transmission rate decreases, leading to a drop in infection prevalence. This reduces the virulent impact on hosts, allowing populations to rebound slightly. The increased host density allows for greater transmission, which increases infection prevalence and overall virulent effects. This process then repeats, leading to a cycle. When overall virulence is not as high and populations are relatively large, the pathogen can transmit at a steadier rate, leading to less variation in infection prevalence, the overall virulence experienced by the population, and therefore population size.

At low levels of direct virulence, indirect virulence has a strong negative effect on population size, since infected adults have high survival and can cannibalize many juveniles before they die. At moderate to high levels of direct virulence, indirect virulence actually increases mean population size slightly, which is driven by the decreased infection prevalence. By removing many infected juveniles from the population, the overall levels of direct virulence suffered by the population are reduced. When direct virulence is strong enough, this effect outweighs the actual reduction in population size via cannibalism, leading to a slight increase in total population size.

Discussion

The indirect virulence pathway can lead to significant suppression of host populations and increase the frequency of host population extinction. Many theoretical and empirical studies of disease note a suppression of host populations (McCallum and Dobson 2002; Gog, Woodroffe, and Swinton 2002; De Castro and Bolker 2004). A combination of high transmission and moderate virulence has been shown to maximize the suppression of host populations in simple disease models (Anderson and May 1992). However, in our model, the indirect virulence pathway allows even higher levels of overall pathogen-induced mortality because it shifts the effects of virulence away from the infected host. If direct virulence is not too high, an infected adult may live for a relatively long time, allowing many cannibalism and transmission events to occur. In our model, the highest degree of host suppression occurs with a combination of low direct and high indirect virulence. Our findings are supported by the example of *Geocoris pallens*, where a pathogen associated with increased cannibalism expression co-occurred with massive depression of host population densities across California's Central Valley (Rosenheim et al. 2019).

Indirect virulence also increases the probability of host population extinction, compared to direct virulence. Extinction of small populations in stochastic models is well-documented (Ovaskainen and Meerson 2010). Oftentimes, extinction at small population sizes is enhanced by Allee effects (Henle, Sarre, and Wiegand 2004; Bascompte 2003; L. J. S. Allen et al. 2005), environmental stochasticity (Giles Leigh 1981; Lande 1993; Foley 1994), or catastrophic perturbations (Assaf, Kamenev, and Meerson 2009; Cairns, Ross, and Taimre 2007; Lande 1993). In our model, host extinction at small population sizes is driven by an intrinsic feature of the disease: increased

cannibalism expression. At small population sizes, infected adults may cannibalize all remaining juveniles in the population, driving reproductive recruitment to zero and leading to host extinction. A combination of small population size and relatively low direct virulence makes this mechanism possible. In our model, the population suffers no Allee effects and at small population sizes often rebounds to pre-disease size after pathogen extinction, indicating that indirect virulence does not simply drive population size below some threshold, but rather provides a distinct mechanism by which host extinction may occur.

When direct virulence is too high, coexistence becomes unlikely, pathogen extinction is more frequent than host population extinction, and the strength of the indirect virulence pathway decreases. In many disease models, there is a critical community size below which the pathogen will “fade out,” as it is unable to persist in the population (Bartlett 1960; Black 1966; Keeling 1997). This effect can be seen in our model, where high rates of pathogen extinction occur when direct virulence is high, as the initial wave of infection drives the population below the critical community size. In some cases, the small population sizes induced by direct virulence alone can lead to host population extinction as well, but pathogen extinction is far more common.

Increased direct virulence also reduces the strength of the indirect virulence pathway, similar to the effects of direct virulence on transmission. When direct virulence is too high, infected adults die before they are able to cannibalize many juveniles or generate many new infections.

Our results demonstrate the potentially high impact of pathogen-induced cannibalism on host population size and extinction. We believe this phenomenon warrants future study, with a few key directions. First, while there are only a few documented examples of increased cannibalism expression in infected hosts (Bunke et al. 2015; Yan, Stevens, and Schall 1994; Rosenheim et al. 2019), there are strong links between energetic stress and cannibalistic behavior (Zhou, Rao, and

Rao 2008; El Husseiny et al. 2018; Yakovlev 2018). This suggests that energetic stress imposed by infection may increase cannibalism in many taxa that exhibit the behavior. Second, because the indirect virulence pathway does not require the pathogen to infect juveniles in order to inflict mortality on them, a pathogen that infects only the adult life stage (Briggs and Godfray 1995) may still inflict high mortality on juveniles. In this case, a failure to document increases in cannibalism may lead to poor estimates of disease impacts on host populations. Finally, the indirect virulence pathway may impact the evolution of disease virulence and host behavior. The close links between cannibalism and energetic stress mean that cannibalistic expression may be an inevitable byproduct of infection. While there may be a relatively continuous relationship between a direct virulence effect, such as increased mortality, and pathogen reproduction, if cannibalism expression is a more discrete behavioral “switch,” then there may be a discontinuous relationship between pathogen reproduction and indirect virulence. This may affect the evolutionary trajectory of the indirect virulence pathway and pathogen virulence as a whole.

Appendix A

ODD Protocol

This is an ODD (Overview, Design Concepts, and Details) protocol used to describe the structure and function of the ABM written in NetLogo (Grimm et al. 2020). Note that the NetLogo model allows for the addition of various complexities that are not implemented in the current study, such as vertical transmission, density-dependent cannibalism by uninfected adults, and trophic transmission via cannibalism.

Purpose and Patterns

The purpose of the model is to explore the effects of pathogen-induced cannibalism, virulence, transmission, and individual movement on pathogen and host population dynamics in a spatially and temporally explicit and discrete context. These effects are explored both broadly, in a non-species specific context, as well as specifically modeling the beneficial insect *Geocoris pallens*.

As this model is investigating a relatively understudied phenomenon, we use only general patterns as criteria for the model's usefulness:

1. Increases in mortality and development time and decreases in fecundity lead to decreased population size
2. Increased horizontal transmission leads to higher pathogen prevalence
3. Increased cannibalism reduces the juvenile population size

Entities, State Variables, and Scales

Entities

This model is relatively general, aiming to understand general processes rather than specific, highly parameterized simulations. The model consists of 6 classes of individuals: uninfected adults, infected adults, uninfected juveniles, and infected juveniles, corpses, and juvenile corpses. Corpses do not interact with other agents or the environment, they are simply dead infected agents, kept in the simulation so their internal states can be retained at the end of the simulation.

Scales

This model is discrete in both space and time. Resources are not modeled explicitly, and multiple agents can occupy a single patch. The boundaries of the spatial grid are reflecting, and there is no immigration or emigration. For the *G. pallens* example, which is used as a relatively well-parameterized system, each patch is assumed to be a single plant within an agricultural field and each time step represents one hour. However, the scales motivated by the *G. pallens* example only serve as a biologically feasible starting point, and the parameters and scales can be scaled as needed to match other systems.

State Variables

There are several internal state variables tracked across agents. Both infected and uninfected juveniles have a `development-level`, set at birth according to a random normal distribution with a mean of 0 and a standard deviation set as by `development_stdev`. At each time step, the `development-level` increases by 1, until it reaches the `maturation_time` parameter, and the juvenile matures into an adult. Varying the starting `development-level` essentially gives some juveniles a head start to reaching the `maturation_time`, while setting others back. Juveniles also record the agent ID of their parents as `parent-id`. Then, each time an infected adult cannibalizes a juvenile, it records whether or not that juvenile's `parent-id` matches their own ID. The infected adults have state variables denoting the number of their own uninfected and infected eggs they have cannibalized (`offspring-cann` and `inf-offspring-cann`, as well as the number of others uninfected and infected eggs they have cannibalized (`other-cann` and `inf-other-cann`).

Infected agents also record the cumulative number of horizontal infections they generate across 4 categories: juvenile->juvenile, juvenile->adult, adult->juvenile, and adult->adult, denoted as jj-infected, ja-infected, aj-infected, and aa-infected. This allows for a calculation of lifetime number of horizontal infections generated across multiple classes. If juveniles and adults have different levels of “host quality” (Sadeh, Northfield, and Rosenheim 2016), then it may be important to track each type of horizontal infection separately, as a new adult case may have more impact than a new juvenile case. Infected adults also track the cumulative number of vertical transmissions they generate, as num-vert-births.

There is another class of internal state variables used, which do not change, but record the time at which certain events occur. Juveniles of both types record the time step at which they are born (birth-time) and the time step at which they mature (hatch-time), carrying these internal state variables through to adulthood. If horizontal infection occurs, the infected agent records the time step and life stage at which it was infected (horiz-inf-time or juv-horiz-inf-time). If an agent was infected through vertical transmission, this internal state will be blank. If trophic transmission occurs, the time step is recorded under trophic-inf-time.

All of the internal state variables that occur in infected agents are carried over into the corpse state, so the states may be collected from every infected agent that completed its life cycle during the course of the simulation. For each corpse, we can note the time it was born, the time it matured into adulthood, the time it was infected (if horizontally or trophically infected), the time it died, and its lifetime number of horizontal and vertical infections generated. Whether the infected agent was the initial infected agent added to the simulation is also recorded as initial-inf, which allows for an empirical calculation of R_0 , as this is a single infected agent introduced to a totally susceptible population.

Process Overview and Scheduling

The model processes are listed in order of their occurrence in the schedule. Within a given procedure, agents are updated asynchronously with a random order. The randomness of the model is controlled by the seed, which can be set explicitly in the NetLogo GUI via the seed parameter or in the scripts used to run the model from the command line.

1. Development

Each juvenile's development level state variable is increased by 1.

2. Death

See Submodels

3. Cannibalism

See Submodels

4. Movement

See Submodels

5. Reproduction

See Submodels

6. Maturation

See Submodels

7. Infection

See Submodels

Design Concepts

Basic Principles

The model focuses on two basic biological concepts: disease and cannibalism. Specifically, it focuses on an intersection of the two, namely the *indirect virulence* pathway, wherein infection induces elevated cannibalism expression that can affect uninfected hosts, creating an indirect effect of the pathogen on uninfected hosts. The model also incorporates basic principles of density-dependent population growth, with density-dependent mortality and fecundity leading to a logistic growth pattern in an uninfected population. Finally, the model incorporates movement of agents in discrete space, which allows for spatial heterogeneity of infection, cannibalism, and density dependence.

Emergence

The impacts of the *indirect virulence* pathway can be observed from the emergent host population and pathogen dynamics, which can be visualized as population time series. By introducing the infection to a quasi-stationary population, the pre- and post-infection population sizes can be compared, and by changing levels of direct virulence, transmission, pathogen-induced cannibalism, and movement, the interactions of these effects on host population and pathogen dynamics can be determined. In the broadest sense, the fate of the population (extinction, disappearance of the pathogen) is an emergent property of the underlying pathogen and cannibalism processes.

Adaptation

No adaptation occurs in this model.

Objectives

Agents in this model have no explicit objectives.

Learning

Agents in this model do not learn.

Prediction

There are no predictive behaviors in this model.

Sensing

There are three types of sensing done by agents in the model: density dependence, cannibalism, and horizontal transmission. Adults reproduce in a density-dependent fashion, with the density of other adults within a certain radius reducing the number of offspring produced by the focal agent.

This same count of adults also has a positive impact on cannibalism by uninfected adults.

Cannibalism involves detecting juveniles within a certain radius to be prospective prey. Finally, horizontal transmission requires the identification of prospective infectees within a given radius of the focal infected agent.

Interaction

The only interactions that occur in the model are cannibalism of juveniles by adults and the transmission of the pathogen horizontally between agents.

Stochasticity

All model processes are stochastic, and the overall model is controlled by a RNG seed, which can be set in the NetLogo GUI or as a parameter in individual model runs. The implementation of stochasticity in each process is described in more detail in the process descriptions.

Collectives

There are no collective groups of agents in this model.

Observation

Time Series

The number of each non-corpse agent class is recorded at every time step, giving population time series with finer details on infection, stage structure, and population variability. Additionally, by introducing the pathogen after a burn-in period, comparisons can be drawn between the pre- and post-pathogen population sizes.

Agent Variables

Due to the corpse agent classes, state variables from dead infected agents can be collected at the end of a simulation run. These variables fall into two main categories: infections generated and juveniles cannibalized. See the above *State Variables* section for a thorough description of each variable.

Initialization

For global sensitivity analyses, the model is initialized with a certain number of uninfected juveniles (determined by the parameter `initial_juveniles`) placed randomly in the landscape,

with development levels randomly set between 0 and the `development_time` parameter. This provides a relatively well-mixed population of adults and juveniles, which alleviates some of the discrete generations that occur if the model is initialized with adults. If adults are used, they begin producing a great number of offspring, which then mature around the same time, creating discrete generations. The number of juveniles used to initialize can be controlled with a model parameter. For the more specific *in silico* experiments, where the baseline demographic parameters are stable, the model can be initialized closer to the quasi-stationary state. To do so, the model is run for 10,000 steps without any infection, and the mean number of adults and juveniles for the last 5,000 steps is calculated. The model can then be initialized with slightly fewer adults and juveniles than this (around 80%), which allows the population to grow slightly to reach the quasi-stationary state, so that the infection can be quickly introduced to a stable population.

Since the seed is set manually, if the seed remains unchanged, the placement of initial juveniles will be the same. The model is then run for a certain amount of time, to allow the population to reach some quasi-stationary state, which will happen as agents die and reproduce with some density dependence. At a time step set by `inf_appear_time`, a certain number of infected individuals are introduced at random locations. This essentially allows for a “burn-in” period, where the population may reach a quasi-stationary state before the introduction of the pathogen.

All model parameters can be set using the NetLogo GUI, but for the analysis of this model, a series of R scripts are used to generate XML files containing parameters that control one or more runs of the model. There is a bash script that runs the model on a computing cluster, and then a series of R scripts that collect and clean the results of the model runs. For each run, the parameters and outcomes are stored together. The R script that generates the XML files

containing model parameters is controlled by a pseudorandom seed, which affects both the generation of model parameters from user-specified ranges as well as the seeds used for each NetLogo model run. This means that if the same seed and parameter ranges are used in the XML generating R script, the model outcomes will be exactly the same. This allows for replicability of all model runs.

Input Data

No input data are used for this model.

Submodels

Death

Death is implemented as a random process each time step, with the per-step probability of death set by parameters for each agent class (*mortality*, *juv_mortality*, *inf_mort_mod*, and *inf_juv_mort_mod*, as well as the density of agents of the same stage within a certain radius.

$$p = mortality * (neighbors + 1)^{dens_dep}$$

Cannibalism

Cannibalism can be expressed by both infected and uninfected adults. The baseline uninfected cannibalism is density-dependent, based on the number of adults within a certain radius at the current time step.

$$p = 1 - e^{-cann_lambda * (neighbors + 1) - cann_level}$$

For infected adults, cannibalism is not density-dependent, as it is assumed that the cannibalism is triggered by infection and is not impacted by the presence or absence of conspecifics. The

probability of cannibalizing a juvenile within the `cann_radius` is set by `inf_cann_level`. When an infected adult cannibalizes a juvenile, it checks the juvenile's infection status and whether the juvenile's `parent_id` matches its own ID. Based on the identity and infection status of the juvenile, one of the following state variables for the adult is increased by 1: `offspring-cann`, `inf-offspring-cann`, `other-cann`, `inf-other-cann`.

Trophic Transmission

Additionally, when an uninfected adult cannibalizes an infected juvenile, there is some probability that the adult becomes infected via trophic transmission, determined by `trophic_trans`. If this occurs, the infected adult has an internal state variable, `trophic-inf-time` set to record the time at which that occurs. This also allows the number of trophic transmission events in a run to be recorded.

Movement

Movement is modeled as a hurdle-Poisson process, which means there are two steps to movement. First, the parameter `movement_odds` controls the probability of whether an agent moves during a given time step. If they do move, a second parameter, `move_dist`, controls the number of steps they take, as a Poisson random variable, plus 1, so that the minimum number of steps taken is 1. Each step taken involves turning to face one of the 4 cardinal directions and moving forward 1 patch. If, after turning to face a direction, the world boundary is in the way of moving forward, the agent turns 180 degrees and moves forward 1 patch.

Reproduction

Reproduction is a density-dependent process with the strength of density dependence controlled by a `dens_dep`. The number of conspecifics for density dependence are measured within a radius of the focal individual. For infected adults, each offspring produced has some probability of having the infection vertically transmitted (`vert_trans`), that is, being born as an infected juvenile.

$$p = fecundity * (1/(neighbors + 1))^{dens_dep}.$$

Maturation

If a juvenile's `development-level` has reached the `maturation_time`, it matures into an adult.

Infection

For each infected agent, the infection process occurs at each time step. All uninfected agents within a certain radius (`horiz_trans_radius`) are identified as potential infectees, and each has a probability of becoming infected. The probability of infection is determined by the class of both the infected (`horiz_trans` or `juv_horiz_trans`) and infectee (`juv_susc_mod` modifies the susceptibility of juvenile infectees). The number of new adult and juvenile infections generated are added to the focal infected agent's state variables for lifetime number of horizontal infections generated, with a state variable for each combination of infected and infectee stage (`jj-infected`, `ja-infected`, `aj-infected`, and `aa-infected`). If an uninfected agent is adjacent to multiple infected adults, they will be a potential infectee for each infected agent's infection procedure, since agents go through each process asynchronously.

Appendix B

Global Sensitivity Analyses

In order to assess the overall sensitivity of the model to its many parameters, both demographic and pathogen-related, we conducted two global sensitivity analyses. They were carried out by first establishing ranges for each parameter and conducting a Latin hypercube sampling of the multidimensional parameter space. 10,000 parameter samples were taken, and a single simulation was performed for each parameter set. When conducting sensitivity analyses of stochastic models, increasing coverage of parameter space is more important than replication of parameter sets (Prowse et al. 2016). To analyze the sensitivity of each outcome listed in Table 1 to each model parameter, a random forest model was fit for each outcome using the *ranger* package. The random forest approach to GSA deals well with high-dimensional data, nonlinear effects, and higher order interactions between parameters (Harper, Stella, and Fremier 2011). Regression random forest models were used for every outcome except time to pathogen extinction and time to population extinction, for which survival random forest models were used. This approach allows for the analysis of censored data, as extinction times are censored at the maximum number of steps in each simulation run.

Each model went through two rounds of hyperparameter tuning using 5-fold cross validation and testing/training data sets. Each model yields a permutation importance score for each parameter, describing the decrease in the model's predictive accuracy if a parameter's values are randomly shuffled. Because importance scores do not describe the direction of effect of a parameter on an outcome, for each of the top 8 variables in each model, a univariate linear model was fit and the

sign of the β coefficient was extracted. While this fails to capture possible nonlinear effects and higher order interactions, it can be useful to determine the general trend of a parameter's effect on an outcome.

Table 2: Simulation outcomes calculated from population counts and infected adult state variables.

Outcome name	Description
Mean juvenile proportion	While population > 0 , mean proportion of juveniles in population
Mean population size	While population > 0 , mean total population size
Mean proportion cannibalism of others	Mean proportion of each infected adult's cannibalism directed at non-offspring
Mean proportion cannibalism of uninfected others	Mean proportion of each infected adult's cannibalism directed at uninfected non-offspring
Mean proportion infected	After pathogen introduction, mean proportion of population infected
Time to disease extinction	Time step after pathogen introduction at which population > 0 and infected population = 0. Censored at 10,000 steps (maximum run time)
Time to population extinction	Time step at which population = 0. Censored at 10,000 steps (maximum run time)

R_0	Number of horizontal infections generated by the initial infected adult introduced to the population
Mean R_{eff}	Mean effective reproductive number, or number of horizontal infections generated by all infected adults, including infections generated as juveniles
R_{eff} overdispersion	The degree of overdispersion in the zero-inflated negative binomial model fit to each run's R_{eff} distribution.
R_{eff} zero inflation	The probability of zero inflation in the zero-inflated negative binomial model fit to each run's R_{eff} distribution.

Broad GSA

The primary goals of this GSA are to determine the broad regions of parameter space that yield various simulation end conditions (such as population extinction) and to determine the sensitivity of various outcomes to these parameters. Understanding the areas of parameter space that allow for coexistence of the host and pathogen is important for selecting parameter values to be held constant during the *in silico* experiments. Ranges for basic demographic parameters were set based on empirical measures of *Geocoris pallens*, for two reasons: first, *G. pallens* was a motivating example for the creation of this model, and second, using demographic parameters that relate reasonably to each other provides a biologically feasible starting point. Some biological parameters (such as the strength of density dependence) are not easily derived from empirical literature, so they were given relatively broad ranges.

Below are the parameter ranges used for the broad global sensitivity analysis. Demographic parameter ranges were determined based on estimates of *Geocoris pallens* from the literature,

whereas pathogen parameters and difficult to estimate parameters (such as strength of density dependence) were given relatively broad ranges.

Table 3: Parameter ranges for the broad global sensitivity analysis.

name	min	q25	median	q75	max	special
cann_lambda	0	0	0	0	0	all_zero
cann_level	0	0	0	0	0	all_zero
cann_radius	0	0	0	0	0	all_zero
dens_dep	0.000194	0.75	1.5	2.25	3	NA
development_stdev	5	6.25	7.5	8.75	10	NA
development_time	170	253	335	417	500	NA
fecundity	0.05	0.0875	0.125	0.162	0.2	NA
horiz_trans	7.05e-05	0.25	0.5	0.75	1	NA
horiz_trans_radius	0	0	0	0	0	all_zero
inf_appear_time	1000	1000	1000	1000	1000	single_value
inf_cann_level	0.5	0.625	0.75	0.875	1	NA
inf_fecund_mod	0.5	0.625	0.75	0.875	1	NA
inf_juv_mort_mod	1	1.5	2	2.5	3	NA
inf_mature_mod	1	1.13	1.25	1.37	1.5	NA
inf_mort_mod	1	1.5	2	2.5	3	NA
inf_move_dist_mod	0.1	1.33	2.55	3.78	5	NA

inf_move_prob_mod	0.1	1.33	2.55	3.78	5	NA
initial_juveniles	100	100	100	100	100	single_value
initial_uninfecteds	0	0	0	0	0	all_zero
juv_horiz_trans	7.05e-05	0.25	0.5	0.75	1	NA
juv_mortality	0.001	0.00325	0.0055	0.00775	0.01	NA
juv_move_dist	0.05	0.162	0.275	0.388	0.5	NA
juv_move_prob	0.01	0.02	0.03	0.04	0.05	NA
juv_susc_mod	1	1	1	1	1	single_value
max-pxcor	10	12.8	15	17.2	20	NA
max-pycor	10	12.8	15	17.2	20	NA
min-pxcor	-20	-17.2	-15	-12.8	-10	NA
min-pycor	-20	-17.2	-15	-12.8	-10	NA
mortality	4e-04	0.00055	7e-04	0.00085	0.001	NA
move_dist	0.0502	1.29	2.52	3.76	5	NA
move_prob	0.01	0.0575	0.105	0.152	0.2	NA
num_inf_appear	1	1	1	1	1	single_value
percep_radius	0	0	0	0	0	all_zero
trophic_trans	0	0	0	0	0	all_zero
vert_trans	0	0	0	0	0	all_zero
inf_appear	NA	NA	NA	NA	NA	true

max_pop_size NA NA NA NA NA 120000

The broad GSA demonstrates that many model outcomes are highly sensitive to baseline demographic parameters such as development time, fecundity, and density dependence. Horizontal transmission rates also heavily influenced outcomes such as mean R_{eff} and time to population extinction. The effect on population extinction is likely due to higher-order interactions with direct virulence levels; if direct virulence and transmission rates are high, the entire population becomes infected and cannot sustain itself with demographic rates imposed by the pathogen. Overall, none of the patterns in sensitivity indicated any major concerns for the parameter ranges used in the *in silico* experiments.

Here is a plot of the various types of end conditions. `ceiling_` refers to hitting the max # of agents in the model (see Methods). `ceiling_post_inf` occurs when the ceiling is reached after the infection has been introduced. This typically occurs when there are many corpses that add to the total agent count. `ceiling_pre_inf` means the ceiling has been reached before the infection is introduced, which occurs when the basic demographic parameters allow the population to grow dramatically, with the ceiling being reached only by living agents.

`dis_extinct_ceiling_post` means the pathogen is introduced, goes extinct, and the released population grows rapidly and reaches the ceiling. `full_run` means the pathogen and the population both reach the full 10,000 steps. `full_run_dis_extinct` means the pathogen goes extinct, but the rest of the population continues all the way to the full 10,000 steps. Finally, `pop_extinct` means the entire population goes extinct before 10,000 steps.

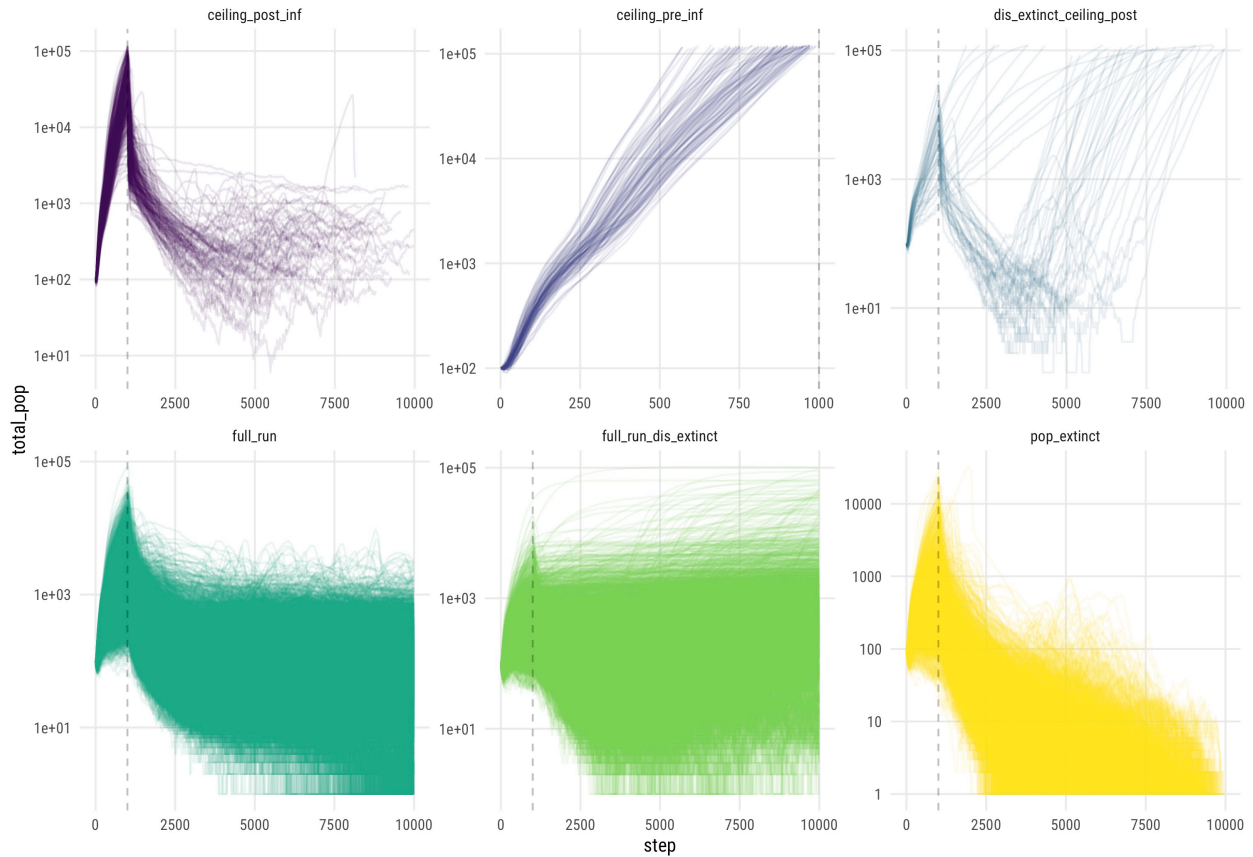


Figure 7: Log of total population size from broad global sensitivity analysis simulations. Each sub-plot corresponds to a different population outcome.

This plot shows the permutation importance scores of the random forest models for each of 10 outcomes. The top 8 predictors for each outcome are shown. Displayed beneath each outcome is the R^2 metric for the random forest model. The time to extinction and time to pathogen extinction models are formulated as survival models, such that there is no R^2 value calculated for the model. Finally, the colors of the bars correspond to the sign of the regression coefficient for a univariate regression between the outcome and parameter. While this does not capture higher-order and nonlinear effects like the random forest approach, it provides a general sense of whether the parameter positively or negatively effects the outcome.

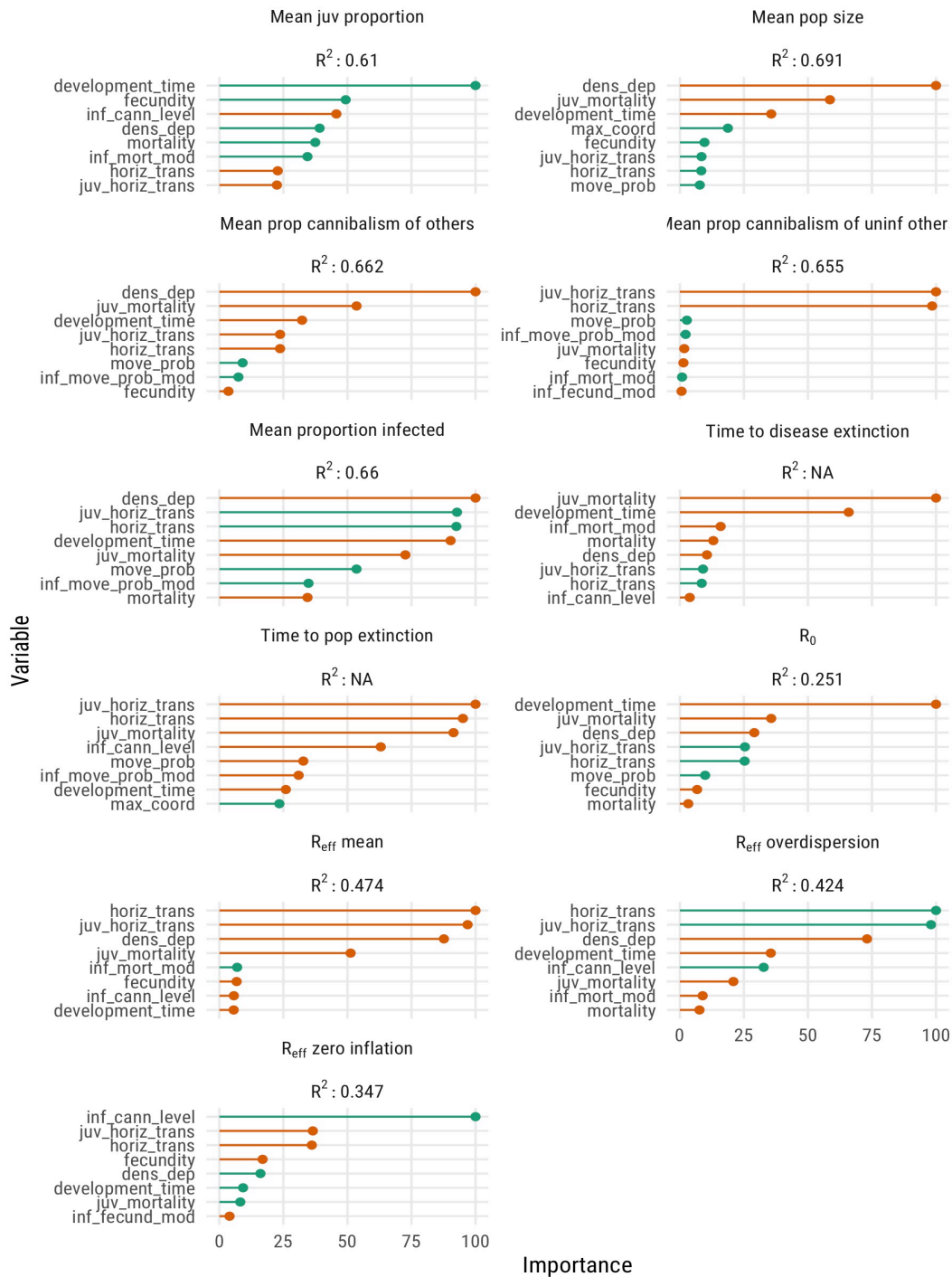


Figure 8: Random forest importance scores for the 8 most important variables within each outcome metric. For regression tree models, an R² value is reported. For each of the variable plus metric combinations, a single linear regression was run using the outcome metric as the outcome and the variable as the predictor, to determine the general sign of the variable's effect. Orange bars correspond to negative beta coefficients, and green bars to positive beta coefficients.

Bibliography

Acevedo, Miguel A., Forrest P. Dilleuth, Andrew J. Flick, Matthew J. Faldyn, and Bret D. Elderd. 2019. “Virulence-Driven Trade-Offs in Disease Transmission: A Meta-Analysis*.” *Evolution* 73 (4): 636–47. <https://doi.org/10.1111/evo.13692>.

Allen, Benjamin G Van, Forrest P Dilleuth, Andrew J Flick, Matthew J Faldyn, David R Clark, Volker H W Rudolf, and Bret D Elderd. 2017. “Cannibalism and Infectious Disease: Friends or Foes?” *American Naturalist* 190 (3): 14.

Allen, Linda J. S., Jesse F. Fagan, Göran Högnäs, and Henrik Fagerholm. 2005. “Population Extinction in Discrete-Time Stochastic Population Models with an Allee Effect.” *Journal of Difference Equations and Applications* 11 (4-5): 273–93. <https://doi.org/10.1080/10236190412331335373>.

Anderson, Roy M, and Robert M May. 1992. *Infectious Diseases of Humans: Dynamics and Control*. Oxford university press.

Assaf, Michael, Alex Kamenev, and Baruch Meerson. 2009. “Population Extinction Risk in the Aftermath of a Catastrophic Event.” *Physical Review E* 79 (1): 011127. <https://doi.org/10.1103/PhysRevE.79.011127>.

Bartlett, M. S. 1960. “The Critical Community Size for Measles in the United States.” *Journal of the Royal Statistical Society. Series A (General)* 123 (1): 37. <https://doi.org/10.2307/2343186>.

Bascompte, Jordi. 2003. “Extinction Thresholds: Insights from Simple Models.” *Annales Zoologici Fennici* 40 (2): 17.

Black, Francis L. 1966. "Measles Endemicity in Insular Populations: Critical Community Size and Its Evolutionary Implication." *Journal of Theoretical Biology* 11 (2): 207–11.

[https://doi.org/10.1016/0022-5193\(66\)90161-5](https://doi.org/10.1016/0022-5193(66)90161-5).

Briggs, C. J., and H. C. J. Godfray. 1995. "The Dynamics of Insect-Pathogen Interactions in Stage-Structured Populations." *The American Naturalist* 145 (6): 855–87.

<https://doi.org/10.1086/285774>.

Bull, J.J. 1994. "Perspective : Virulence." *Evolution* 48 (5): 1423–37.

Bunke, M., M. E. Alexander, J. T. A. Dick, M. J. Hatcher, R. Paterson, and A. M. Dunn. 2015. "Eaten Alive: Cannibalism Is Enhanced by Parasites." *Royal Society Open Science* 2 (3):

140369–69. <https://doi.org/10.1098/rsos.140369>.

Cairns, B.J., J.V. Ross, and T. Taimre. 2007. "A Comparison of Models for Predicting Population Persistence." *Ecological Modelling* 201 (1): 19–26.

<https://doi.org/10.1016/j.ecolmodel.2006.07.018>.

Claessen, D., A. M. de Roos, and L. Persson. 2004. "Population Dynamic Theory of Size-Dependent Cannibalism." *Proceedings of the Royal Society B: Biological Sciences* 271 (1537):

333–40. <https://doi.org/10.1098/rspb.2003.2555>.

Costantino, R. F., R. A. Desharnais, J. M. Cushing, and B. Dennis. 1997. "Chaotic Dynamics in an Insect Population." *Science* 275 (5298): 389–91.

<https://doi.org/10.1126/science.275.5298.389>.

Croft, B A, and J A Murray. 1972. "Comparative Studies on Four Strains of *Typhlodromus Occidentalis* Nesbitt (Acarina: Phytoseiidae). IV. Life History Studies." *Acarologia*, 12.

Day, Troy. 2002. "On the Evolution of Virulence and the Relationship Between Various Measures of Mortality." *Proceedings of the Royal Society of London. Series B: Biological Sciences* 269 (1498): 1317–23. <https://doi.org/10.1098/rspb.2002.2021>.

De Castro, Francisco, and Benjamin Bolker. 2004. "Mechanisms of Disease-Induced Extinction: Mechanisms of Disease-Induced Extinction." *Ecology Letters* 8 (1): 117–26. <https://doi.org/10.1111/j.1461-0248.2004.00693.x>.

El Husseiny, Iman, Hanaa Elbrense, Thomas Roeder, and Samar El Kholy. 2018. "Hormonal Modulation of Cannibalistic Behaviors in Mosquito (*Culex Pipiens*) Larvae." *Journal of Insect Physiology* 109 (August): 144–48. <https://doi.org/10.1016/j.jinsphys.2018.08.001>.

Englert, DuWayne C., and Don W. Raibley. 1977. "GENETIC ANALYSIS OF EGG CANNIBALISM AND OVIPOSITION SITES FOR *TRIBOLIUM CASTANEUM*." *Canadian Journal of Genetics and Cytology* 19 (1): 119–24. <https://doi.org/10.1139/g77-014>.

Faure, Mathieu, and Sebastian J. Schreiber. 2014. "Quasi-Stationary Distributions for Randomly Perturbed Dynamical Systems." *The Annals of Applied Probability* 24 (2). <https://doi.org/10.1214/13-AAP923>.

Foley, Patrick. 1994. "Predicting Extinction Times from Environmental Stochasticity and Carrying Capacity." *Conservation Biology* 8 (1): 124–37. <https://doi.org/10.1046/j.1523-1739.1994.08010124.x>.

Fox, Laurel R. 1975. "Cannibalism in Natural Populations." *Annual Review of Ecology and Systematics*, 21.

Giles Leigh, Egbert. 1981. "The Average Lifetime of a Population in a Varying Environment." *Journal of Theoretical Biology* 90 (2): 213–39. [https://doi.org/10.1016/0022-5193\(81\)90044-8](https://doi.org/10.1016/0022-5193(81)90044-8).

Gog, Julia, Rosie Woodroffe, and Jonathan Swinton. 2002. "Disease in Endangered Metapopulations: The Importance of Alternative Hosts." *Proceedings of the Royal Society of London. Series B: Biological Sciences* 269 (1492): 671–76. <https://doi.org/10.1098/rspb.2001.1667>.

Grimm, Volker, Steven F. Railsback, Christian E. Vincenot, Uta Berger, Cara Gallagher, Donald L. DeAngelis, Bruce Edmonds, et al. 2020. "The ODD Protocol for Describing Agent-Based and Other Simulation Models: A Second Update to Improve Clarity, Replication, and Structural Realism." *Journal of Artificial Societies and Social Simulation* 23 (2). <https://doi.org/10.18564/jasss.4259>.

Halloran, M. Elizabeth, Ira M. Longini, and Claudio J. Struchiner. 2010. "Binomial and Stochastic Transmission Models." In, 6384. New York, NY: Springer New York. <https://doi.org/10.1007/978-0-387-68636-34>.

Harper, Elizabeth B, John C Stella, and Alexander K Fremier. 2011. "Global Sensitivity Analysis for Complex Ecological Models : A Case Study of Riparian Cottonwood Population Dynamics." *Ecological Applications* 21 (4): 1225–40.

Hassell, M. P. 1975. "Density-Dependence in Single-Species Populations." *The Journal of Animal Ecology* 44 (1): 283. <https://doi.org/10.2307/3863>.

Hastings, Alan, and R. F. Costantino. 1987. "Cannibalistic Egg-Larva Interactions in *Tribolium*: An Explanation for the Oscillations in Population Numbers." *The American Naturalist* 130 (1): 36–52. <https://doi.org/10.1086/284696>.

Henle, Klaus, Stephen Sarre, and Kerstin Wiegand. 2004. "The Role of Density Regulation in Extinction Processes and Population Viability Analysis." *Biodiversity and Conservation* 13 (1): 9–52. <https://doi.org/10.1023/B:BIOC.0000004312.41575.83>.

Jaenike, John. 1996. "SUBOPTIMAL VIRULENCE OF AN INSECT-PARASITIC NEMATODE." *Evolution* 50 (6): 2241–47. <https://doi.org/10.1111/j.1558-5646.1996.tb03613.x>.

Keeling, M. J. 1997. "Disease Extinction and Community Size: Modeling the Persistence of Measles." *Science* 275 (5296): 65–67. <https://doi.org/10.1126/science.275.5296.65>.

Lande, Russell. 1993. "Risks of Population Extinction from Demographic and Environmental Stochasticity and Random Catastrophes." *The American Naturalist* 142 (6): 911–27. <https://doi.org/10.1086/285580>.

Law, Yao Hua, and Jay A. Rosenheim. 2011. "Effects of Combining an Intraguild Predator with a Cannibalistic Intermediate Predator on a Species-Level Trophic Cascade." *Ecology* 92 (2): 333–41. <https://doi.org/10.1890/10-0156.1>.

———. 2013. "Presence of Conspecific Females Motivates Egg Cannibalism Owing to Lower Risk of Filial Cannibalism." *Animal Behaviour* 85 (2): 403–9. <https://doi.org/10.1016/j.anbehav.2012.11.015>.

Manica, Andrea. 2004. "Parental Fish Change Their Cannibalistic Behaviour in Response to the Cost-to-Benefit Ratio of Parental Care." *Animal Behaviour* 67 (6): 1015–21.

<https://doi.org/10.1016/j.anbehav.2003.09.011>.

McCallum, Hamish, and Andy Dobson. 1995. "Detecting Disease and Parasite Threats to Endangered Species and Ecosystems." *Trends in Ecology & Evolution* 10 (5): 190–94.

[https://doi.org/10.1016/S0169-5347\(00\)89050-3](https://doi.org/10.1016/S0169-5347(00)89050-3).

———. 2002. "Disease, Habitat Fragmentation and Conservation." *Proceedings of the Royal Society of London. Series B: Biological Sciences* 269 (1504): 2041–49.

<https://doi.org/10.1098/rspb.2002.2079>.

O’Keefe, Kara J., and Janis Antonovics. 2002. "Playing by Different Rules: The Evolution of Virulence in Sterilizing Pathogens." *The American Naturalist* 159 (6): 597–605.

<https://doi.org/10.1086/339990>.

Ovaskainen, Otso, and Baruch Meerson. 2010. "Stochastic Models of Population Extinction." *Trends in Ecology & Evolution* 25 (11): 643–52. <https://doi.org/10.1016/j.tree.2010.07.009>.

Perez, Liliana, and Suzana Dragicevic. 2009. "An Agent-Based Approach for Modeling Dynamics of Contagious Disease Spread" 17: 1–17. <https://doi.org/10.1186/1476-072X-8-50>.

Polis, Gary A. 1981. "The Evolution and Dynamics of Intraspecific Predation." *Annual Review of Ecology and Systematics* 12 (1): 225–51.

<https://doi.org/10.1146/annurev.es.12.110181.001301>.

Prowse, Thomas A A, Corey J A Bradshaw, Steven Delean, Phillip Cassey, Robert C Lacy, Konstans Wells, Matthew E Aiello-lammens, H R Akçakaya, and Barry W Brook. 2016. "An

Efficient Protocol for the Global Sensitivity Analysis of s Toochastic Ecological Models” 7
(March): 1–17.

Radwan, Jacek. 1995. “Male Morph Determination in Two Species of Acarid Mites.” *Heredity* 74 (6): 669–73. <https://doi.org/10.1038/hdy.1995.91>.

Read, Andrew F. 1994. “The Evolution of Virulence.” *Trends in Microbiology* 2 (3): 4.

Reynolds, K Tracy, Linda J Thomson, and Ary A Hoffmann. 2003. “The Effects of Host Age, Host Nuclear Background and Temperature on Phenotypic Effects of the Virulent Wolbachia Strain Popcorn in *Drosophila Melanogaster*.” *Genetics* 164 (3): 1027–34.
<https://doi.org/10.1093/genetics/164.3.1027>.

Rosenheim, Jay A., Nicholas A. Booster, Michael Culshaw-Maurer, Tobias G. Mueller, Randall L. Kuffel, Yao-Hua Law, Peter B. Goodell, et al. 2019. “Disease, Contagious Cannibalism, and Associated Population Crash in an Omnivorous Bug, *Geocoris Pallens*.” *Oecologia* 190 (1): 69–83. <https://doi.org/10.1007/s00442-019-04407-y>.

Rudolf, Volker H W, and Janis Antonovics. 2007. “Disease Transmission by Cannibalism: Rare Event or Common Occurrence?” *Proceedings. Biological Sciences / The Royal Society* 274 (1614): 1205–10. <https://doi.org/10.1098/rspb.2006.0449>.

Sadeh, Asaf, Tobin D. Northfield, and Jay A. Rosenheim. 2016. “The Epidemiology and Evolution of Parasite Transmission Through Cannibalism.” *Ecology* 97 (8): 2003–11.
<https://doi.org/10.1890/15-0884.1>.

Sadeh, Asaf, and Jay A. Rosenheim. 2016. “Cannibalism Amplifies the Spread of Vertically Transmitted Pathogens.” *Ecology* 97 (8): 1994–2002. <https://doi.org/10.1890/15-0825.1>.

Smith, K. F., K. Acevedo-Whitehouse, and A. B. Pedersen. 2009. “The Role of Infectious Diseases in Biological Conservation.” *Animal Conservation* 12 (1): 1–12.

<https://doi.org/10.1111/j.1469-1795.2008.00228.x>.

Tracey, Jeff A., Sarah N. Bevins, Sue VandeWoude, and Kevin R. Crooks. 2014. “An Agent-Based Movement Model to Assess the Impact of Landscape Fragmentation on Disease Transmission.” *Ecosphere* 5 (9): art119. <https://doi.org/10.1890/ES13-00376.1>.

Vijendravarma, Roshan K., Sunitha Narasimha, and Tadeusz J. Kawecki. 2013. “Predatory Cannibalism in *Drosophila Melanogaster* Larvae.” *Nature Communications* 4 (1): 1789.

<https://doi.org/10.1038/ncomms2744>.

Wilensky, Uri. 1999. “NetLogo.” Northwestern University, Evanston, IL.

<http://ccl.northwestern.edu/netlogo/>.

Wise, David H. 2006. “Cannibalism, Food Limitation, Intraspecific Competition, and the Regulation of Spider Populations.” *Annual Review of Entomology* 51 (1): 441–65.

<https://doi.org/10.1146/annurev.ento.51.110104.150947>.

Yakovlev, I. K. 2018. “Effects of Octopamine on Aggressive Behavior in Red Wood Ants.” *Neuroscience and Behavioral Physiology* 48 (3): 279–88. <https://doi.org/10.1007/s11055-018-0561-0>.

Yan, G Y, L Stevens, and J J Schall. 1994. “Behavioral-Changes in *Tribolium* Beetles Infected with a Tapeworm - Variation in Effects Between Beetle Species and Among Genetic Strains.” *American Naturalist* 143 (5): 830–47. <https://doi.org/10.1086/285635>.

Zhou, Chuan, Yong Rao, and Yi Rao. 2008. "A Subset of Octopaminergic Neurons Are Important for *Drosophila* Aggression." *Nature Neuroscience* 11 (9): 1059–67.

<https://doi.org/10.1038/nn.2164>.

Łukasik, Piotr. 2010. "Trophic Dimorphism in Alternative Male Reproductive Morphs of the Acarid Mite *Sancassania Berlesei*." *Behavioral Ecology* 21 (2): 270–74.

<https://doi.org/10.1093/beheco/arp186>.